Universidade Estadual de Campinas
Faculdade de Engenharia Química

Luciana de Souza Guedes

Quantificação de compostos bioativos da palmeira *Elaeis guineensis* por cromatografia com fluido supercrítico de ultra alta eficiência e por espectroscopia no infravermelho com transformada de Fourier

Campinas
2019

Luciana de Souza Guedes

Quantificação de compostos bioativos da palmeira *Elaeis guineensis* por cromatografia com fluido supercrítico de ultra alta eficiência e por espectroscopia no infravermelho com transformada de Fourier

Tese apresentada à Faculdade de Engenharia Química da Universidade Estadual de Campinas como parte dos requisitos exigidos para a obtenção do título de Doutora em Engenharia Química.

Orientador: Prof. Dr. Cesar Costapinto Santana
Coorientadoras: Profa. Dra. Marisa Masumi Beppu e Profa. Dra. Márcia Cristina Breitkreitz

ESTE EXEMPLAR CORRESPONDE À VERSÃO FINAL DA TESE DEFENDIDA PELA ALUNA LUCIANA DE SOUZA GUEDES E ORIENTADA PELO PROFESSOR DOUTOR CESAR COSTAPINTO SANTANA.

Campinas

2019

Ficha catalográfica
Universidade Estadual de Campinas
Biblioteca da Área de Engenharia e Arquitetura
Rose Meire da Silva - CRB 8/5974

G935q

Guedes, Luciana de Souza, 1975-
Quantificação de compostos bioativos da palmeira *Elaeis guineensis* por cromatografia com fluido supercrítico de ultra alta eficiência e por espectroscopia no infravermelho com transformada de Fourier / Luciana de Souza Guedes. – Campinas, SP : [s.n.], 2019.

Orientador: Cesar Costapinto Santana.
Coorientadores: Marisa Masumi Beppu e Márcia Cristina Breitkreitz.
Tese (doutorado) – Universidade Estadual de Campinas, Faculdade de Engenharia Química.

1. Carotenoides. 2. Coenzima Q10. 3. Óleo de palma. 4. Cromatografia com fluido supercrítico de ultra alta eficiência. 5. Espectroscopia no infravermelho com transformada de Fourier. I. Santana, Cesar Costapinto, 1948-. II. Beppu, Marisa Masumi, 1972-. III. Breitkreitz, Márcia Cristina,1979-. IV. Universidade Estadual de Campinas. Faculdade de Engenharia Química. V. Título.

Informações para Biblioteca Digital

Título em outro idioma: Quantification of bioactive compounds from *Elaeis guineensis* palm tree by ultra-high performance supercritical fluid chromatography and Fourier transform infrared spectroscopy
Palavras-chave em inglês:
Carotenoids
Coenzyme Q10
Palm oil
Ultra-high performance supercritical fluid chromatography (UHPSFC)
Fourier transform infrared spectroscopy (FTIR)
Área de concentração: Engenharia Química
Titulação: Doutora em Engenharia Química
Banca examinadora:
Cesar Costapinto Santana [Orientador]
Priscilla Carvalho Veggi
Adalberto Pessoa Júnior
Maurício Ariel Rostagno
Carla Beatriz Grespan Bottoli
Data de defesa: 27-06-2019
Programa de Pós-Graduação: Engenharia Química

Identificação e informações acadêmicas do(a) aluno(a)
- ORCID do autor: https://orcid.org/0000-0003-3972-915X
- Currículo Lattes do autor: http://lattes.cnpq.br/1288835097644799

Folha de Aprovação da Defesa de Tese de Doutorado defendida por Luciana de Souza Guedes aprovada em 27 de junho de 2019 pela banca examinadora constituída pelos seguintes doutores:

Dr. Cesar Costapinto Santana

FEQ / UNICAMP

Profa. Dra. Carla Beatriz Grespan Bottoli

IQ / UNICAMP

Dr. Adalberto Pessoa Junior

FCF /USP

Dra. Priscilla Carvalho Veggi

Universidade Federal de São Paulo

Dr. Maurício Ariel Rostagno

Universidade Estadual de Campinas

ATA da Defesa com as respectivas assinaturas dos membros encontra-se no SIGA/Sistema de Fluxo de Dissertação/Tese e na Secretaria do Programa da Unidade.

Aos meus pais, Antonio e Eudália, e à
minha querida irmã Erika pelo apoio.

Agradecimentos

Primeiramente, gostaria de agradecer minha família pelo apoio e compreensão por não estar presente em todos os momentos. À minha querida irmã Erika pelos conselhos valiosos.

Aos professores Cesar Costapinto Santana, Marisa Masumi Beppu e Márcia Cristina Breitkreitz pela oportunidade e confiança. Foram muitos os momentos de aprendizado. À professora Isabel Cristina Sales Fontes Jardim pela leitura dedicada das publicações. Aos professores Douglas Neil Rutledge e José Licarion Pinto Segundo Neto pela generosa contribuição na análise dos resultados.

À Universidade Tiradentes pela oportunidade de estágio e aos alunos Kelvis Vieira Campos, Larissa Ferreira Torres e Ronney José Oliveira Santos pelo auxílio com os experimentos de extração. As professoras Nicole Labbé e Danielle Julie Carrier pela orientação e acolhida durante o meu estágio no *Center of Renewable Carbon, The University of Tennessee*. Agradeço também à Kalavathy Rajan, Choo Hamilton, Chris Helton e Anna Kim pelo auxílio no laboratório.

O presente trabalho foi realizado com o apoio do CNPq, Conselho Nacional de Desenvolvimento Científico e Tecnológico - Brasil, processo 140467/2015-7. À Waters Technologies do Brasil Ltda. pela doação das colunas cromatográficas e pela parceria para a publicação da nota técnica.

Aos meus queridos amigos da Faculdade de Engenharia Química, João Batista Neto, Thiago B. Taketa, Laise M. Lopes, Rogério Bataglioli, Luiz G. L. Germiniani, Gabriel A. T. da Silveira, Reginaldo Neto e os demais pela amizade e carinho. Agradeço também aos meus queridos amigos do Instituto de Química, Lucília V. de Melo, Hery Mitsutake, Fabiane Pires, Marcella E. P. Schmidt, Jucélio L. Saturno, Gabriela B. Almeida, Letícia S. Shiroma, Igor M. Santana, Camila Honda, Camila D. L. dos Santos, Luana Macedo, Mary A. Perez, Felipe Campanaro e os demais pela convivência e oportunidade de aprendizado.

La vie n'est facile pour aucun de nous. Mais quoi, il faut avoir de la persévérance, et surtout de la confiance en soi. Il faut croire que l'on est doué pour quelque chose, et que, cette chose, il faut l'atteindre coûte que coûte.

Marie Curie

Resumo

Neste estudo, método para separação e quantificação do licopeno, betacaroteno, coenzima Q10 e luteína no óleo de palma foi desenvolvido por cromatografia com fluido supercrítico de ultra alta eficiência (UHPSFC). Primeiramente, as condições de operação foram otimizadas com a mistura padrão. Os analitos foram separados em menos de 7 minutos nas condições de pressão de 1500 psi, temperatura 40 ℃ e porcentagem de etanol 15,5%. No entanto, essas condições de operação não se mostraram adequadas para a separação dos compostos bioativos no óleo de palma devido à co-eluição dos mesmos com componentes da matriz. Novas condições experimentais foram avaliadas e as condições de pressão de 1600 psi, temperatura 40 ℃ e porcentagem de etanol 18% foram selecionadas. O método quimiométrico Análise Multivariada de Curvas com Mínimos Quadrados Alternantes (MCR-ALS) foi empregado na análise dos dados cromatográficos para identificar e quantificar os compostos investigados. A concentração determinada para o betacaroteno, coenzima Q10 e luteína foi 176, 8,29 e 2,90 μg/mL, respectivamente. O licopeno não foi quantificado devido à baixa pureza do padrão secundário. A concentração desses compostos foi determinada também por espectroscopia no infravermelho com transformada de Fourier (FTIR). Os resultados apresentaram concordância com os resultados obtidos por UHPSFC usado como referência. A concentração determinada para o betacaroteno, coenzima Q10 e luteína foi 178, 12,8 e 2,90 μg/mL, respectivamente. O estudo mostrou que as técnicas UHPSFC e FTIR podem ser empregadas para quantificação de constituintes minoritários do óleo de palma como os carotenoides e a coenzima Q10.

Palavras-chave: carotenoides, coenzima Q10, óleo de palma, cromatografia com fluido supercrítico de ultra alta eficiência (UHPSFC), espectroscopia no infravermelho com transformada de Fourier (FTIR)

Abstract

In this study, a method for separation and quantification of lycopene, beta-carotene, coenzyme Q10 and lutein in palm oil was developed by ultra-high performance supercritical fluid chromatography (UHPSFC). First, the operating conditions were optimized with a standard mixture. Analytes were separated in less than 7 minutes under conditions of pressure 1500 psi, temperature 40 ℃ and 15.5% of ethanol. However, these operating conditions were not adequate for separation of the bioactive compounds in palm oil due to co-elution of the target compounds with matrix constituents. New experimental conditions were evaluated and the conditions of pressure 1600 psi, temperature 40 ℃ and 18% of ethanol were selected. The chemometric method Multivariate Curve Resolution with Alternating Least Squares (MCR-ALS) was applied on the chromatographic data to properly identify and quantify the target compounds. Concentration of beta-carotene, coenzyme Q10 and lutein was determined as 176, 8.29 and 2.90 μg/mL, respectively. Lycopene was not quantified because of the low purity of its secondary standard. Concentration of the bioactive compounds were also determined by Fourier transform infrared spectroscopy (FTIR). The results showed good agreement with results obtained by UHPSFC used as reference method. Concentration of beta-carotene, coenzyme Q10 and lutein was determined as 178, 12.8 and 2.90 μg/mL, respectively. The study showed that UHPSFC and FTIR techniques may be employed for quantification of palm oil minor constituents as carotenoids and coenzyme Q10.

Keywords: carotenoids, coenzyme Q10, palm oil, ultra-high performance supercritical fluid chromatography (UHPSFC), Fourier transform infrared spectroscopy (FTIR)

Lista de Ilustrações

Lista de Tabelas

Lista de Abreviaturas e Siglas

ANOVA	Análise da variância, do inglês *Analysis of Variance*
ATR	Espectroscopia por refletância total atenuada, do inglês *Attenuated Total Reflectance Spectroscopy*
CCD	Planejamento composto central, do inglês *Central Composite Design*
CPO	Óleo de palma cru, do inglês *Crude Palm Oil*
CV	Coeficiente de variação, do inglês *Coeficient of Variation*
DOBI	Índice de deterioração de branqueabilidade, do inglês *Deterioration of Bleachability Index*
DOE	Planejamento experimental, do inglês *Design of Experiments*
FIR	Espectroscopia no infravermelho longínquo, do inglês *Far Infrared Spectroscopy*
FTIR	Espectroscopia no infravermelho com transformada de Fourier, do inglês *Fourier Transform Infrared Spectroscopy*
HCA	Agrupamento por métodos hierárquicos, do inglês *Hierarchical Cluster Analysis*
HPLC	Cromatografia líquida de alta eficiência, do inglês *High-Performance Liquid Chromatography*
MCR-ALS	Resolução multivariada de curvas com mínimos quadrados alternantes, do inglês *Multivariate Curve Resolution with Alternating Least Squares*
MIR	Espectroscopia no infravermelho médio, do inglês *Mid Infrared Spectroscopy*
NIR	Espectroscopia no infravermelho próximo, do inglês *Near Infrared Spectroscopy*
PCA	Análise de componentes principais, do inglês *Principal Component Analysis*
PCR	Regressão por componentes principais, do inglês *Principal Component Regression*
PDA	Detector do tipo arranjo de diodos, do inglês *Photodiode Array*
PFO	Fibra prensada, do inglês *Palm Fibre Oil*
PKO	Óleo de palmiste, do inglês *Palm Kernel Oil*
PLS	Mínimos quadrados parciais, do inglês *Partial Least Squares*
POME	Efluentes líquidos da indústria de palma, do inglês *Palm Oil Mill Effluent*

PRESS	Soma dos quadrados predita do erro, do inglês *Predicted Residual Error Sum of Squares*
R	Coeficiente de correlação, do inglês *Correlation coefficient*
R^2	Coeficiente de determinação, do inglês *Coefficient of determination*
RMSE	Raiz quadrada do erro médio quadrático, do inglês *Root Mean Square Error*
RMSEC	Raiz quadrada do erro médio quadrático de calibração, do inglês *Root Mean Square Error of Calibration*
RMSECV	Raiz quadrada do erro médio quadrático de validação cruzada, do inglês *Root Mean Square Error of Cross-Validation*
RMSEP	Raiz quadrada do erro médio quadrático de previsão, do inglês *Root Mean Square Error of Prediction*
RSM	Metodologia de superfície de resposta, do inglês *Response Surface Methodology*
SEC	Erro padrão de calibração, do inglês *Standard Error of Calibration*
SECV	Erro padrão de validação cruzada, do inglês *Standard Error of Cross-Validation*
SF	Fluido supercrítico, do inglês *Supercritical Fluid*
SFC	Cromatografia com fluido supercrítico, do inglês *Supercritical Fluid Chromatography*
UHPSFC	Cromatografia com fluido supercrítico de ultra alta eficiência, do inglês *Ultra-High Performance Supercritical Fluid Chromatography*

Sumário

1 | Introdução

1.1 Estrutura da Tese

A tese foi organizada em capítulos, onde cada capítulo apresenta as principais etapas do trabalho. O capítulo 1 contempla a justificativa do estudo. O objetivo principal e os objetivos específicos são apresentados no capítulo 2. A revisão bibliográfica da matriz estudada (óleo de palma), dos compostos bioativos investigados (carotenoides e coenzima Q10) e das técnicas utilizadas (UHPSFC e FTIR) é apresentada no capítulo 3.

Os resultados do trabalho são reportados nos capítulos 4, 5 e 6, e foram organizados em formato de artigo. O capítulo 4 intitulado como *Study of the effect of the operating parameters on the separation of bioactive compounds of palm oil by ultra-high performance supercritical fluid chromatography using a design of experiments approach* apresenta os resultados do desenvolvimento do método de separação com a mistura padrão do licopeno, betacaroteno, coenzima Q10 e luteína por UHPSFC. Esta parte do trabalho foi publicada no *The Canadian Journal of Chemical Engineering*, DOI 10.1002/cjce.22969.

O capítulo 5 intitulado como *Quantification of bioactive compounds from palm oil by ultra-high performance supercritical fluid chromatography* descreve o desenvolvimento do método de separação dos compostos estudados por UHPSFC e do emprego do método quimiométrico MCR-ALS para a identificação e quantificação do betacaroteno, coenzima Q10 e luteína no óleo de palma.

O capítulo 6 intitulado como *Application of Fourier transform infrared spectroscopy (FTIR) combined with partial least squares (PLS) regression for determination of minor constituents in palm oil* apresenta os resultados dos estudos desenvolvidos com a técnica FTIR para a quantificação do betacaroteno, coenzima Q10 e luteína no óleo de palma. Esta parte do trabalho foi realizada no *Center for Renewable*

Carbon, The University of Tennessee sob a supervisão das professoras Nicole Labbé e Danielle Julie Carrier.

O capítulo 7 apresenta as conclusões dos estudos desenvolvidos com as técnicas UHPSFC e FTIR para quantificação do betacaroteno, coenzima Q10 e luteína no óleo de palma, e as sugestões para projetos futuros são apresentadas no capítulo 8.

1.2 Justificativa

Carotenoides e coenzima Q10 são potentes antioxidantes naturais encontrados em plantas, microorganismos e animais. Uma grande atenção tem sido dada a esses compostos devido aos benefícios apresentados para a saúde humana e também às suas aplicações industriais [1]. Estudos recentes demonstraram que a capacidade antioxidante dos carotenoides e da coenzima Q10 auxilia no processo de prevenção de doenças cardiovasculares, cancerígenas e outras doenças crônicas [2]. Na indústria, esses compostos são usados como suplemento alimentar, aditivo de produtos farmacêuticos e em produtos cosméticos [3],[4] e [5].

Técnicas cromatográficas têm sido bastante usadas na separação e análise de carotenoides e coenzima Q10 presentes em diferentes matrizes. São reportados na literatura diversos estudos empregando a Cromatografia Líquida de Alta Eficiência (HPLC) na determinação desses compostos em amostras de origem animal, vegetal e biológica. É representativa a revisão de Rivera *et al.* (2012) de técnicas cromatográficas para análise de carotenoides [6]. Outra contribuição importante é o estudo desenvolvido por Lunetta *et al.* (2008) para a determinação de coenzima Q10 em matérias-primas e suplementos alimentares [7].

A cromatografia com fluido supercrítico (SFC) tem sido empregada mais recentemente no estudo de carotenoides e coenzima Q10 devido à modernização da instrumentação e a excelente seletividade da técnica. Além disso, a SFC permite obter tempos de análise inferiores aos observados por HPLC e reduzir o consumo de solventes orgânicos [8]. A grande maioria dos estudos de separação desses compostos encontrados na literatura foi realizada com sistema modelo. Um número menor de publicações tem reportado resultados da determinação desses compostos em matrizes complexas. Choo *et al.* (2005) utilizaram a SFC na análise quantitativa de carotenoides, vitamina E, esteróis e esqualeno presentes no óleo extraído da

palmeira *Elaeis guineensis* Jacq. (óleo de palma). Neste estudo, os pesquisadores determinaram os carotenoides totais da amostra [9]. Outro resultado importante foi obtido por Han *et al.* (2006) que estudaram a separação da coenzima Q10 presente no óleo de palma cru (CPO, *crude palm oil*) e na fibra prensada (PFO, *palm fibre oil*) por SFC [10].

Técnicas espectroscópicas também têm sido usadas para a quantificação de constituintes do óleo de palma e para identificação da sua origem geográfica. Moh *et al.* (1999) empregaram a espectroscopia no UV-Visível, no infravermelho próximo (NIR) e FTIR para quantificar o betacaroteno no óleo de palma. Os resultados mostraram que as técnicas FTIR e NIR podem ser uma alternativa a espectroscopia UV-Visível para a determinação desse constituinte do óleo de palma [11]. Em outro estudo, Ammawath *et al.* (2010) quantificaram o betacaroteno na fração líquida do óleo de palma (oleína) por FTIR. Os resultados obtidos foram semelhantes aos do método de referência (HPLC). Os autores ressaltaram as vantagens do método desenvolvido por FTIR, como menor consumo de solventes orgânicos e menor tempo de análise [12].

Os estudos mencionados anteriormente mostram o potencial expressivo do emprego das técnicas UHPSFC e FTIR para a quantificação de constituintes do óleo de palma.

2 | Objetivos

O objetivo principal do trabalho foi o desenvolvimento de método para separação e quantificação do licopeno, betacaroteno, coenzima Q10 e luteína presentes no óleo de palma (*Elaeis guineensis* Jacq.) por UHPSFC. Os objetivos específicos do estudo foram:

- Desenvolvimento do método de separação com a mistura padrão (licopeno, betacaroteno, coenzima Q10 e luteína) por UHPSFC;
- Identificação das condições ótima de separação empregando métodos quimiométricos;
- Desenvolvimento do método de separação com a amostra do óleo de palma por UHPSFC;
- Identificação e quantificação do betacaroteno, coenzima Q10 e luteína presentes no óleo de palma por UHPSFC empregando o método quimiométrico MCR-ALS;
- Avaliação da espectroscopia FTIR em conjunto com o método quimiométrico Mínimos Quadrados Parciais (PLS, do inglês *Partial Least Squares*) para quantificação do betacaroteno, coenzima Q10 e luteína no óleo de palma.

3 | Revisão Bibliográfica

3.1 Óleo de Palma

A espécie *Elaeis guineensis* Jacq. é uma palmeira de origem africana conhecida no Brasil como dendê. Essa palmácea é cultivada em 42 países, ocupando 11 milhões de hectares, sendo a maior plantação para produção de óleo comestível do mundo [13]. Os cinco principais países produtores de óleo de palma são Indonésia, Malásia, Tailândia, Colômbia e Nigéria. Os frutos da palmeira *Elaeis guineensis* Jacq. produzem dois tipos de óleo, o óleo de palma obtido a partir do mesocarpo do fruto e o óleo de palmiste extraído da amêndoa [14]. O óleo de palma é rico em carotenoides, contém entre 500 e 700 ppm desses compostos, sendo que esta quantidade é de 10 a 200 vezes maior do que a quantidade presente em vegetais como cenoura e tomate [15]. Além disso, o óleo de palma é fonte de vitamina E (600-1000 ppm), coenzima Q10 (10-80 ppm), esteróis (250-620 ppm), esqualeno (200-600 ppm) e fosfolipídios (20-100 ppm) [9],[16],[17], [18].

3.2 Carotenoides

Carotenoides são tetraterpenóides de 40 carbonos formados por 8 unidades isoprenóides de 5 carbonos. Esses compostos são divididos em dois grandes grupos nomeados carotenos e xantofilas. Carotenos são moléculas formadas somente por carbono e hidrogênio como o licopeno e o betacaroteno, e xantofilas são os derivados com grupos substituintes contendo oxigênio como, por exemplo, a luteína. A Figura 3.1 apresenta a estrutura dos carotenoides estudados. A presença de conjugações no cromóforo (onze no licopeno e betacaroteno, e dez na luteína) explica a coloração intensa desses compostos. Os carotenoides podem ser classificados também com base em sua coloração: pigmentos amarelo-alaranjados como o betacaroteno e a luteína cuja absorção máxima é observada em 450 nm; e pigmentos avermelhados como,

por exemplo, a criptoxantina, a capsorubina e a capsantina que possuem um ou dois grupos oxigenados conjugados às duplas ligações e apresentam absorção máxima em 480 nm [19].

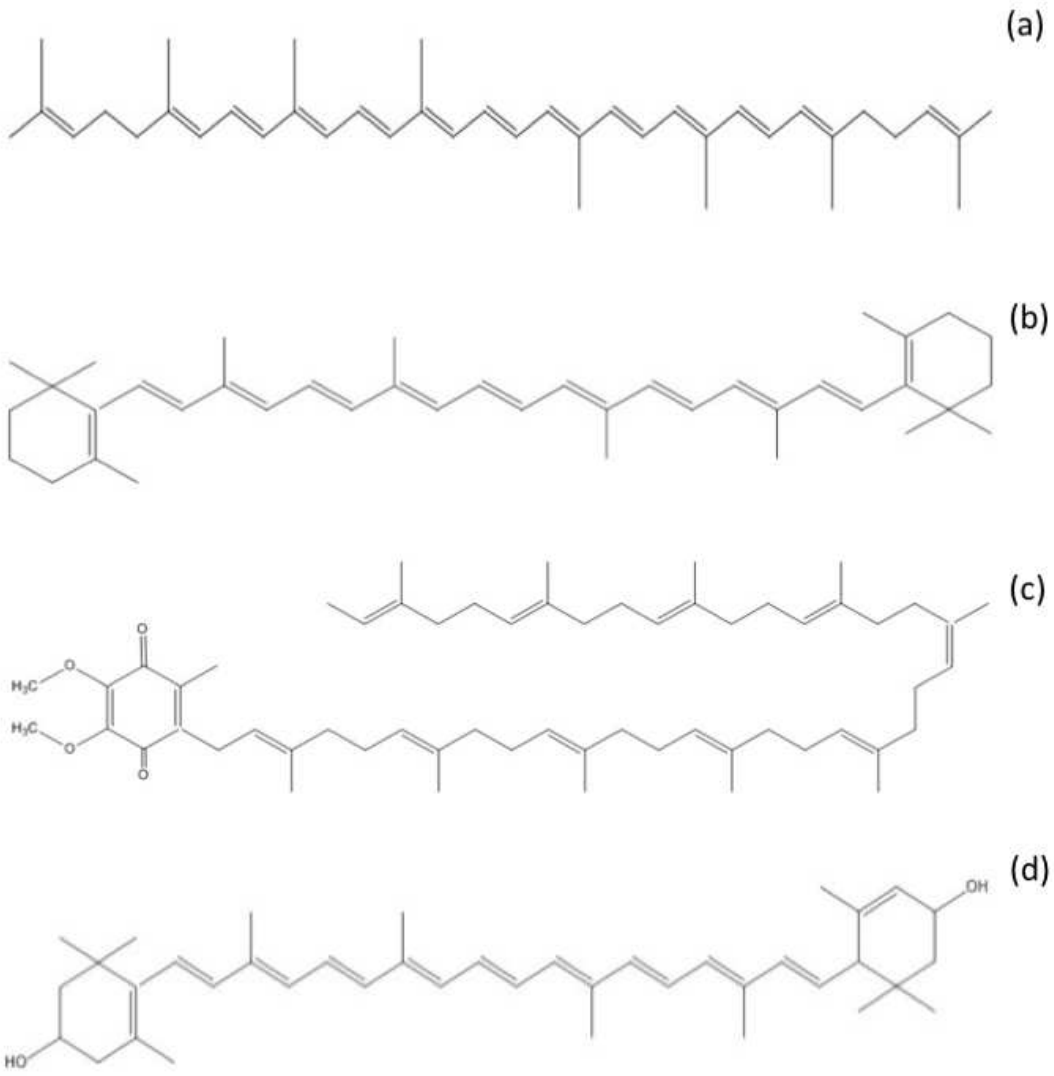

Figura 3.1: Fórmula estrutural do (a) licopeno, (b) betacaroteno, (c) coenzima Q10 e (d) luteína.

A presença de ligações duplas na cadeia de hidrocarbonetos faz com que esses compostos sejam susceptíveis a reações como oxidação e isomerização (*cis-trans*). Ciclização, hidrogenação, desidrogenação e introdução de grupos contendo oxigênio são algumas das modificações que podem ocorrer na estrutura dos carotenoides e

que resultam na diversidade de estruturas observadas para esses compostos [20]. A Tabela 3.1 apresenta as propriedades físico-químicas dos carotenoides estudados.

Tabela 3.1: Fórmula molecular, massa molar e valores de logP do licopeno, betacaroteno, coenzima Q10 e luteína.

Composto	**Fórmula Molecular**	**Massa Molar (g/mol)**	**logP**
Licopeno	$C_{40}H_{56}$	536,885	11,93
Betacaroteno	$C_{40}H_{56}$	536,885	11,12
Coenzima Q10	$C_{59}H_{90}O_4$	863,361	11,00
Luteína	$C_{40}H_{56}O_2$	568,833	8,55

Referências [21],[22].

Carotenoides são pigmentos naturais lipossolúveis encontrados em uma grande variedade de plantas, animais e micro-organismos. Existem mais de 500 carotenoides na natureza, sendo que os mais estudados são betacaroteno, alfacaroteno, licopeno, luteína, astaxantina, fucoxantina e cantaxantina. Além de apresentarem capacidade antioxidante, alguns carotenoides são precursores da vitamina A que é essencial para o sistema imunológico, o funcionamento do ciclo visual e para o crescimento, desenvolvimento e manutenção das células do epitélio [2], [23]. Seres humanos não são capazes de sintetizar carotenoides e, portanto, necessitam obtê-los pela dieta [6]. Frutas e vegetais são as maiores fontes de carotenoides na dieta humana. O consumo desses compostos tem sido associado a inúmeros benefícios para a saúde como a prevenção de câncer, doenças vasculares e degenerativas [20], [23]. Carotenoides são usados na indústria como corantes, suplementos alimentares, aditivos de produtos farmacêuticos, em produtos para alimentação animal e em fragrâncias [5]. O mercado global de carotenoides deve atingir aproximadamente US$ 1,8 bilhão em 2019 [24].

Carotenoides são encontrados na natureza na forma livre e esterificada com ácidos graxos, sendo esta última a forma mais estável [25]. Esses compostos degradam com facilidade devido à sensibilidade a luz, calor, ácido e oxigênio [19],[20]. Além disso, a grande variedade de carotenoides com estruturas semelhantes e a limitada disponibilidade de padrões analíticos dificulta a análise desses compostos [20], [23]. Devido a essas limitações, algumas medidas são necessárias no preparo, análise e armazenamento das amostras para manter a integridade dos carotenoides.

São reportados na literatura estudos que recomendam a determinação de carotenoides após a saponificação da amostra. Este procedimento é utilizado para remover interferentes como, por exemplo, clorofila e lipídios. Amorim-Carrilho *et al.* (2014) avaliaram diversos estudos que empregaram este procedimento no preparo de amostra. Alguns estudos observaram aumento da recuperação de carotenoides após a saponificação, enquanto que outros estudos observaram redução na recuperação desses compostos após o procedimento. Os pesquisadores concluíram que a recuperação de carotenoides não depende somente do emprego ou não da saponificação, mas também do tipo de matriz em que esses compostos estão presentes, do tempo e da concentração dos tratamentos alcalinos utilizados [19], [20].

Além do procedimento citado acima, podem ser mencionados também a importância da proteção da amostra da presença de ácidos e íons metálicos, a seleção adequada do solvente, o armazenamento em ambiente refrigerado (-20 ℃) e na ausência de luz como medidas para manter a integridade das amostras. As soluções de carotenoides não são estáveis por períodos longos, e suas concentrações e purezas devem ser avaliadas com frequência para se detectar alterações [19],[26],[27].

3.3 Coenzima Q10

Coenzima Q10 ou ubiquinona é uma vitamina-símile lipossolúvel que está presente em quase todas as células do organismo humano, sendo encontrada em maior concentração na membrana mitocondrial. Desempenha papel essencial no transporte de elétrons e na geração de energia na forma de adenosina trifosfato (ATP) [28], [29], [30], [31]. A coenzima Q10 é produzida de forma endógena, mas também pode ser obtida pela suplementação ou pela dieta a partir de alimentos como carnes, ovos, peixes, cereais e vegetais [28],[29], [30]. A estrutura da coenzima Q10 é apresentada na Figura 3.1 e suas propriedades físico-químicas são reportadas na Tabela 3.1.

A coenzima Q10 apresenta capacidade antioxidante cujo efeito é 10 vezes mais potente que o da vitamina E. Devido à essa propriedade, a coenzima Q10 tem sido empregada no tratamento de pacientes cardíacos e com síndrome parkinsoniana [32]. Além disso, este composto tem se mostrado efetivo na prevenção da peroxidação lipídica e da degeneração oxidativa da hemoglobina, e na redução de

mediadores inflamatórios [33], [34]. A coenzima Q10 tem sido utilizada em produtos farmacêuticos, cosméticos e alimentícios [3], [4].

3.4 Cromatografia com Fluido Supercrítico de Ultra Alta Eficiência

A técnica de HPLC é a principal técnica empregada na análise de carotenoides e coenzima Q10. Recentemente, o emprego de fluidos supercríticos (SF) como por exemplo, o dióxido de carbono supercrítico tem se tornado uma alternativa promissora ao HPLC visto que o uso de SF possibilita a redução do tempo de análise e da quantidade de solvente usada [19].

O emprego de fluidos supercríticos apresenta vantagens como maior poder de solvatação de substâncias apolares quando comparada à solubilidade em condições normais de temperatura e pressão em solventes orgânicos, sua baixa viscosidade em relação aos gases provoca menor queda de pressão na coluna favorecendo a percolação e permitindo que partículas de tamanhos menores possam ser usadas no leito recheado, o que gera maior eficiência para a coluna [35], [36].

A SFC tem sido bastante estudada devido à sua versatilidade na separação quiral, o que tem levado a um melhor entendimento da técnica e consequentemente rápido desenvolvimento da parte instrumental [37]. Esta técnica é um método de separação muito atrativo, pois os fluidos usados como fase móvel são sustentáveis, têm baixo custo, não são tóxicos (em concentrações abaixo de 2% no ar) e não são inflamáveis. O dióxido de carbono (CO_2) tem sido bastante empregado como fase móvel na SFC, pois suas propriedades críticas (P_c = 73,773 bar, T_c = 304,13 K) são próximas as condições ambiente, além de não ser explosivo ou tóxico [23],[38], [39]. A técnica utilizava inicialmente CO_2 puro como fase móvel. Atualmente são empregadas condições subcríticas onde a fase móvel é modificada pela adição de solvente orgânico de forma a aumentar a solubilidade de compostos polares [37], [40].

Ao contrário do HPLC, a SFC permite o uso de vazões altas com menor queda de pressão ao longo da coluna, o que resulta em separações mais rápidas e eficientes por unidade de tempo [40]. O CO_2 supercrítico, sendo uma fase móvel ambientalmente compatível, é vantajoso nas separações em larga escala, permitindo reduzir o consumo de solventes orgânicos. Esta técnica possibilita o uso de colunas acopladas

com o mesmo tipo de fase ou combinações de fases, gerando elevado número de pratos e aumentando assim a eficiência da separação [41],[42].

Os primeiros equipamentos de SFC apresentavam algumas desvantagens em relação aos equipamentos de cromatografia gasosa e líquida, como menor sensibilidade e pouca repetibilidade. A modernização da instrumentação solucionou essas limitações, melhorando o desempenho dos equipamentos. Além disso, essa nova geração de equipamentos é compatível com colunas de partículas totalmente porosas sub-2μm e com colunas de partículas superficialmente porosas sub-3μm que melhoraram a eficiência e o poder de separação [37], [43]. Esses avanços elevaram a técnica à chamada Cromatografia com Fluido Supercrítico de Ultra Alta Eficiência (UHPSFC). Atualmente, esta tecnologia está disponível nos equipamentos Waters Acquity UPC^2, Agilent 1260 Infinity Analytical SFC, Shimadzu Nexera UC e Jasco SFC-4000 [37], [43].

A Figura 3.2 mostra um sistema típico de SFC composto por um cilindro pressurizado contendo CO_2, duas bombas de alta pressão para fornecimento da fase móvel e do solvente orgânico, injetor, forno contendo a coluna, detector e restritor. A temperatura na cabeça da bomba de fornecimento de CO_2 é mantida a -4 ℃ por meio de unidade de resfriamento eletrônico ou banho termostático. A separação por SFC emprega detectores usados no HPLC, sendo a pressão controlada por um regulador de contrapressão localizado antes do detector para detecção por espectrometria de massas ou depois para detector do tipo arranjo de diodos (PDA) [35],[40].

McLaren *et al.* (1968) publicaram os resultados do primeiro estudo de separação de carotenoides por SFC em 1968 [40], [45]. Estudos posteriores mostraram que a SFC pode ser uma alternativa ao HPLC na separação de isômeros *cis-trans*. Lesellier *et al.* (1993) estudaram a influência de dezesseis modificadores orgânicos na separação do alfa e betacaroteno, incluindo os isômeros *cis-trans* do betacaroteno (equipamento Jasco e colunas Ultrabase UB 225, 250 x 4,6 mm, 5 μm; e Brownlee Spherical 5 ODS, 250 x 4,6 mm, 5 μm). Os resultados mostraram que a constante dielétrica e o parâmetro de solubilidade dos solventes foram os fatores que mais afetaram a variação da força de eluição dos modificadores orgânicos estudados. Os pesquisadores verificaram também modificação no comportamento da fase estacionária dependendo do tipo de solvente usado e que, consequentemente, afetaram

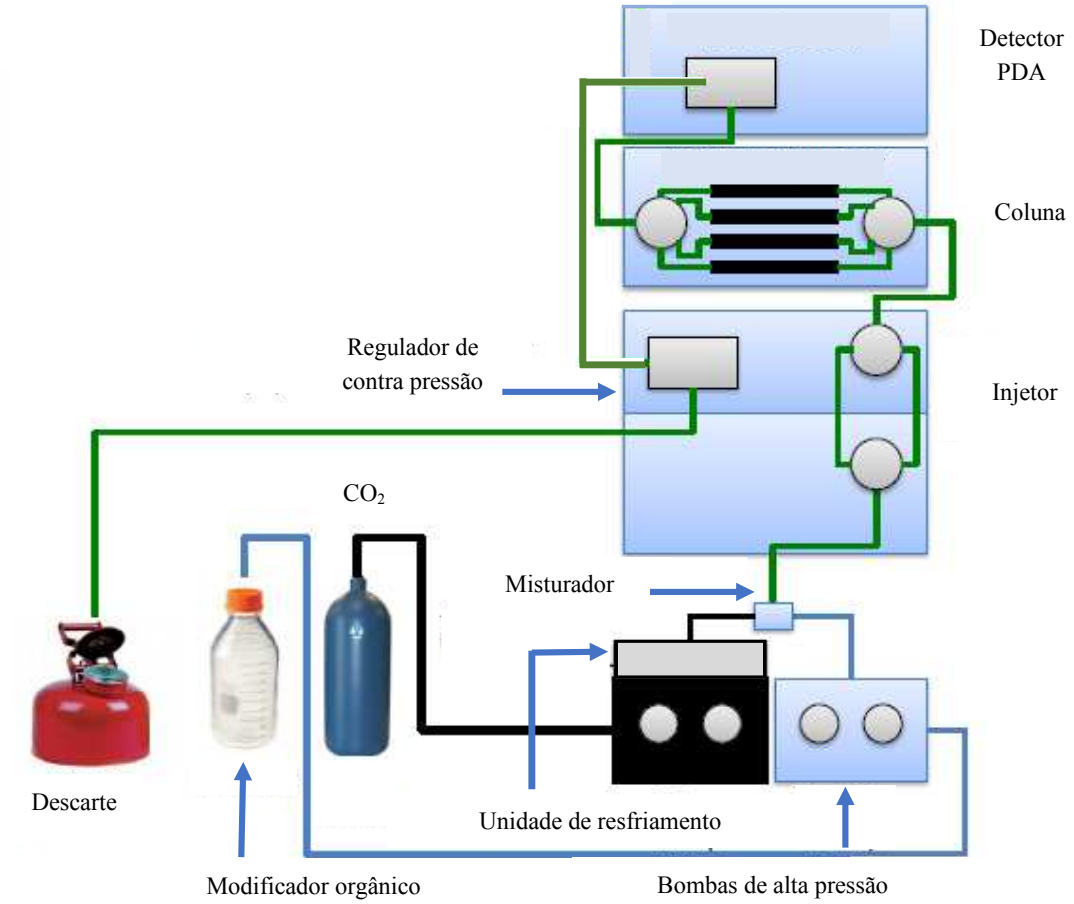

Figura 3.2: Diagrama esquemático do sistema SFC. Adaptado de [44].

o fator de separação dos isômeros cis-trans [19], [40]. Abrahamsson *et al.* (2012) desenvolveram método de separação por SFC para determinação quantitativa de oito carotenoides presentes em uma mistura modelo e no extrato da microalga *Scenedesmus sp.* Os experimentos foram realizados em equipamento Thar Investigator, empregando duas colunas acopladas em série (SunFire C18, 250 x 4,6 mm, 5 μm; Viridis SFC Sílica 2-Etilpiridina, 250 x 4,6 mm, 5 μm). Os resultados mostraram que o fator de separação foi mais afetado pela temperatura do que pela pressão, mesmo alterações de 4 °C na temperatura tiveram grande efeito no fator de separação. Por outro lado, alterações na pressão afetaram substancialmente o fator de retenção. A separação dos oito carotenoides presentes na mistura modelo foi realizada em 10 minutos, enquanto que a separação dos carotenoides presentes no extrato foi obtida em 20 minutos [23], [40].

Carotenoides, vitamina E, esteróis e esqualeno presentes na fibra prensada e no óleo de palma foram determinados por SFC (equipamento Jasco e coluna LiChrosorb 60A Sílica, 250 x 4,6 mm, 5μm). Os carotenoides foram quantificados como betacaroteno totais visto que este é o composto presente em maior quantidade na amostra. No óleo de palma cru (CPO) a quantidade de carotenoides totais foi de 550 $\pm$10 ppm, enquanto que na fibra prensada (PFO) foi de 2400 $\pm$30 ppm [9]. Outro resultado importante foi obtido por Han *et al.* (2006) que quantificaram a coenzima Q10 presente em amostras de CPO e PFO por SFC. Os experimentos foram realizados em equipamento Jasco modelo SUPER-200 com coluna Metaphase RP C18, 250 x 4,6 mm. Metanol foi usado como modificador orgânico. A faixa de concentração da coenzima Q10 determinada com a amostra de CPO foi de 10-80 ppm. Por outro lado, uma faixa de concentração maior foi obtida com a amostra de PFO, 1000-1500 ppm [10].

3.5 Planejamento Experimental

Os estudos mencionados anteriormente mostram a dependência complexa das propriedades da fase móvel e dos parâmetros cromatográficos nas condições de operação. O uso de um planejamento experimental adequado é importante no estudo da influência das condições de operação na separação de compostos bioativos. O planejamento experimental pode ser empregado para avaliar quais fatores (variáveis independentes) têm efeitos relevantes nas respostas (variáveis dependentes). Além disso, o método multivariado permite verificar como o efeito de um fator varia com os níveis de outros fatores, bem como, determinar as interações entre diferentes fatores [46], [47].

A seleção do tipo de planejamento experimental depende do objetivo que se quer alcançar com os experimentos. Quando o objetivo principal é otimizar o sistema, isto é, maximizar ou minimizar determinadas respostas, a metodologia de superfícies de resposta (RSM) associada ao planejamento composto central (CCD) é uma ferramenta eficaz na obtenção das condições ótimas. Esta abordagem permite obter informações relevantes sobre o sistema em estudo com um número menor de experimentos quando comparado com o processo univariado de otimização [47], [48].

A RSM é um conjunto de técnicas estatísticas e matemáticas que geralmente emprega modelos lineares ou quadráticos para descrever o sistema. Esta metodologia tem sido usada com grande sucesso na modelagem de diversos processos industriais e é composta basicamente de três etapas, sendo que a primeira etapa consiste na determinação dos fatores e seus níveis, seguida da seleção do tipo de planejamento experimental, da construção e avaliação da qualidade dos modelos, e finalizando com a obtenção da representação gráfica dos resultados e determinação das condições ótimas [49].

O CCD é um planejamento fatorial de três níveis (ponto central) que permite estimar os efeitos principais, as interações e o grau de curvatura na superfície de resposta [50]. O CCD consiste das seguintes partes: (1) uma parte fatorial (ou cúbica); (2) uma parte axial (ou em estrela) com todas as coordenadas nulas, exceto uma que é igual a $\pm\alpha$; (3) ensaios no ponto central. O número total de experimentos do CCD é $n = 2^x + 2x + m$, onde 2^x é o número de ensaios fatoriais, 2x o número de ensaios axiais e m o número de replicatas no ponto central [47], [51], [52]. A Figura 3.3 ilustra a representação geométrica dos pontos do CCD.

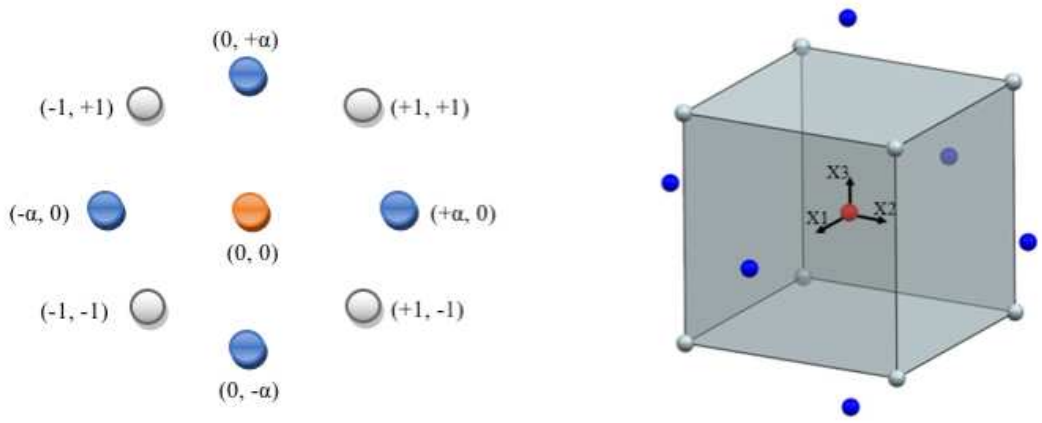

Figura 3.3: Planejamento composto central para três fatores. Os pontos cinzas formam a parte cúbica, os pontos azuis representam a parte axial e em vermelho o ponto central. Adaptado de [52].

As três partes do CCD desempenham papéis importantes e bastante diferentes na construção do modelo. Os ensaios da parte fatorial contribuem para a estimativa dos termos lineares e dos termos de interação entre os fatores. Já os ensaios da parte axial permitem estimar os termos quadráticos. Esta parte do planejamento não contribui com o cálculo dos termos de interação, visto que nesses ensaios os

fatores não estão variando simultaneamente e sim um de cada vez. As repetições no ponto central têm a finalidade de estabilizar a variância da resposta prevista e fornecer uma medida do erro puro, sendo que a estimativa do erro pode ser obtida com poucas repetições, normalmente entre 3 e 5 [47], [50]. As interações são a principal componente de muitos processos de otimização. Sem o uso do planejamento experimental, importantes interações de fatores não são detectadas e a otimização máxima do sistema pode levar mais tempo para ser alcançada [46], [47].

O método mais usado para se avaliar numericamente a qualidade do ajuste do modelo é a análise da variância (ANOVA). Na ANOVA a variação total da resposta é definida como a soma quadrática de dois componentes: a soma quadrática da regressão SQ_R e a soma quadrática dos resíduos SQ_r. A soma da variação total corrigida para a média SQ_T pode ser escrita como a equação 3.1:

$$SQ_T = SQ_R + SQ_r \tag{3.1}$$

onde os termos SQ_T, SQ_R e SQ_r são apresentados com mais detalhe pelas equações 3.2, 3.3 e 3.4, respectivamente.

$$SQ_T = \sum (y_i - \overline{y})^2 \tag{3.2}$$

$$SQ_R = \sum (\hat{y}_i - \overline{y})^2 \tag{3.3}$$

$$SQ_r = \sum (y_i - \hat{y}_i)^2 \tag{3.4}$$

onde $\hat{y}_i$ é o valor previsto, $\overline{y}$ a média global e y_i a resposta individual. Quanto maior a fração descrita pela regressão, melhor será o ajuste do modelo, sendo este ajuste quantificado pela equação 3.5:

$$R^2 = \frac{SQ_R}{SQ_T} = \frac{\sum (\hat{y}_i - \overline{y})^2}{\sum (y_i - \overline{y})^2} \tag{3.5}$$

R^2 é o coeficiente de determinação do modelo. Quanto mais perto de 1 estiver o valor de R^2, melhor terá sido o ajuste do modelo as respostas observadas [47], [50].

Ahmad *et al.* (2010) empregaram o CCD para otimizar a recuperação de carotenoides presentes nos efluentes líquidos da indústria de palma (POME, *palm oil mill effluent*). O estudo teve como objetivo identificar os fatores relevantes para a recuperação desses compostos por cromatografia de adsorção. Foram selecionados como fatores, a temperatura, o volume de hexano e a razão óleo:adsorvente e como respostas a recuperação de carotenoides, a concentração desses compostos e a recuperação de óleo. Em relação aos termos principais, o volume de hexano e a razão óleo:adsorvente foram os termos significativos para os modelos para a recuperação de carotenoides e de óleo. Enquanto que para o modelo da concentração de carotenoides, o termo significativo foi a razão óleo:adsorvente. As condições ótimas para a recuperação de carotenoides foram 40 ℃, 200 mL de solvente e razão 1:4,36 de óleo:adsorvente. Os valores previstos pelos modelos foram 83,36% para a recuperação de carotenoides, 23,628 ppm para a concentração de carotenoides e 100% para a recuperação de óleo. Os resultados experimentais apresentaram concordância com os valores previstos indicando a significância dos modelos gerados [46].

Planejamento fatorial completo foi usado no estudo da separação da mistura racêmica de óxido de trans-estilbeno (TSO) e 1,1'-bi-2-naftol (BINOL) por SFC na escala analítica e preparativa. O estudo avaliou o efeito da pressão, temperatura e porcentagem de metanol na produtividade e nos fatores de retenção e separação. Os resultados demonstraram que os fatores de retenção foram afetados principalmente pela porcentagem de metanol e pela pressão. Por outro lado, a porcentagem de metanol e a temperatura foram os fatores que mais influenciaram o fator de separação. A produtividade na escala preparativa foi mais afetada pela porcentagem de metanol e pela pressão. Os resultados indicaram também que no domínio experimental estudado, altas porcentagens de metanol e altas temperaturas resultaram na maximização da produtividade [53].

Os estudos mencionados anteriormente ilustram o uso da quimiometria na avaliação do efeito de variáveis do processo nas respostas investigadas. O emprego do planejamento experimental possibilitou a identificação das condições ótimas para a recuperação e separação dos compostos de interesse. Um ponto fundamental a ser considerado no desenvolvimento de métodos de separação é a avaliação dos parâmetros cromatográficos [54].

3.6 Parâmetros Cromatográficos

O desenvolvimento de método de separação por SFC requer o estudo da dependência complexa e geralmente não linear das propriedades da fase móvel e dos parâmetros cromatográficos nas condições de operação (pressão, temperatura e porcentagem de modificador orgânico). Considerando que separações cromatográficas resultam da combinação da influência de todas as interações entre as moléculas do soluto com a superfície da fase estacionária e com as moléculas da fase móvel. A interação das moléculas do soluto com a superfície da fase estacionária leva a seletividade do sistema e a separação dos componentes da amostra. No entanto, o transporte das moléculas do soluto pela fase móvel pode ter consequências como redução da seletividade, dependendo de como a velocidade da fase móvel afeta o alargamento da banda e, portanto a eficiência da coluna [39].

Na SFC, a solubilidade pode variar significativamente com a densidade local e, por isso pode ser usada como um indicador confiável do comportamento de retenção. Além da solubilidade, outras duas propriedades físicas da fase móvel afetam diretamente os parâmetros cromatográficos, sua viscosidade e a difusividade do soluto. A viscosidade determina a queda de pressão para uma vazão específica e, consequentemente o perfil da densidade e as condições ao longo da coluna. Por outro lado, a difusividade do soluto controla diretamente o fenômeno de transferência de massa [39].

A discussão acima mostra que a solubilidade é a propriedade da fase móvel que mais influencia a retenção do soluto. Enquanto que a eficiência é controlada principalmente pela difusividade do soluto e em menor grau, pelo fator de retenção dos analitos. Visto que as propriedades da fase móvel na SFC são ajustáveis, o entendimento dos efeitos individuais das três propriedades (solubilidade, difusividade e viscosidade) é importante na investigação da separação por SFC [39].

O sistema SFC é normalmente operado no intervalo de pressão entre 74 e 300 bar (1.073 e 4.351 psi) e na faixa de temperatura entre 280 e 374 K. Nessas condições de temperatura e pressão, o CO_2 é altamente compressível de forma que os parâmetros que afetam a pressão de entrada e, consequentemente a pressão média na coluna, irão afetar a densidade da fase móvel. A Figura 3.4 ilustra como esses parâmetros

influenciam a densidade levando a diferentes valores de fator de retenção e de fator de separação [37], [39].

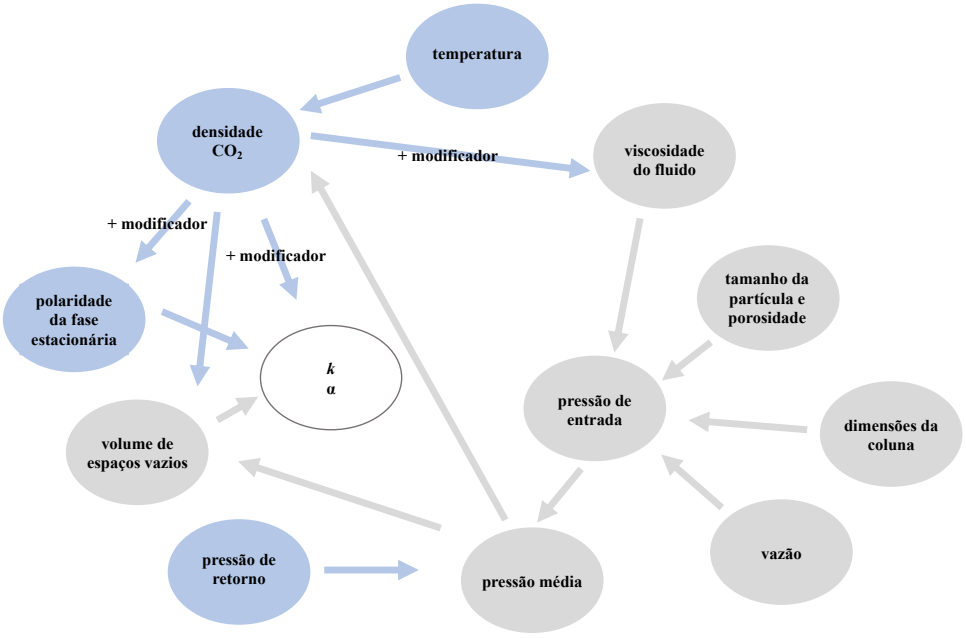

Figura 3.4: Multiplicidade de efeitos que afetam os parâmetros cromatográficos. Setas azuis indicam os efeitos do CO_2 e a indicação + modificador demonstra os efeitos da composição CO_2/solvente. Setas em cinza indicam os efeitos observados com fluidos compressíveis. Adaptado de [37].

Condições subcríticas são empregadas nas separações por SFC devido à redução da variação da viscosidade e da força de eluição do solvente. Além disso, as altas temperaturas necessárias para manter a mistura CO_2/solvente acima da temperatura crítica podem danificar a coluna e degradar os analitos. Temperatura entre 25 e 30 ℃ e pressão de 15 MPa (2.175 psi) são recomendadas [37].

É indicado o emprego de modificador orgânico na análise de amostras contendo analitos com uma grande variedade de polaridade, sendo que essas separações são realizadas por gradiente. Geralmente, uma programação de gradiente iniciando entre 2-5% até 30-40% de modificador orgânico é usada nos experimentos. Solventes polares, como metanol, etanol e acetonitrila são bastante utilizados para aumentar a força de eluição da fase móvel. Metanol altera significativamente as propriedades da fase móvel, sendo considerado a primeira escolha para a eluição de compostos polares. Este solvente é completamente miscível em CO_2 em um amplo intervalo de temperatura e pressão. Outros álcoois, como, por exemplo, etanol e isopropanol

também são bastante utilizados. Acetonitrila causa diferenças significativas na seletividade e na ordem de eluição dos analitos. Além disso, aumento na retenção e assimetria dos picos são observados. Essas alterações são atribuídas à baixa capacidade da acetonitrila para formar ligações de hidrogênio e, consequentemente inativar grupos silanóis residuais. Por esta razão, a composição CO_2/acetonitrila é raramente usada. Entretanto, a combinação com álcoois se mostra vantajosa para o ajuste fino da seletividade. Etanol é uma alternativa aos solventes apresentados anteriormente por ser mais sustentável e causar efeitos mínimos na retenção e seletividade [35], [37].

A seleção do modificador orgânico é uma etapa importante no desenvolvimento do método de separação, visto que este afeta os parâmetros cromatográficos e sua seleção deve considerar a polaridade e a estrutura dos compostos investigados. Geralmente solventes apolares, como o hexano são selecionados para análise de carotenoides apolares ou esterificados, enquanto que solventes polares como o etanol são mais apropriados para análise de carotenoides polares [20]. Licopeno, luteína e beta-caroteno têm pouca solubilidade em metanol e apresentam picos alargados quando as amostras são preparadas em isopropanol [55]. A variação da porcentagem do modificador orgânico permite avaliar possíveis alterações no comportamento de retenção [56]. Além disso, adição de modificador orgânico de 5 a 50% aumenta a solubilidade de compostos polares. Por outro lado, os modificadores podem influenciar a qualidade da separação de diversas formas, como, por exemplo, alterar a densidade e o poder de solvatação da fase móvel, desativar sítios ativos da fase estacionária inibindo a adsorção, sendo que o modificador adsorvido pode aumentar o volume da mesma levando a uma alteração da razão entre as fases e, consequentemente, podendo alterar o fator de retenção [57].

No desenvolvimento do método de separação a correta seleção da fase estacionária, do modificador orgânico, bem como das condições de operação levará a uma boa separação dos analitos de forma que estes possam ser identificados e quantificados. O método de separação pode ser avaliado pela análise de alguns parâmetros cromatográficos, como por exemplo, o fator de retenção, fator de separação, resolução e eficiência [54].

O fator de retenção, k, é determinado pela razão entre os tempos que o analito permanece na fase estacionária e na fase móvel. Este parâmetro representa a afinidade do analito pela fase estacionária e é calculado pela equação 3.6, onde o tempo de retenção, t_R, é o tempo que o analito permanece no sistema cromatográfico e t_M o tempo gasto pela fase móvel para percorrer a coluna [54], [58]. As condições cromatográficas são normalmente definidas para se obter fatores de retenção entre 0,5 e 20 [59].

$$k = \frac{t_R - t_M}{t_M} \tag{3.6}$$

O fator de separação, α, é a razão entre dois picos adjacentes e é expresso pela equação 3.7 [54], [58]. A seletividade depende de vários fatores, entre os quais, a composição da fase estacionária, a densidade e a composição da fase móvel [37].

$$\alpha = \frac{k_2}{k_1} \tag{3.7}$$

Quanto maior o valor do fator de separação for do valor unitário, maior a distância entre os máximos de picos adjacentes. No entanto, os picos podem estar parcialmente coeluídos devido à espessura das suas bases. De forma que, um terceiro parâmetro é usado para analisar a resolução de picos adjacentes e expresso pela equação 3.8, onde w_b representa a largura do pico em sua base [54]. Resolução maior que 1 indica que os picos não estão sobrepostos podendo ser analisados para identificação e quantificação [54].

$$R_s = \frac{t_{R2} - t_{R1}}{(w_{b2} - w_{b1})/2} = \frac{2(t_{R2} - t_{R1})}{w_{b2} - w_{b1}} \tag{3.8}$$

A eficiência de uma coluna cromatográfica é medida pelo número de pratos gerados, isto é, o número de estágios de equilíbrio presentes no interior da coluna. Quanto maior o número de estágios de equilíbrio, maior será a eficiência da coluna e, portanto melhor a separação. O número de pratos é obtido pela equação 3.9 [54], [58].

$$N = 16(\frac{t_R}{w_b})^2 \tag{3.9}$$

O número de pratos pode ser afetado por vários fatores como por exemplo, condição de operação, tipo da amostra e comprimento da coluna. Por esta razão, outra forma de comparar a eficiência de colunas cromatográficas é a determinação da altura equivalente a um prato, ou seja, a determinação da altura dos estágios de equilíbrio que é expressa pela equação 3.10, onde L é o comprimento da coluna cromatográfica [54], [58].

$$H = \frac{L}{N} \tag{3.10}$$

3.7 Espectroscopia no Infravermelho com Transformada de Fourier

A espectroscopia é o estudo da interação da radiação eletromagnética com a matéria. Esta interação pode ocorrer por três processos distintos: absorção, emissão e espalhamento da radiação. A espectroscopia de absorção no infravermelho estuda a transição das vibrações normais moleculares. Estas vibrações podem ser do tipo estiramento de ligação, deformação angular e torção. A vibração normal de estiramento (*stretching*) pode ser simétrica ou assimétrica, enquanto que a deformação angular (*bending*) pode ocorrer no plano, como do tipo tesoura (*scissoring*) e rotação (*rocking*), e fora do plano, como as deformações do tipo balanço (*wagging*) e torção (*twisting*) [60].

A espectroscopia no infravermelho pode ser dividida em três regiões: infravermelho longínquo (FIR), de 400-10 cm^{-1}, região que possui baixa energia e está relacionada as transições rotacionais das moléculas. A região FIR tem aplicação limitada na análise de alimentos [61], [62], [63]. Infravermelho médio (MIR), de 4000-400 cm^{-1}, onde se localizam as frequências vibracionais fundamentais das moléculas, e infravermelho próximo (NIR), de 14000-4000 cm^{-1}, que correspondem as transições vibracionais entre o nível de energia fundamental e os níveis de energia de ordem superior [61], [62].

Informação química pode ser extraída do espectro infravermelho pela análise da posição das bandas de absorção, da sua intensidade e formato [61], [64]. As bandas de absorção na região do MIR são geralmente mais intensas do que as bandas observadas na região do NIR. Além disso, os espectros na região do NIR se originam

principalmente da sobreposição ou combinação dos modos e sobretons, resultando em espectros mais complexos para serem interpretados do que os espectros obtidos na região do MIR [61].

O primeiro espectrômetro foi desenvolvido no final de 1940, e as primeiras aplicações foram reportadas na década seguinte. No entanto, foi somente em 1960 que a técnica foi empregada na análise de alimentos. Os avanços mais significativos na técnica foram observados com a introdução de espectrômetros com transformada de Fourier (FTIR) que apresentaram vantagens como detecção simultânea dos comprimentos de onda, maior razão sinal/ruído, melhor precisão e exatidão [60], [61] [63].

Os espectrômetros FTIR consistem de fonte de radiação, interferômetro, compartimento de amostra, detector e componentes ópticos (espelhos e divisor de feixe). O diagrama esquemático de um espectrômetro FTIR é ilustrado na Figura 3.5. A fonte de radiação eletromagnética é geralmente um sólido inerte aquecido eletricamente entre 1000 e 1800 ℃. Na região do FIR, a fonte de radiação mais usada é o vapor de mercúrio, enquanto que para a região do MIR, o Globar (CSi) refrigerado a água, a espiral de níquel-cromo ou o bastão de cerâmica, ambos refrigerados a ar, são utilizados. Na região NIR a lâmpada de tungstênio refrigerada a água ou ar é empregada [60], [61], [65].

A unidade interferométrica divide a radiação eletromagnética em dois feixes (A e B), cada um correspondendo a 50% do feixe original. O feixe A é direcionado para um espelho plano fixo, sendo refletido de volta para o divisor de feixe, onde parte é refletida para a fonte e parte para o detector. O feixe B é direcionado para um espelho plano móvel e também é refletido de volta para o divisor de feixe, onde parte é refletida para a fonte e parte para o detector. Os feixes são recombinados, gerando interferências construtivas, quando os dois feixes estão em fase, ou interferências destrutivas, se os dois feixes estiverem fora de fase. A radiação resultante passa pelo compartimento de amostra e é direcionada por um espelho côncavo para o detector. O interferograma obtido é convertido em espectro através da transformada de Fourier [60], [61], [62], [65]. O divisor de feixe pode ser de filme de Mylar (politereftalato de etileno-PET de diferente espessuras) para espectrômetros FIR, de KBr para espectrômetros MIR e de CaF_2 ou quartzo para espectrômetros NIR [60].

O detector do espectrômetro varia de acordo com as regiões do infravermelho. Nos espectrômetros FIR são usados o bolômetro ou o detector DTGS-polietileno (*deuterated triglycine sulfate* com janela de polietileno). Os detectores DTGS com janela de KBr, MCT (*mercury cadmium telluride*, HgCdTe) resfriado à temperatura do nitrogênio líquido ou fotoacústico são utilizados nos espectrômetros MIR, enquanto que detectores de Si, InSb ou PbSe são usados em espectrômetros NIR [60], [61], [65].

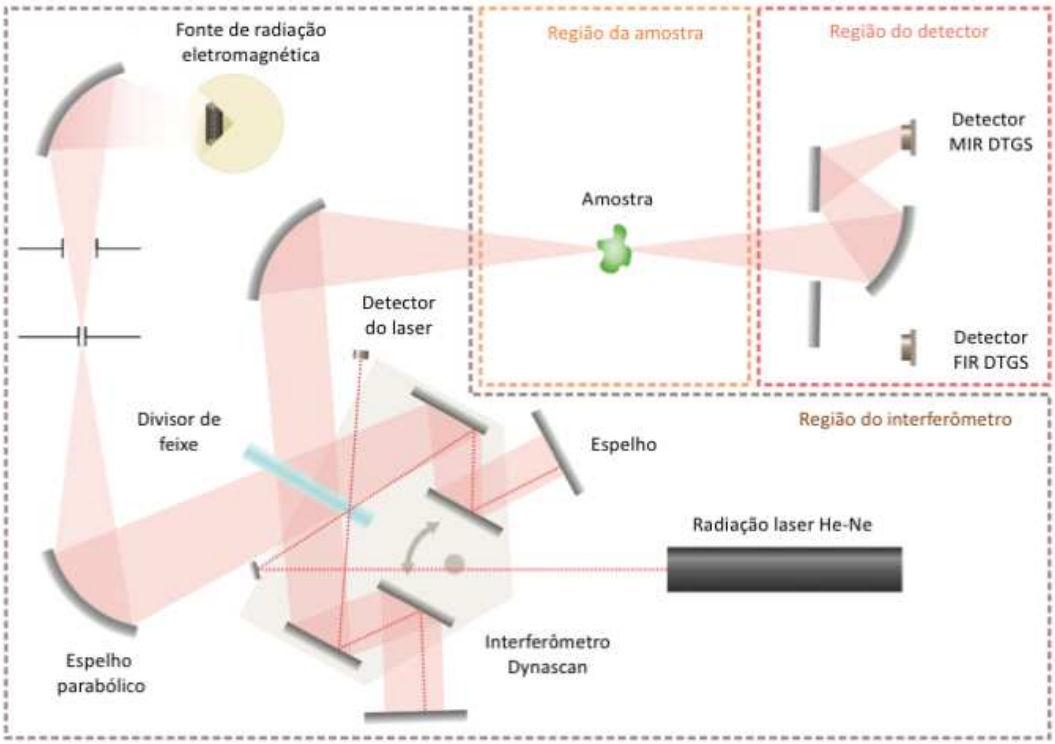

Figura 3.5: Diagrama esquemático do espectrômetro FTIR. Adaptado de [66].

Uma das vantagens da espectroscopia no infravermelho é sua versatilidade para análise de amostras sólidas, líquidas ou gasosas [61], [67]. O uso do acessório de refletância total atenuada (ATR) elimina algumas limitações relacionadas à análise de amostras sólidas e líquidas como o preparo de amostra e a reprodutibilidade espectral [67], [68]. O acessório é montado no compartimento de amostra, cujo elemento principal é o cristal. Este deve ser transparente à radiação infravermelho e ter alto índice de refração [67]. Cristais de diamante, ZnSe, silício, AMTIR, KRS-5 e germânio são usados [62], [64]. O acessório de ATR possui também dois espelhos planos, onde um espelho direciona o feixe de radiação incidente para o cristal e o

outro orienta o feixe refletido do cristal para o detector [67]. A Figura 3.6 ilustra o acessório ATR.

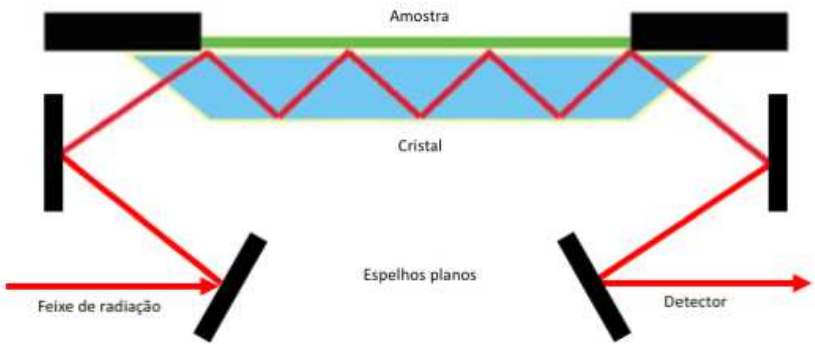

Figura 3.6: Acessório ATR. Adaptado de [60], [67].

Na espectroscopia por ATR, o feixe de radiação incide no cristal e sofre o fenômeno de reflexão completa. No ponto de reflexão, o feixe penetra uma pequena profundidade (0,5-5 μ) na superfície da amostra que está em contato com o cristal, se amostra absorver parte da radiação, esta fração será detectada. A radiação que penetra a amostra e é atenuada é chamada onda evanescente, e o termo refletância total atenuada advém desse fenômeno [60], [62], [64], [67].

No espectro infravermelho de sistemas de um componente ou misturas simples, a posição das bandas pode ser facilmente relacionada à estrutura molecular do componente ou dos componentes da mistura, enquanto que a intensidade das mesmas é relacionada à concentração do componente na amostra pela lei de Lambert-Beer [60], [61]. A análise de sistemas complexos resulta em espectros com sobreposição de bandas que demandam ferramentas estatísticas e matemáticas mais avançadas para extrair informação dos dados espectrais [61].

Métodos multivariados são empregados na análise de dados espectrais para reduzir a dimensão da matriz de dados e extrair informação relevante sobre a amostra [61]. O conjunto de dados pode ser inicialmente investigados por métodos exploratórios. Esses métodos não requerem o conhecimento prévio das propriedades da amostra, como por exemplo, análise de agrupamentos por métodos hierárquicos (HCA) e análise de componentes principais (PCA) [68], [69]. Posteriormente, modelos quantitativos podem ser construídos utilizando métodos de regressão por componentes principais (PCR) e mínimos quadrados parciais (PLS) [61], [69]. Os modelos

de regressão estabelecem relação entre a propriedade quantitativa da amostra e um conjunto de variáveis independentes que é usado para prever a propriedade de interesse em amostras desconhecidas [61]. A construção do modelo de regressão consiste das seguintes etapas: pré-tratamento dos dados, seleção do conjunto de calibração, validação e teste, seleção das variáveis, construção e validação do modelo [61].

O pré-tratamento de dados é usado para remover interferências contidas no espectro de forma a aumentar a linearidade entre as variáveis antes da modelagem dos dados [61], [70]. Centralização, normalização, correção da linha de base e aplicação de derivadas são alguns pré-tratamentos utilizados. Outras técnicas de pré-tratamento, como suavização e deconvolução auxiliam e melhoram a interpretação dos dados espectrais [61], [70]. A aplicação de pré-tratamento deve ser avaliada para preservar a informação espectral da amostra [60].

O conjunto de calibração deve conter amostras que contemplam uma ampla variabilidade da propriedade de interesse. O mesmo deve ser observado para os conjuntos de validação e teste. O conjunto de calibração, validação e teste são usados na construção do modelo de regressão, validação e previsão, respectivamente [61]. Para o tratamento de dados pode-se utilizar o espectro inteiro ou realizar seleção de variáveis empregando apenas regiões que contém informação relevante para a regressão. O espectro completo é mais usado porque previne o sobre-ajuste, visto que a quantidade de dados é reduzida sem a eliminação de informação relevante [61], [71].

O modelo de regressão é validado para verificar sua capacidade preditiva e reprodutibilidade. A validação pode ser realizada com um conjunto independente de amostras (validação externa) ou com o conjunto de treinamento (validação cruzada) [61]. Na validação cruzada, as amostras do conjunto de calibração são usadas no conjunto de treinamento.

No procedimento de validação cruzada, um modelo de regressão é construído com parte das amostras, e usado para prever as amostras restantes. Na sequência, um novo modelo é construído com um novo conjunto de amostras e usado para estimar o valor das amostras não usadas na construção do modelo. Este procedimento é realizado até que todas as amostras são previstas [72], [73]. A qualidade do ajuste do modelo é avaliada pelo coeficiente de determinação R^2 e as incertezas nas estimativas

da propriedade de interesse é avaliada pela raiz quadrada do erro médio quadrático (RMSE) que mede a diferença entre os valores previstos e os obtidos pelo método de referência [61], [71].

Diversos estudos têm sido reportados na literatura demonstrando a viabilidade do emprego da espectroscopia FTIR associada a métodos quimiométricos para análise do óleo de palma e seus derivados [71], [74], [75], [76], [77], [78]. Nokkaew *et al.* (2019) determinaram a concentração de carotenoides e o índice de deterioração de branqueabilidade (DOBI, *Deterioration Of Bleachability Index*) do óleo de palma por espectroscopia Raman e NIR. Os autores avaliaram procedimentos de pré-tratamento dos dados, sendo que os melhores modelos foram obtidos com a aplicação da primeira derivada. A qualidade do ajuste do modelo de regressão por PLS para a concentração de carotenoides foi determinada pelo coeficiente de correlação (R) 0,71, coeficiente de determinação (R^2) 0,50 e raiz quadrada do erro médio quadrático da previsão (RMSEP) 86,70 ppm. Os autores explicaram que a limitação do modelo foi devido à baixa concentração dos carotenoides no óleo de palma, e a necessidade de um conjunto de amostras mais representativo para a construção de modelos mais precisos [74].

Che Man *et al.* (2005) determinaram α-tocoferol em oleína de palma desodorizada, branqueada e refinada por espectroscopia FTIR. O modelo para quantificação foi construído utilizando o método de regressão PLS. Apenas a região de 3100-2750 cm^{-1} do espectro infravermelho foi empregada na construção do modelo. Os resultados obtidos apresentaram concordância com os resultados do método de referência (HPLC). Os autores destacaram alguns vantagens do uso da técnica como menor tempo de análise e menor consumo de solventes orgânicos [76]. Moh *et al.* (1999) avaliaram a espectroscopia FTIR e NIR associadas ao método de regressão PLS para determinar a concentração do betacaroteno no óleo de palma. Os resultados foram comparados aos resultados da espectroscopia UV-Vis usada como método de referência. Os autores observaram variação de 5% nos valores das concentrações previstas pelas duas técnicas quando comparados aos valores de referência [11]. Os estudos mencionados ilustram o potencial da espectroscopia FTIR associada a métodos quimiométricos para análise do óleo de palma.

4 | Study of the effect of the operating parameters on the separation of bioactive compounds of palm oil by ultra-high performance supercritical fluid chromatography using a design of experiments approach

In this study, an analytical method based on Design of Experiments and response surface methodology for the separation of lycopene, beta-carotene, coenzyme Q10 and lutein was developed by ultra-high performance supercritical fluid chromatography technique. A Central Composite Design was used to evaluate the influence of temperature, pressure and ethanol percentage on the retention and separation factors of these compounds. In the designed experiments, the temperature was varied between 25 and 50 ℃, the pressure within the interval of 1500 and 2200 psi and the ethanol percentage between 15 and 24 (v/v) %. Each variable was tested at 3 levels and 5 replicated central points were added. It was found for the studied system that the ethanol percentage and pressure were the parameters that most influenced the retention factors whereas the ethanol percentage, pressure and temperature affected the separation factors. Quadratic models were necessary to describe the retention and separation of these compounds. Furthermore, it was observed interactions among the factors, justifying the DOE approach used in this work. Considering the retention and separation factors, the selected operating conditions for further experiments were: 15.5% of ethanol at 40 ℃ and 1500 psi.

4.1 Introduction

Carotenoids form an important class of natural pigments that are found in microorganisms, plants and animals. They are fat-soluble compounds and play an important role in physiological and biological processes. In addition to the provitamin A activity of some carotenoids, these compounds have been associated with a wide number of health benefits. Several studies have shown that their antioxidant capacity help prevent cancer, diabetes and cardiovascular diseases [20], [79]. Besides their medicinal use, the importance of carotenoids has also increased due to their use in the food, cosmetic and feed industries [46].

Coenzyme Q10 (CoQ10, ubiquinone-10) is a fat-soluble, vitamin-like nutrient that is involved in the mitochondrial respiratory chain. Like carotenoids, coenzyme Q10 is also a powerful antioxidant. Its antioxidant capacity is ten times greater than vitamin E. Many therapeutic values of coenzyme Q10 have been reported, such as prevention of lipid peroxidation and oxidative damage of haemoglobin. Furthermore, coenzyme Q10 shows promising results when administered to hypertensive patients [17], [28].

Supercritical fluid chromatography (SFC) has been intensively studied due to its versatility in chiral and achiral separations. The technique is suitable to the analysis of thermally unstable compounds like carotenoids and the separation kinetics is faster than in High Performance Liquid Chromatography (HPLC) due to the lower viscosity of the mobile phase [17]. The fluids employed as mobile phase in SFC are environmentally friendly, nontoxic and non-flammable. Carbon dioxide (CO_2) is the most used compound for several reasons: it is not expensive, has good miscibility with most polar and non-polar organic solvents and is easily available with analytical quality. Furthermore, its critical properties (P_c = 73.773 bar, T_c = 304.13 K) are easily attainable [8], [39], [80]. SFC experiments were initially performed with pure CO_2 as the mobile phase. Nowadays, a mixture of CO_2 and organic modifier is very often used in order to increase the solubility of polar compounds and allow their elution [37], [38], [40]. Recently, there has been a revival of interest in the SFC technique due to the introduction of new state-of-the-art instrumentation, in which the pressure control system was improved, proving superior repeatability of the results. This fact, together with the possibility of using sub-2 μm particle stationary

phases gave rise to the new generation of SFC, named Ultra-High Performance Supercritical Fluid Chromatography (UHPSFC).

In SFC and UHPSFC method development, the stationary phase, mobile phase composition (the type and percentage of the organic modifier) and operating conditions (pressure and temperature) should be evaluated. Since CO_2 is a non-polar compound, the addition of organic modifier (for example methanol, ethanol, acetonitrile, etc.) is necessary to improve the solubility of the analytes in the mobile phase and therefore extend the domain for chromatographic applications. Studies have demonstrated that retention of polar solutes is more sensitive to the percentage of the organic modifier, which is the most important parameter after the selection of the stationary phase [37], [53].

Temperature and pressure also play an important role in SFC and UHPSFC, since they control the density of the fluid. Changes in the mobile phase density induce variable retention times which can affect the repeatability and reproducibility of the chromatographic separation. Additionally, temperature also affects the vapour pressure of the solute and influences the solubility parameters of both solute and supercritical fluid. Unlike in liquid chromatography, when temperature is increased (at a constant pressure) retention increases due to the reduction of the mobile phase density. On the other hand, when pressure is increased, it is observed a reduction in retention due to increase density of the supercritical fluid. Since temperature, pressure and mobile phase composition influence the chromatographic parameters, these parameters should be evaluated on a method development [35], [37].

Design of Experiments (DOE) is a multivariate effective tool for optimizing systems that are subject to the influence of several experimental parameters and their interactions. This methodology allows quantifying the relationship between the input parameters (operating conditions) and the desired responses through the estimation of linear and quadratic effects as well as interactions among them, with a small number of experiments. By using a Response Surface Methodology (RSM), mathematical models are fit by the Least Squares method and the 3D response surface plots and contour plots obtained provide information about the system and facilitate the understanding of the relationships among variables and responses, supporting the decision-making [46], [81], [82].

The objective of this study was to identify the key factors that affect the separation of lycopene, beta-carotene, coenzyme Q10 and lutein by ultra-high performance supercritical fluid chromatography and determine the chromatographic operating conditions that could lead to adequate selectivity and retention by using response surface methodology. Parts of this work have been presented at the XXI Brazilian Congress of Chemical Engineering (COBEQ 2016) in Fortaleza, Brazil [16].

4.2 Materials and Methods

4.2.1 Chemicals and Reagents

Ethanol and methyl tert-butyl ether (MTBE) used were of HPLC-grade (Panreac). Ultrapure CO_2 (99.99%) was provided by White Martins. Analytical standards of lycopene, beta-carotene, coenzyme Q10 and lutein were acquired from Sigma-Aldrich. A mixture of the standards was prepared in MTBE in a concentration of 0.2 mg/mL and filtered through a 0.45 μm syringe filter prior injection.

4.2.2 Chromatographic Conditions

All experiments were performed with a Waters Acquity UPC^2 system. The column was an Acquity UPC^2 HSS C18 SB 150 x 3.0 mm column with particle diameter of 1.8 μm. CO_2 and ethanol were used as mobile phase. The sample manager temperature was 5 ℃, flow rate was 1.5 mL/min and injection volume was 1 μL. All injections were carried out in duplicate and the average was calculated. After scanning in the 210-600 nm range, analytes were detected at 275 nm.

The experimental domain was defined taking into account instrumental constrains such as maximum pressure of the system and reasonable analysis time. Considering that the maximum allowed temperature for the HSS C18 SB column is 60 ℃, a temperature range of 25-50 ℃ was selected. The ethanol percentage range (15–24 v/v %) was chosen based on preliminary experiments. The pressure range of 1500-2200 psi was evaluated to allow the use of ethanol range selected previously. The maximum analysis time was set at 10 min to enable the separation to be performed at a reasonable time.

4.2.3 Experimental Design

A Central Composite Design (CCD) was used to design a series of experiments to provide data to determine the relationship between the three operating parameters, pressure, temperature and ethanol percentage and the responses, retention factors (k) of each analyte and separation factors ($\alpha = k_n/k_{n-1}$), especially for the critical pair (beta-carotene and coenzyme Q10). The CCD consisted of 19 experiments, run in a randomized order to estimate the model coefficients and their corresponding errors. More specifically, 8 factorial runs (2^x, x is the number of studied variables), 6 axial runs (2x, on axes at a distance of $\pm\alpha$ from the center) and 5 replicates of the central point were carried out. The range and levels of experimental variables investigated are presented in Table 4.1.

Table 4.1: Coded and actual levels of the independent variables for UHPSFC experiments.

Symbol	**Variables**	**Coded Levels**		
		-1	**0**	**+1**
A	Pressure (psi)	1500	1850	2200
B	Temperature (°C)	25	37.5	50
C	Ethanol percentage (%)	15	19.5	24

Statistical analyzes were carried out by Design Expert software version 9.0 (Stat-Ease). All retention factors were transformed logarithmically to ln k. The second order model was obtained as follows:

$$y = \beta_0 + \sum_{j=1}^{k} \beta_j X_j + \sum \sum_{i<j} \beta_{ij} X_i X_j + \sum_{j=1}^{k} \beta_{jj} X_j^2 \tag{4.1}$$

where β_0, β_j, β_{ij} and β_{jj} are regression coefficients for intercept, linear, interaction and quadratic coefficients respectively and X_i and X_j are coded independent variables [49]. The regression models for each response was assessed by analysis of variance (ANOVA), diagnostics graphs (residuals and predicted vs actual values) and coefficient of determination (R^2). The contour plots were generated by holding one of the independent variable at constant value and changing the levels of the other two variables.

4.3 Results and Discussion

The first step of the method development consisted in the selection of a suitable stationary phase. Acquity UPC^2 HSS C18 SB column was selected due to its non-polar character, which ensures the proper interaction of the non-polar bioactive compounds with the hydrophobic particle surface. This stationary phase has been already described for the separation of the two geometrical isomers, lycopene and beta-carotene using UHPSFC technique [55].

Besides the selection of the stationary phase, various parameters potentially affect the UHPSFC separation process, and therefore the optimization of the experimental conditions represents a critical step in the method development. The chromatograms of three selected runs are shown in Figure 4.1 as an example. In the chromatogram shown in Figure 4.1a, 2200 psi, 25 ℃, 24% of ethanol, no separation between beta-carotene and coenzyme Q10 was observed. Changes in the operating conditions, decreasing the ethanol percentage to 15%, keeping constant temperature and pressure, provided a better resolution between beta-carotene and coenzyme Q10 (Figure 4.1b). Decreasing the pressure to 1500 psi (Figure 4.1c) has improved even more the separation of beta-carotene and coenzyme Q10, providing the baseline resolution for the four compounds. In this example, temperature change was not considered; however, the three variables temperature, pressure and ethanol percentage are closely related since they modify the fluid density and therefore the retention of the compounds. For this reason, they were studied together using a DOE approach.

It should be noted that the range of the organic modifier to be used in the DOE study was selected based on previous retention experiments of the four compounds in C18 stationary phase (retention curves of the four compounds are shown in Figure 4.7 in Supplementary Material). Suitable retention factors ($2 < k < 10$) for all compounds was achieved within the range of 15 to 24% of ethanol. The use of lower amounts of organic modifier could be beneficial for the separation of beta-carotene and coenzyme Q10. However, unacceptable retention of lutein, the highly retained compound, would be achieved. Gradient elution was not considered because this method is intended to be scaled-up in the next steps of the project. Therefore, the approach used was to simultaneously evaluate pressure, temperature and ethanol

percentage in the range of 15-24% in order to accomplish the best possible separation in isocractic mode.

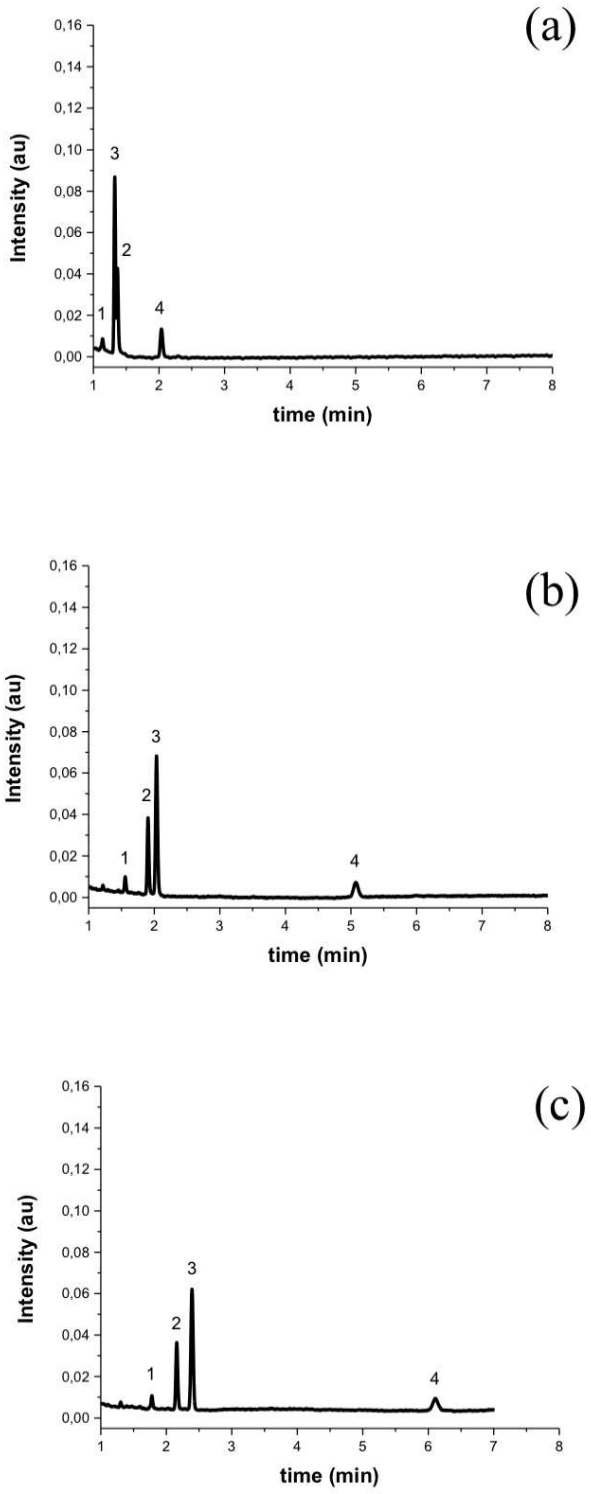

Figure 4.1: Chromatograms of the separation: 1. Lycopene, 2. Beta-carotene, 3. Coenzyme Q10, 4. Lutein. Experimental conditions: (a) 24% of ethanol, temperature 25 ℃ and pressure 2200 psi; (b) 15% of ethanol, temperature 25 ℃ and pressure 2200 psi; (c) 15% of ethanol, temperature 25 ℃ and pressure 1500 psi.

4.3.1 Experimental Design and Data Analysis

The experimental design points and all responses experimentally obtained are shown in Table 4.4 and the corresponding chromatograms are shown in Figures 4.8, 4.9 and 4.10 in Supplementary Material.

Retention factors

ANOVA showed that the quadratic model was suitable to describe the retention of the four analytes where Prob < 0.05 indicates that the model coefficients are significant in a 95% confidence level (Table 4.2). The F-values of regression significance were 1205.66, 123.54, 1017.81 and 5016.07 for lycopene, beta-carotene, coenzyme Q10 and lutein models, respectively, indicating that the retention strongly depends on the operational conditions within the studied range of the factors. The results indicated that all linear, quadratic and interaction coefficients were significant for lycopene, coenzyme Q10 and lutein. On the other hand, for the beta-carotene model, only the main factors, ethanol percentage (C_E, A), temperature (B) and pressure (C); the interaction terms AB and BC were significant. The other model coefficients were not significant which included the interaction term AC and the second-order effects A^2, B^2 and C^2. The results showed that the interaction coefficients were significant for the four models, except the interaction term AC for the beta-carotene model. It is interesting to point out that the interaction among factors would have been missed if the approach of varying one factor at a time had been used. This highlights the importance of using a multivariate approach based on Design of Experiments.

The F-values of lack of fit were 2.45, 10.73, 4.73 and 4.11 for lycopene, beta-carotene, coenzyme Q10 and lutein models, respectively, indicating that only for the beta-carotene model a slight lack of fit was observed (the tabulated value of F 5.4, 95% is 6.26). However this lack of fit was not worrisome, considering the analysis of diagnostics graphs and R^2, as will be described below.

Besides ANOVA, the fit of the models was evaluated by diagnostics graphs: predicted vs actual values and residual analysis. If the model is adequate to represent the experimental data, the predicted values should be in good agreement with the actual values, indicating small error of prediction. The residuals should show no

Table 4.2: ANOVA for the quadratic model for the retention factors of lycopene, beta-carotene, coenzyme Q10 and lutein.

Source	Sums of squares	DF	Mean square	F value	Prob> F
Lycopene					
Model	0.97	9	0.11	1205.66	< 0.0001
A-C$_E$	0.71	1	0.71	7902.19	< 0.0001
B-T	6.2×10^{-4}	1	6.2×10^{-4}	6.90	0.0275
C-P	0.18	1	0.18	1968.25	< 0.0001
AB	0.02	1	0.02	202.27	< 0.0001
AC	3.7×10^{-3}	1	3.7×10^{-3}	40.96	0.0001
BC	0.03	1	0.03	286.52	< 0.0001
A^2	3.8×10^{-3}	1	3.8×10^{-3}	41.90	0.0001
B^2	6.3×10^{-3}	1	6.3×10^{-3}	69.83	< 0.0001
C^2	1.4×10^{-3}	1	1.4×10^{-3}	15.13	0.0037
Beta-carotene					
Model	0.86	9	0.10	123.54	< 0.0001
A-C$_E$	0.65	1	0.65	844.98	< 0.0001
B-T	5.6×10^{-3}	1	5.6×10^{-3}	7.24	0.0247
C-P	0.16	1	0.16	204.94	< 0.0001
AB	5.2×10^{-3}	1	5.6×10^{-3}	6.69	0.0294
AC	7.4×10^{-4}	1	7.4×10^{-4}	0.96	0.3536
BC	0.02	1	0.02	32.39	0.0003
A^2	2.1×10^{-4}	1	2.1×10^{-4}	0.27	0.6187
B^2	2.7×10^{-3}	1	2.7×10^{-3}	3.53	0.0928
C^2	7.0×10^{-4}	1	7.0×10^{-4}	0.91	0.3653
Coenzyme Q10					
Model	1.44	9	0.16	1017.81	< 0.0001
A-C$_E$	1.11	1	1.11	7108.26	< 0.0001
B-T	8.8×10^{-4}	1	8.8×10^{-4}	5.61	0.0420
C-P	0.21	1	0.21	1351.94	< 0.0001
AB	0.02	1	0.02	144.47	< 0.0001
AC	4.9×10^{-3}	1	4.9×10^{-3}	31.47	0.0003
BC	0.03	1	0.03	190.43	< 0.0001
A^2	6.1×10^{-3}	1	6.1×10^{-3}	38.96	0.0002
B^2	7.6×10^{-3}	1	7.6×10^{-3}	48.21	< 0.0001
C^2	1.3×10^{-3}	1	1.3×10^{-3}	8.25	0.0184
Lutein					
Model	3.46	9	0.38	5016.07	< 0.0001
A-C$_E$	3.17	1	3.17	41281.33	< 0.0001
B-T	3.1×10^{-3}	1	3.1×10^{-3}	40.15	0.0001
C-P	0.19	1	0.19	2465.30	< 0.0001
AB	0.01	1	0.01	170.59	< 0.0001
AC	3.2×10^{-3}	1	3.2×10^{-3}	41.55	0.0001
BC	0.02	1	0.02	289.25	< 0.0001
A^2	0.01	1	0.01	160.53	< 0.0001
B^2	7.1×10^{-3}	1	7.1×10^{-3}	92.30	< 0.0001
C^2	9.1×10^{-4}	1	9.1×10^{-4}	11.87	0.0073

tendency over time (residuals vs run) or according to the levels of the factors (residuals vs predicted values). The last graph is an indicative of heteroscedasticity, i.e., prediction is not homogeneous for all levels of the factors. The diagnostics graphs for the beta-carotene regression model are shown in Figure 4.11 in Supplementary Material. As can be seen, there was no indicative of lack of fit in these graphs, therefore the model could be safely used for prediction. The other models were evaluated in the same way.

The coefficients of determination (R^2) obtained for lycopene, beta-carotene, coenzyme Q10 and lutein models were 0.9992, 0.9920, 0.9990 and 0.9998, respectively. The R^2 values showed that only 0.08, 0.8, 0.1 and 0.02% of the total variation were not explained by the respective model. The adjusted coefficients of determination (adjusted R^2) were 0.9983, 0.9839, 0.9980 and 0.9996 for lycopene, beta-carotene, coenzyme Q10 and lutein models, respectively. There was only a small difference between the R^2 and the adjusted R^2 values indicating that the experimental data were well described by the regression models.

The graphical representation of the coefficients for the regression models of the retention factor is presented in Figure 4.2. The main effect of ethanol percentage (C_E, A) was the most significant parameter for the retention of all analytes, with negative effect, i.e., a decrease in ethanol percentage in the mobile phase lead to an increase of the retention factor.

Because the temperature range was rather small due to stationary phase limitations and the low thermal stability of the compounds, temperature (B) had a minor effect on the retention factors. It is interesting to notice that the coefficients of the models for lycopene and beta-carotene were negative whereas the coefficients for coenzyme Q10 and lutein models were positive. The interaction term BC was significant for all models and the second-order effect B^2 was significant for all models, except beta-carotene, as already mentioned. Pressure (C) was the second most significant factor studied and it had nearly the same influence on the retention factors of all compounds. The second-order effect C^2 was only significant for lycopene, coenzyme Q10 and lutein models. Figure 4.3 shows contour plots of lycopene, beta-carotene, coenzyme Q10 and lutein retention factors illustrating the dependency of the retention factor on ethanol percentage and pressure at 25 ℃.

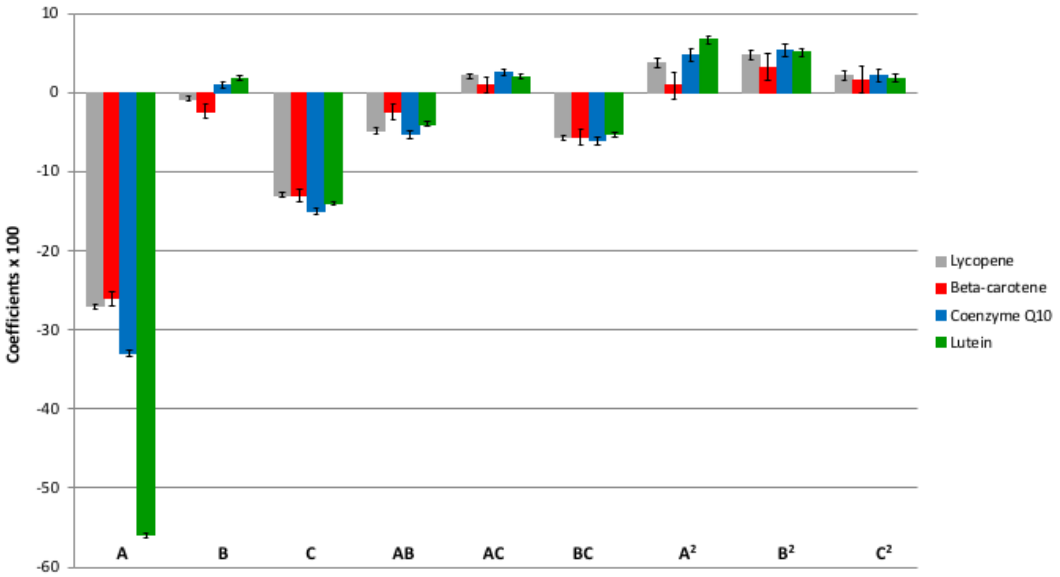

Figure 4.2: Coefficients of the model for the retention factor of lycopene, beta-carotene, coenzyme Q10 and lutein. The error bars represent the 95% confidence interval of the coefficients. A is the ethanol percentage (C_E), B is the temperature and C is the pressure; AB, AC and BC are the interaction terms; A^2, B^2 and C^2 are the second-order terms.

The second order models obtained for the retention factors in terms of coded factors were:

$$\begin{aligned} lnk_{lycopene} &= 0.63 - 0.27A - 7.87 \times 10^{-3}B - 0.13C - 0.05AB \\ &\quad + 0.02AC - 0.06BC + 0.04A^2 + 0.05B^2 + 0.02C^2 \end{aligned} \tag{4.2}$$

$$\begin{aligned} lnk_{beta-carotene} &= 0.92 - 0.26A - 0.02B - 0.13C - 0.02AB + 9.60 \times 10^{-3}AC \\ &\quad - 0.06BC + 8.671 \times 10^{-3}A^2 + 0.03B^2 + 0.02C^2 \end{aligned} \tag{4.3}$$

$$\begin{aligned} lnk_{coenzymeQ10} &= 0.94 - 0.33A + 9.38 \times 10^{-3}B - 0.15C - 0.05AB \\ &\quad + 0.02AC - 0.06BC + 0.05A^2 - 0.05B^2 + 0.02C^2 \end{aligned} \tag{4.4}$$

$$\begin{aligned} lnk_{lutein} &= 1.77 - 0.56A + 0.02B - 0.14C - 0.04AB + 0.02AC \\ &\quad - 0.05BC + 0.07A^2 + 0.05B^2 + 0.02C^2 \end{aligned} \tag{4.5}$$

The response surfaces are shown in Figure 4.12 in Supplementary Material. It can be clearly seen in these Figures that the edges of a given response surface are not parallel. An increase in pressure when the mobile phase has a lower amount of ethanol causes retention to decrease much more than when mobile phase has a

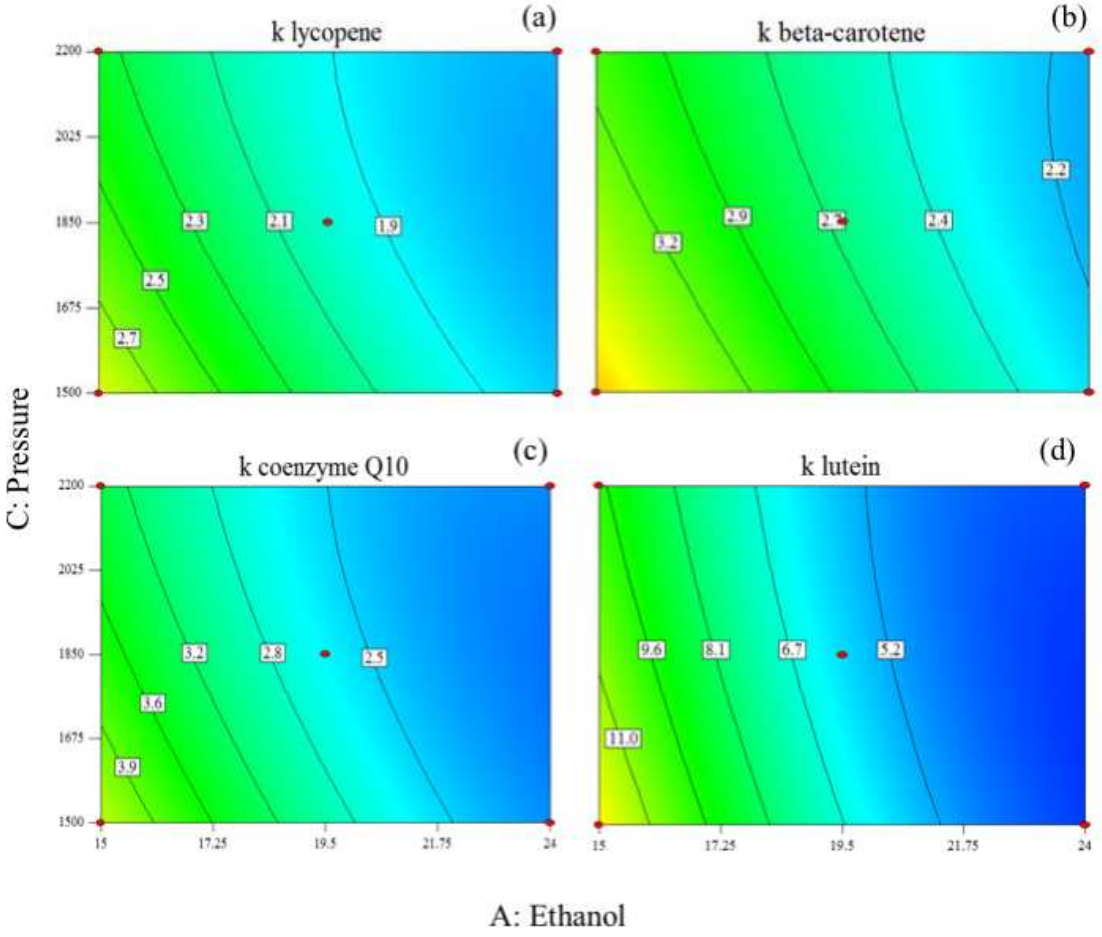

Figure 4.3: Contour plot of the retention factor of lycopene (a), beta-carotene (b), coenzyme Q10 (c) and lutein (d) as a function of the pressure and ethanol percentage at 25 ℃.

higher amount of ethanol. This clearly indicates the interaction between these two variables. The chemical explanation is related to the fact that the density of the fluid is not so influenced by pressure when the content of organic modifier in the mobile phase is high, due to its lower compressibility.

Selectivity

The separation factor (α) describes the separation of two components, it is calculated by the ratio between their retention factors, and therefore represents the selectivity of the analysis [53]. Table 4.3 shows ANOVA results for the calculated models where values of Prob < 0.05 indicate that the model term is significant within a 95% confidence interval. Beta-carotene and coenzyme Q10 were the analytes that

presented separation issues inside the experimental domain and therefore this pair of peaks was considered critical in order to obtain adequate overall separation.

The separation of lycopene and beta-carotene (α_{12}) was not significantly affected by the experimental variables ethanol percentage and pressure, the only significant factor was temperature. In fact, it can be seen that the regression was only slightly significant by the ANOVA, according to Table 4.3. This was due to the fact that the range of α for this pair was too small (1.2 – 1.3). For the other two pairs, the range of the separation factor was broader and therefore the regression was significant. For the pair beta-carotene and coenzyme Q10 (α_{23}), the three main factors, the interaction term AB and the quadratic term A^2 were significant. Regarding the pair coenzyme Q10 and lutein (α_{34}), all terms except the quadratic terms B^2 and C^2 were significant.

The predictive capability of the models was evaluated by the diagnostics graphs and coefficient of determination (R^2). The R^2 values were 0.7795, 0.9584 and 0.9993 and the adjusted coefficients of determination (adjusted R^2) were 0.5589, 0.9168 and 0.9987 for α_{12}, α_{23} and α_{34} models, respectively. The low values of R^2 for the pair α_{12} can be explained by the low regression significance, as already mentioned, and therefore residual analysis were not carried out for this pair. For the pairs α_{23} and α_{34} residual were random without signal of heteroscedasticity and the predicted values were in good agreement with the experimental values.

Figure 4.4 shows how changes in temperature and ethanol percentage affect the separation factors α_{12}, α_{23} and α_{34}. In the case of the separation factor α_{12}, changes in ethanol percentage and pressure provided minor effects on selectivity. On the other hand, an increase in separation was achieved by lowering temperature. For the separation factor α_{23}, which is related to the critical pair beta-carotene and coenzyme Q10, an increase in temperature provided a better separation of the two analytes. It is important to note that an increase in ethanol percentage resulted in a decrease of the separation factor, as can be seen in Figure 4.1. The results for the separation factor α_{34} showed that an increase in separation follows a decrease in ethanol percentage while temperature had a minor effect. The response surfaces are shown in Figure 4.13 in Supplementary Material. The models obtained for the separation factors in terms of coded factors were:

Table 4.3: ANOVA for the response surface quadratic model for the separation factors α_{12}, α_{23} and α_{34}.

Source	Sums of squares	DF	Mean square	F value	Prob> F
		$\alpha_{12} = k_{beta-carotene}/k_{lycopene}$			
Model	0.03	9	3.4×10^{-3}	3.53	0.0369
A-C$_E$	1.9×10^{-3}	1	1.9×10^{-3}	2.00	0.1909
B-T	4.0×10^{-3}	1	4.0×10^{-3}	4.10	0.0735
C-P	8.5×10^{-4}	1	8.5×10^{-4}	0.87	0.3741
AB	6.4×10^{-3}	1	6.4×10^{-3}	6.56	0.0306
AC	1.8×10^{-3}	1	1.8×10^{-3}	1.86	0.2059
BC	3.4×10^{-6}	1	3.4×10^{-6}	3.7×10^{-3}	0.9529
A^2	3.8×10^{-3}	1	3.8×10^{-3}	3.93	0.0786
B^2	1.2×10^{-3}	1	1.2×10^{-3}	1.24	0.2942
C^2	1.8×10^{-4}	1	1.8×10^{-4}	0.19	0.6753
		$\alpha_{23} = k_{coenzymeQ10}/k_{beta-carotene}$			
Model	0.12	9	0.01	23.03	< 0.0001
A-C$_E$	0.07	1	0.07	123.22	< 0.0001
B-T	0.01	1	0.01	23.59	0.0009
C-P	5.1×10^{-3}	1	5.1×10^{-3}	8.50	0.0172
AB	8.7×10^{-3}	1	8.7×10^{-3}	14.39	0.0043
AC	2.7×10^{-3}	1	2.7×10^{-3}	4.44	0.0645
BC	4.1×10^{-4}	1	4.1×10^{-4}	0.68	0.4315
A^2	5.1×10^{-3}	1	5.1×10^{-3}	8.50	0.0172
B^2	1.5×10^{-3}	1	1.5×10^{-3}	2.47	0.1507
C^2	1.2×10^{-4}	1	1.2×10^{-4}	0.20	0.6692
		$\alpha_{34} = k_{lutein}/k_{coenzymeQ10}$			
Model	2.94	9	0.33	1492.19	< 0.0001
A-C$_E$	2.87	1	2.87	13129.40	< 0.0001
B-T	2.0×10^{-3}	1	2.0×10^{-3}	8.95	0.0152
C-P	4.5×10^{-3}	1	4.5×10^{-3}	20.39	0.0015
AB	5.4×10^{-3}	1	5.4×10^{-3}	24.88	0.0008
AC	2.0×10^{-3}	1	2.0×10^{-3}	9.26	0.0140
BC	3.8×10^{-3}	1	3.8×10^{-3}	17.39	0.0024
A^2	0.03	1	0.03	146.33	< 0.0001
B^2	6.4×10^{-5}	1	6.4×10^{-5}	0.29	0.6027
C^2	2.2×10^{-4}	1	2.2×10^{-4}	1.02	0.3385

$$\alpha_{12} = 1.34 + 0.01A - 0.02B + 9.2 \times 10^{-3}C + 0.03AB - 0.02AC + 6.7 \times 10^{-4}BC - 0.04A^2 - 0.02B^2 - 8.2 \times 10^{-3}C^2 \quad (4.6)$$

$$\alpha_{23} = 1.02 - 0.09A + 0.04B - 0.02C - 0.03AB + 0.02AC - 7.1 \times 10^{-3}BC + 0.04A^2 + 0.02B^2 + 6.6 \times 10^{-3}C^2 \quad (4.7)$$

$$\alpha_{34} = 2.28 - 0.54A + 0.01B + 0.02C + 0.03AB - 0.02AC + 0.02BC + 0.11A^2 - 4.8 \times 10^{-3}B^2 - 9.0 \times 10^{-3}C^2 \quad (4.8)$$

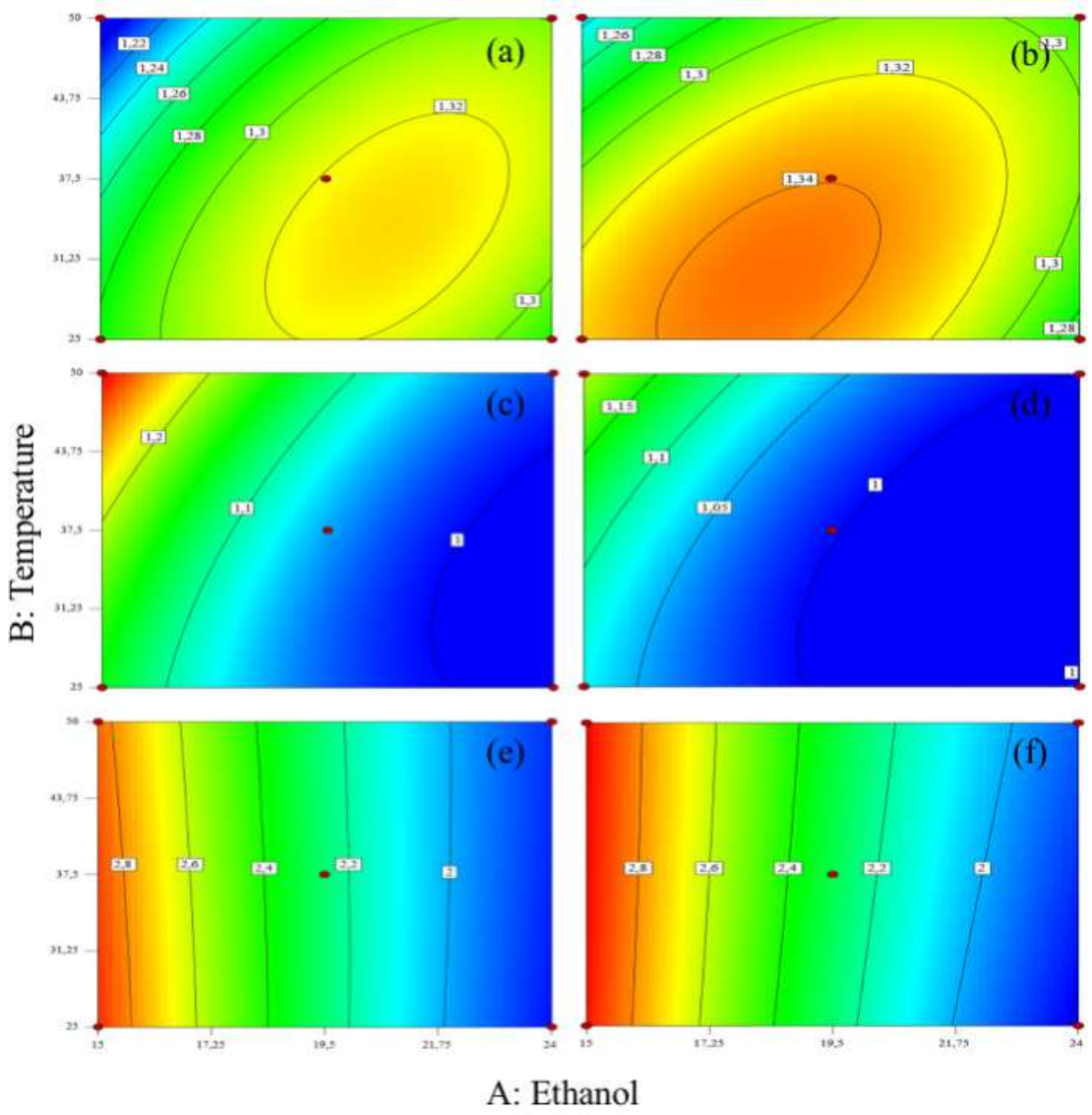

Figure 4.4: Contour plots of the separation factors as a function of the temperature and ethanol percentage for the pairs: (a and b) lycopene and beta-carotene (α_{12}), (c and d) beta-carotene and coenzyme Q10 (α_{23}) and (e and f) coenzyme Q10 and lutein (α_{34}) at 1500 psi on the left and 2200 psi on the right.

In order to find the optimal conditions for retention and separation of all analytes, a multiple response optimization procedure was carried out employing to restrictions: the retention factor (k) should be higher than 2 for all analytes (especially lycopene, which was the first eluted) and a separation criterion measured by α should be higher than 1.15 for the critical pair beta-carotene and coenzyme Q10. The experimental region that encompasses both criteria is shown in Figure 4.5, for 1500 psi (a) and 2200 psi (b). The selected operating conditions for further experiments were: 15.5% of ethanol at 40 ℃ and 1500 psi, which is located inside the experimental domain for both retention and separation factors (Figure 4.6).

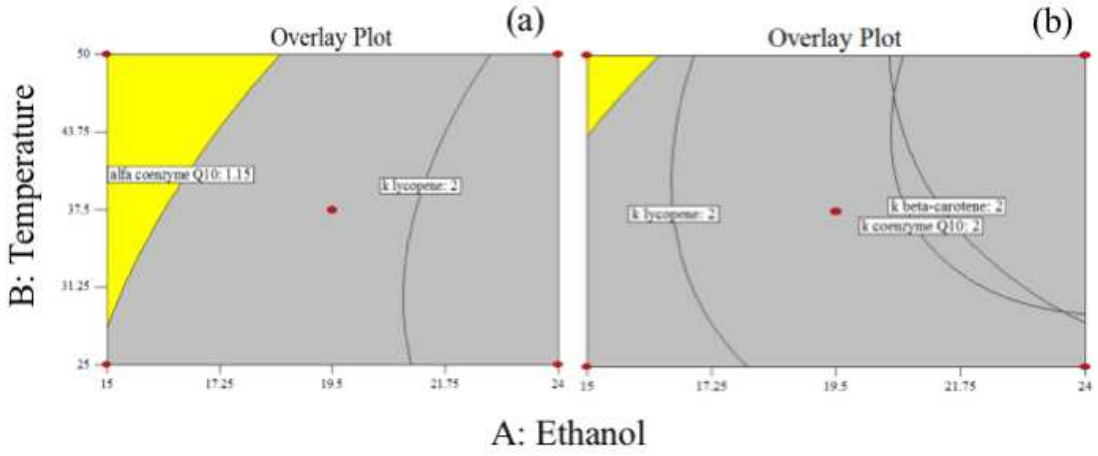

Figure 4.5: Overlay plots of retention and separation for 1500 psi (a) and 2200 psi (b). The yellow region shows the combination of operating factors that satisfy simultaneously $k > 2$ for all the analytes and $\alpha > 1.15$ for the critical pair beta-carotene and coenzyme Q10.

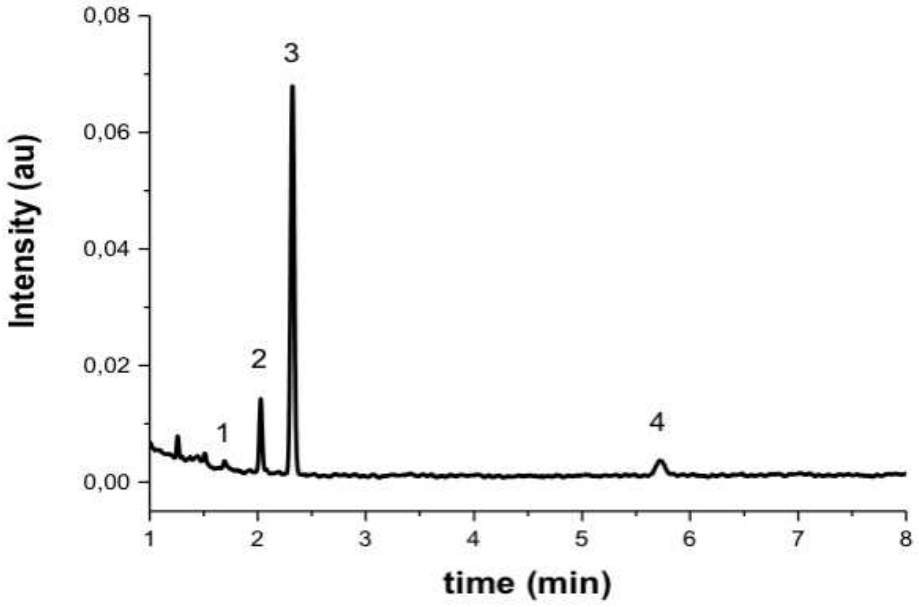

Figure 4.6: Chromatogram of the separation: 1. Lycopene, 2. Beta-carotene, 3. Coenzyme Q10, 4. Lutein. Experimental conditions: 15.5 % of ethanol, temperature 40 °C and pressure 1500 psi.

4.4 Conclusions

The individual and combined effects of ethanol percentage, temperature and pressure were investigated using a Central Composite Design to describe their impact on the retention and separation factors in the UHPSFC technique. Retention factors were found to be strongly dependent on the amount of ethanol and pressure, followed by temperature. The interaction factors and quadratic terms were significant, indicating the need for a response surface multivariate approach to properly describe the system. Beta-carotene and coenzyme Q10 was the critical pair for separation, which was shown to be dependent on the three operating parameters. All polynomial regression models were in good agreement with the experimental results. An experimental domain was delimited in which retention and separation factors were satisfied, $k > 2$ and $\alpha > 1.15$. Therefore, the operating conditions selected for further experiments were 15.5% of ethanol at 40 ℃ and 1500 psi.

4.5 Supplementary Material

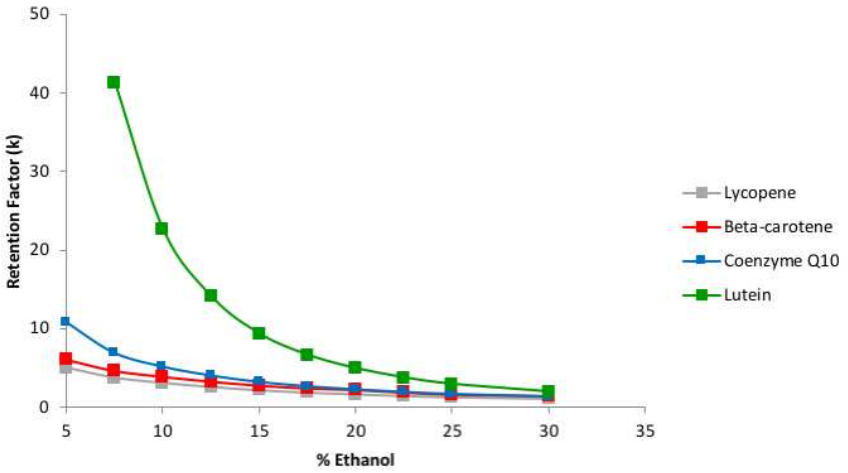

Figure 4.7: Retention curves of the analytes in the HSS C18 SB stationary phase used to select the range of organic modifier to provide retention factors between 2 and 10. Experimental conditions: pressure 2190 psi, column temperature 40 ℃, sample temperature 5 ℃, flowrate 1.5 mL/min and injection volume 1μL.

Table 4.4: Central composite design in the original and coded (between brackets) form of the independent variables percentage of modifier (A), temperature (B) and pressure (C) and experimental results for the response variables, retention factors of lycopene (k_1), beta-carotene (k_2), coenzyme Q10 (k_3) and lutein (k_4) and separation factors of the pairs lycopene/beta-carotene (α_{12}), beta-carotene/ coenzyme Q10 (α_{23}) and coenzyme Q10/lutein (α_{34}), between brackets the standard deviation.

Run	**Factor**			**Response**						
	Percentage of modifier (A)	Temperature (B)	Pressure (C)	k_1	k_2	k_3	k_4	α_{12}	α_{23}	α_{34}
1	24 (+1)	25 (−1)	2200 (+1)	1.59 (±0.02)	2.01 (±0.02)	2.01 (±0.02)	3.63 (±0.02)	1.27 (< 0.01)	0.97 (±0.04)	1.80 (< 0.01)
2	24 (+1)	50 (+1)	1500 (−1)	1.79 (±0.02)	2.36 (±0.02)	2.36 (±0.02)	4.40 (±0.04)	1.32 (< 0.01)	1.00 (< 0.01)	1.87 (< 0.01)
3	24 (+1)	25 (−1)	1500 (−1)	1.80 (±0.02)	2.32 (±0.02)	2.32 (±0.02)	4.19 (±0.02)	1.29 (< 0.01)	1.00 (< 0.01)	1.81 (< 0.01)
4	15 (−1)	25 (−1)	2200 (+1)	2.39 (±0.01)	3.15 (±0.01)	3.43 (±0.01)	10.06 (±0.04)	1.32 (< 0.01)	1.09 (< 0.01)	2.93 (< 0.01)
5	19.5 (0)	37.5 (0)	1850 (0)	1.89 (< 0.01)	2.57 (< 0.01)	2.57 (< 0.01)	5.86 (< 0.01)	1.36 (< 0.01)	1.00 (< 0.01)	2.28 (< 0.01)

Continue on next page

Run	**Factor**			**Response**						
	Percentage of modifier (A)	Temperature (B)	Pressure (C)	k_1	k_2	k_3	k_4	α_{12}	α_{23}	α_{34}
6	19.5 (0)	37.5 (0)	1850 (0)	1.88 (< 0.01)	2.57 (< 0.01)	2.57 (< 0.01)	5.85 (< 0.01)	1.36 (< 0.01)	1.00 (< 0.01)	2.28 (< 0.01)
7	19.5 (0)	25 (-1)	1850 (0)	2.00 (±0.01)	2.68 (±0.01)	2.68 (±0.01)	6.06 (±0.01)	1.34 (< 0.01)	1.00 (< 0.01)	2.26 (< 0.01)
8	19.5 (0)	37.5 (0)	2200 (+1)	1.68 (< 0.01)	2.27 (< 0.01)	2.27 (< 0.01)	5.21 (< 0.01)	1.35 (< 0.01)	1.00 (< 0.01)	2.29 (< 0.01)
9	15 (-1)	37.5 (0)	1850 (0)	2.52 (±0.01)	3.21 (±0.01)	3.70 (±0.01)	10.89 (±0.04)	1.27 (< 0.01)	1.15 (< 0.01)	2.94 (< 0.01)
10	19.5 (0)	37.5 (0)	1850 (0)	1.88 (±0.01)	2.56 (±0.01)	2.56 (±0.01)	5.84 (±0.02)	1.36 (< 0.01)	1.00 (< 0.01)	2.28 (< 0.01)
11	24 (+1)	37.5 (0)	1850 (0)	1.50 (< 0.01)	1.94 (< 0.01)	1.94 (< 0.01)	3.58 (±0.01)	1.29 (< 0.01)	1.00 (< 0.01)	1.85 (< 0.01)
12	19.5 (0)	37.5 (0)	1850 (0)	1.87 (< 0.01)	2.55 (< 0.01)	2.55 (< 0.01)	5.82 (±0.01)	1.36 (< 0.01)	1.00 (< 0.01)	2.28 (< 0.01)

Continue on next page

Run	**Factor**			**Response**						
	Percentage of modifier (A)	Temperature (B)	Pressure (C)	k_1	k_2	k_3	k_4	α_{12}	α_{23}	α_{34}
13	19.5 (0)	37.5 (0)	1500 (-1)	2.18 (±0.01)	2.78 (±0.01)	3.00 (±0.01)	6.78 (±0.01)	1.27 (< 0.01)	1.08 (< 0.01)	2.26 (< 0.01)
14	15 (-1)	25 (-1)	1500 (-1)	2.88 (< 0.01)	3.71 (±0.01)	4.21 (±0.01)	12.29 (±0.04)	1.29 (< 0.01)	1.13 (< 0.01)	2.92 (< 0.01)
15	15 (-1)	50 (+1)	1500 (-1)	3.55 (±0.02)	4.26 (±0.03)	5.51 (±0.04)	15.85 (±0.10)	1.20 (< 0.01)	1.29 (< 0.01)	2.88 (< 0.01)
16	19.5 (0)	37.5 (0)	1850 (0)	1.90 (±0.01)	2.50 (±0.11)	2.59 (±0.02)	5.92 (±0.05)	1.32 (±0.06)	1.04 (±0.05)	2.28 (< 0.01)
17	24 (+1)	50 (+1)	2200 (+1)	1.29 (±0.01)	1.66 (±0.01)	1.67 (±0.01)	3.16 (< 0.01)	1.29 (< 0.01)	1.00 (< 0.01)	1.90 (±0.02)
18	15 (-1)	50 (+1)	2200 (+1)	2.29 (< 0.01)	2.84 (< 0.01)	3.39 (< 0.01)	10.06 (±0.02)	1.24 (< 0.01)	1.19 (< 0.01)	2.97 (< 0.01)
19	19.5 (0)	50 (+1)	1850 (0)	1.94 (< 0.01)	2.42 (< 0.01)	2.70 (±0.01)	6.22 (< 0.01)	1.25 (< 0.01)	1.11 (< 0.01)	2.30 (< 0.01)

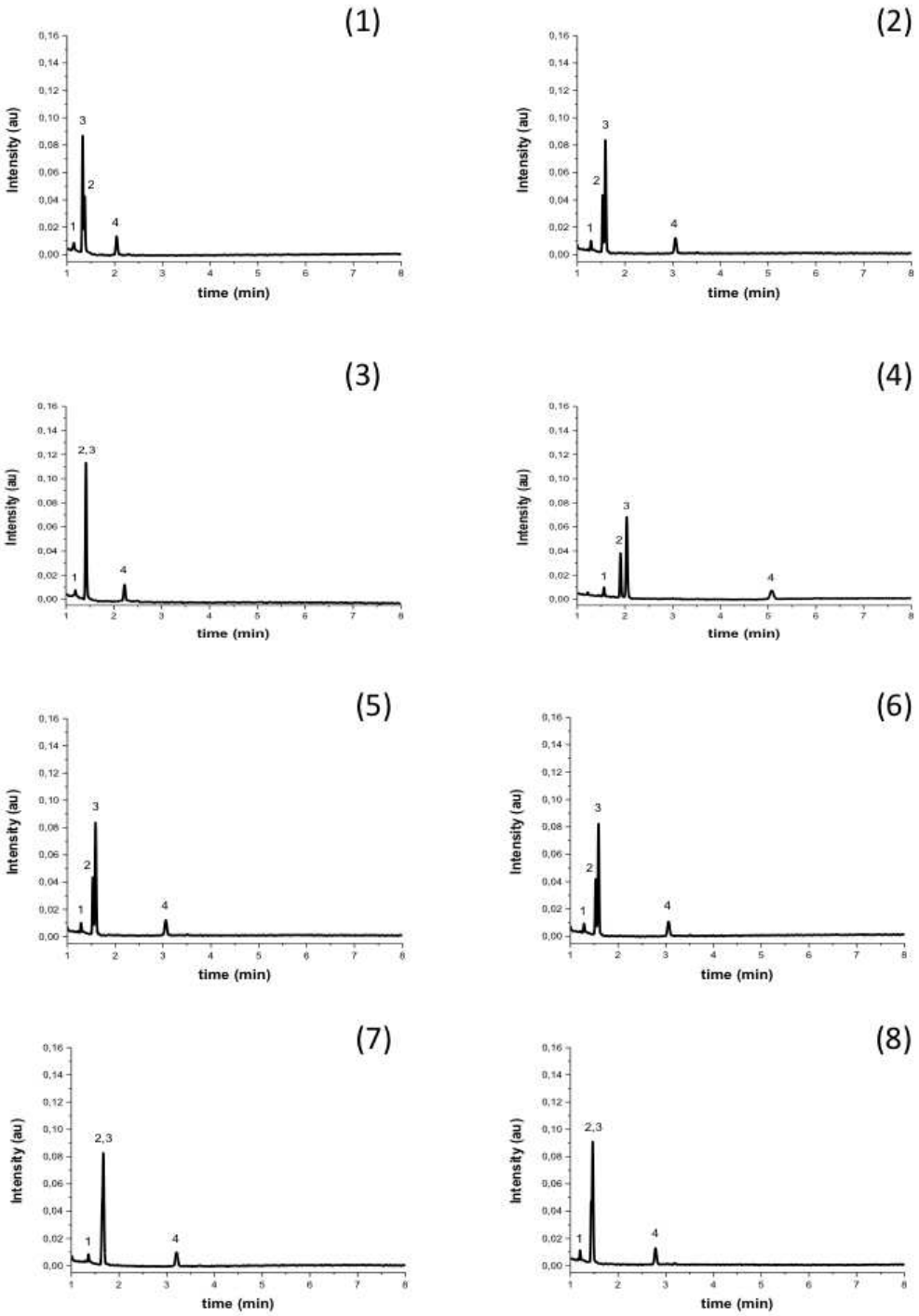

Figure 4.8: Chromatograms of the separation: 1. Lycopene, 2. Beta-carotene, 3. Coenzyme Q10, 4. Lutein at the experimental design conditions. The chromatograms were numbered according to each run. See the experimental conditions on Table 4.4.

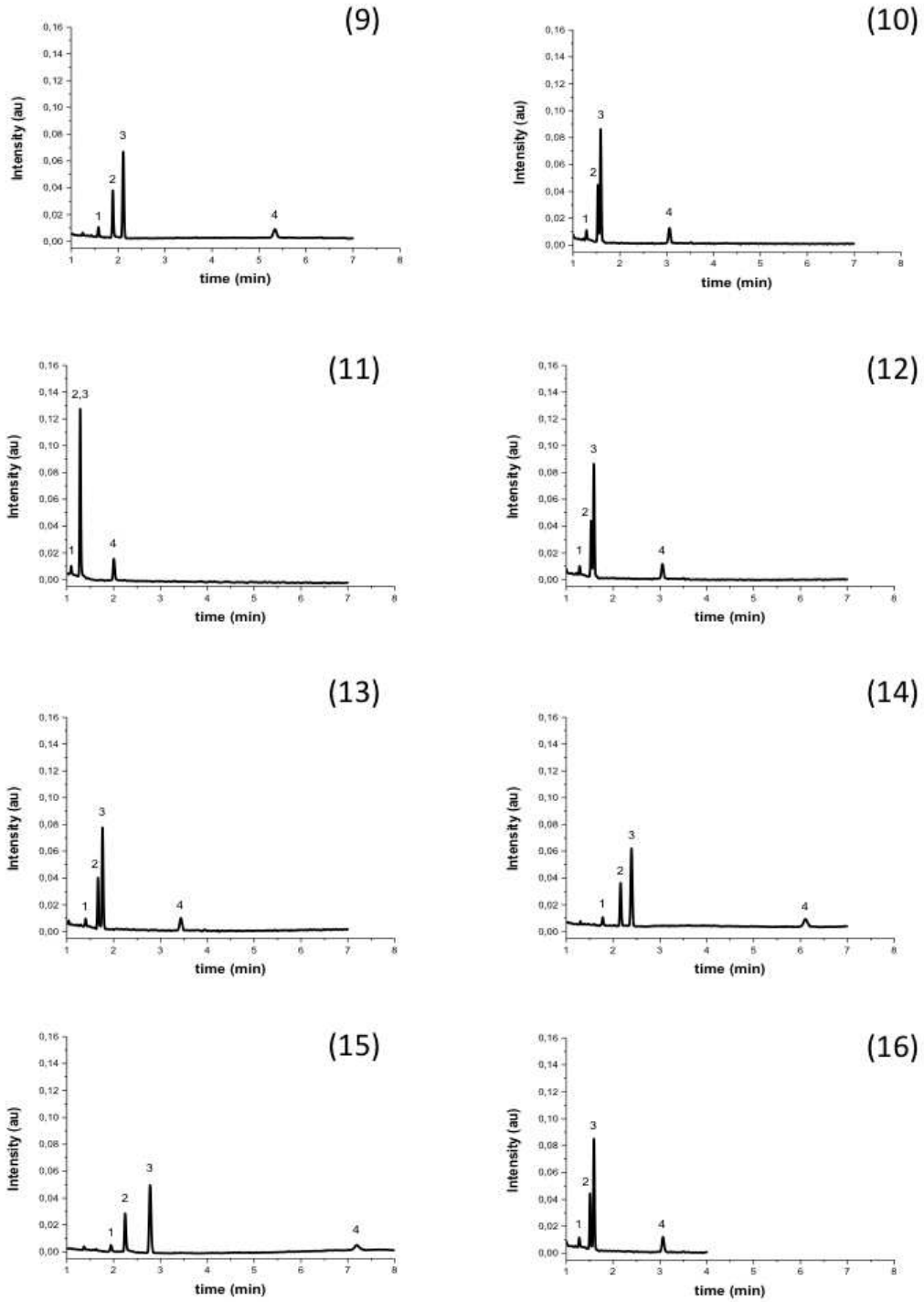

Figure 4.9: Chromatograms of the separation: 1. Lycopene, 2. Beta-carotene, 3. Coenzyme Q10, 4. Lutein at the experimental design conditions. The chromatograms were numbered according to each run. See the experimental conditions on Table 4.4.

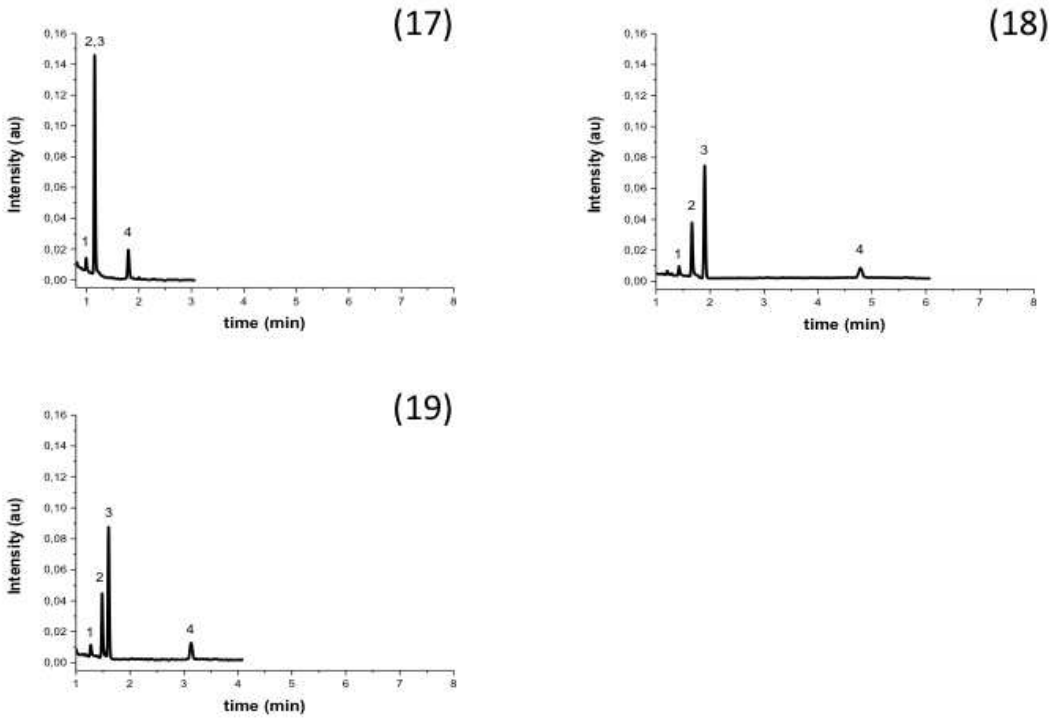

Figure 4.10: Chromatograms of the separation: 1. Lycopene, 2. Beta-carotene, 3. Coenzyme Q10, 4. Lutein at the experimental design conditions. The chromatograms were numbered according to each run. See the experimental conditions on Table 4.4.

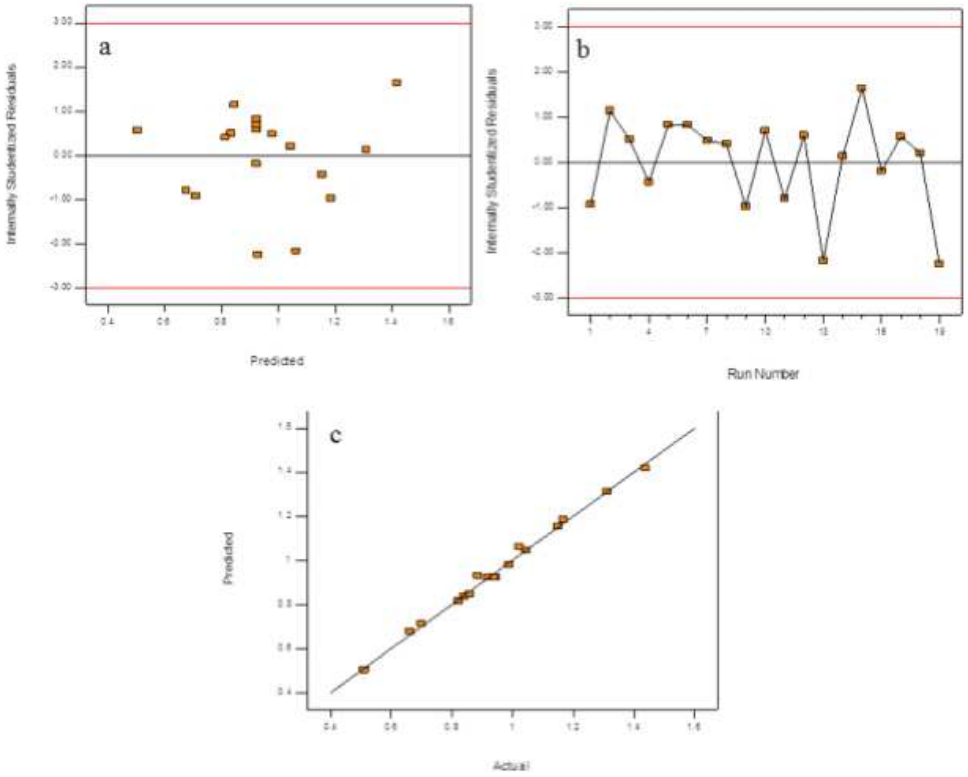

Figure 4.11: Diagnostics graphs for beta-carotene retention model: a) standardized residuals vs predicted values; b) standardized residuals vs run number; c) predicted vs actual values.

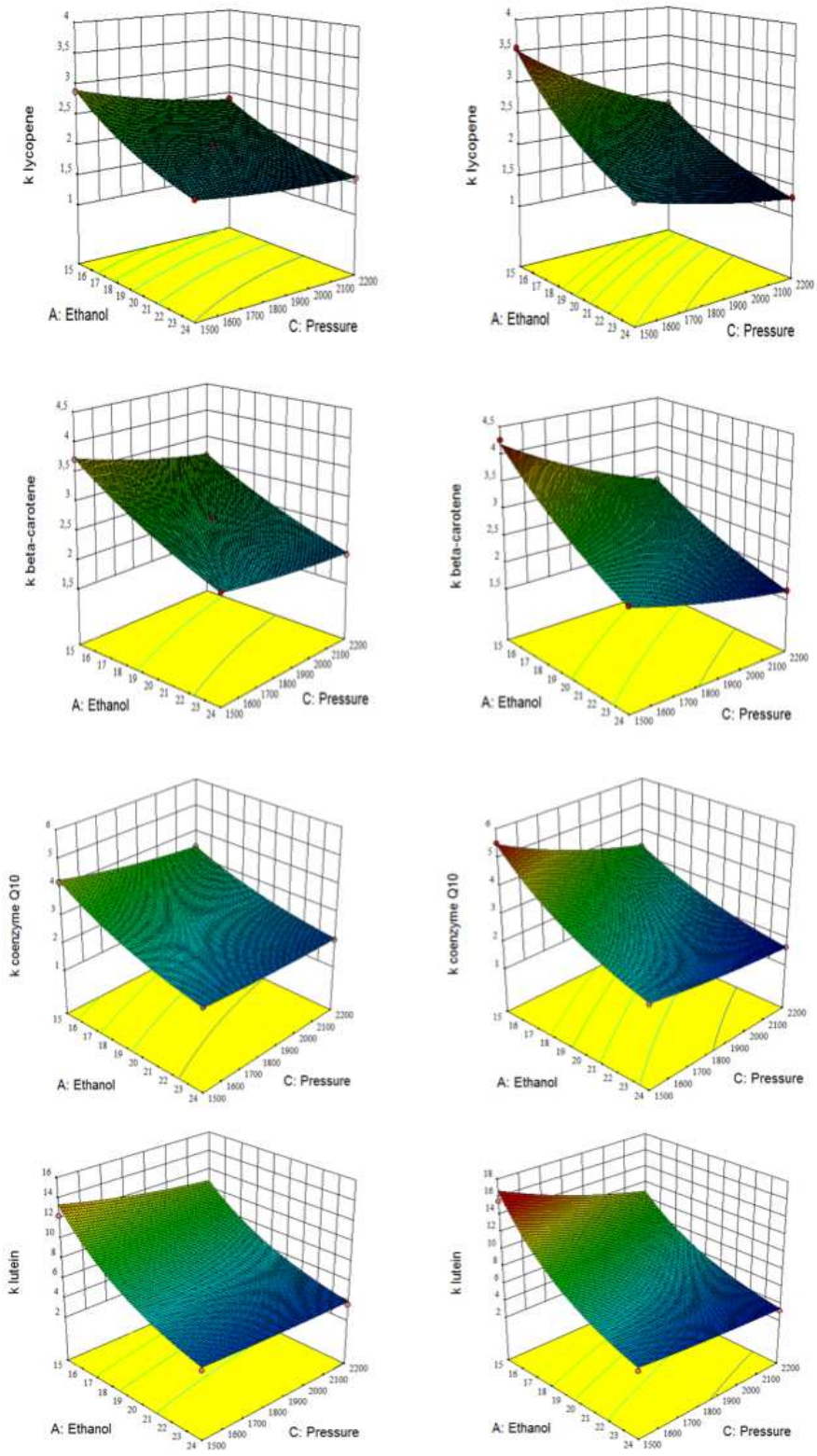

Figure 4.12: Response surface plots of the retention factors as a function of the percentage of organic modifier and pressure at 25 ℃ on the left and 50 ℃ on the right.

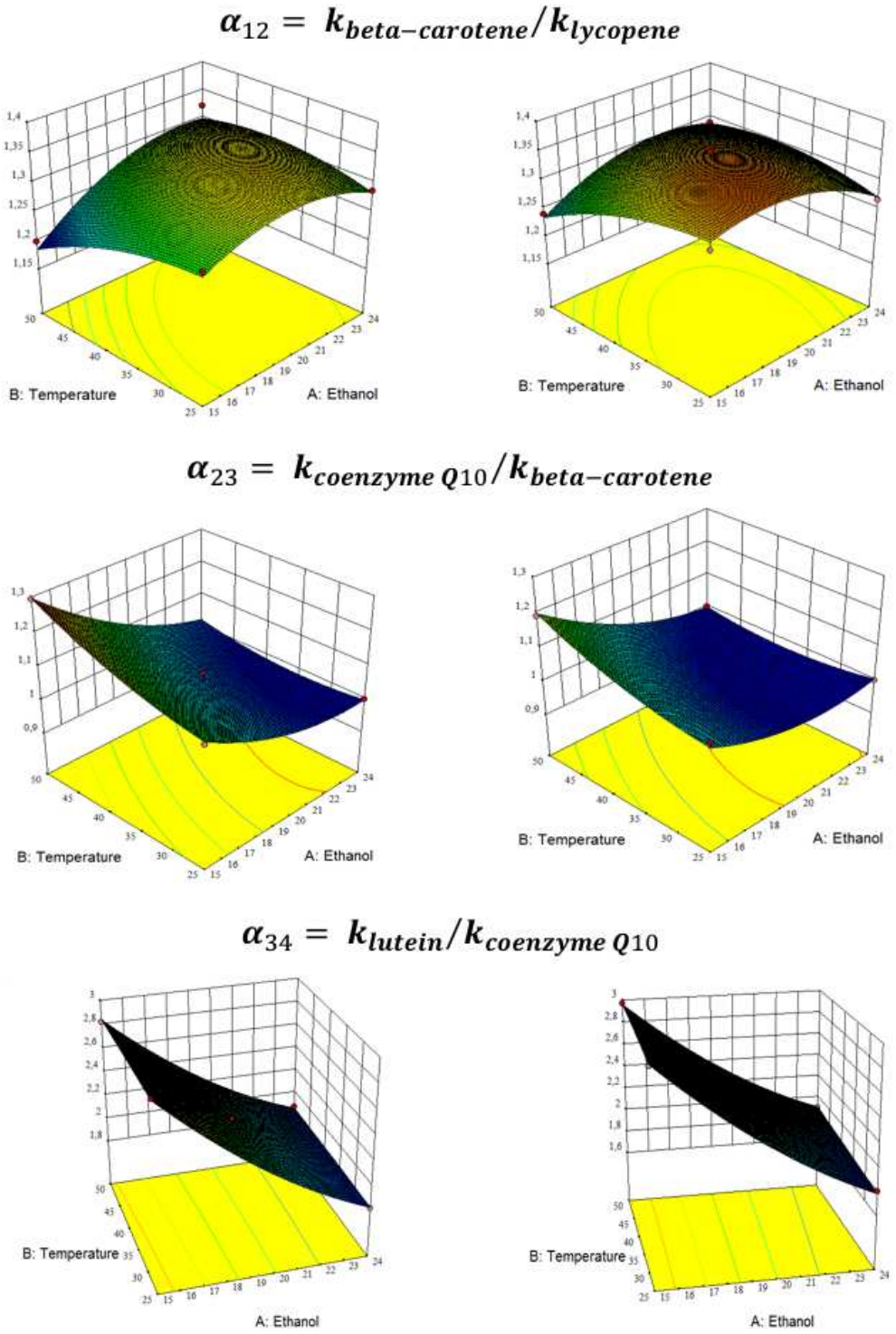

Figure 4.13: Response surface plots of the separation factors as a function of the percentage of organic modifier and temperature at 1500 psi on the left and 2200 psi on the right.

5 | Quantification of bioactive compounds from palm oil by ultra-high performance supercritical fluid chromatography

Carotenoids and coenzyme Q10 are high valuable minor constituents of palm oil that are removed during biodiesel production to produce light-colored oils. Quantification of these bioactive compounds from palm oil was investigated by ultra-high performance supercritical fluid chromatography. In the preliminary results, co-elution of some matrix constituents with the target compounds was observed. Due to co-elution, the clean-up procedures solid-phase extraction, dispersive solid-phase extraction, liquid-liquid extraction with hexane, Amberlite XAD7HP resin and saponification were evaluated to physically remove interferences from palm oil matrix. The results showed that the clean-up procedures could not completely remove interferences. Based on these findings, a separation method was developed without a clean-up procedure, and design of experiments was employed to evaluate the influence of pressure, temperature and ethanol percentage on retention and separation factors of the bioactive compounds. The optimum operating conditions were: 18% of ethanol, 40 ℃ and 1600 psi. Data analysis was carried out with the chemometric method Multivariate Curve Resolution-Alternating Least Squares to resolve and quantify the target compounds. This chemometric method was employed to mathematically remove interferences which could lead to an overestimated quantification of the bioactive compounds. Concentration of beta-carotene, coenzyme Q10 and lutein were determined as being 176, 8.29 and 2.90 μg/mL, respectively. The results demonstrated that ultra-high performance supercritical fluid chromatography coupled with chemometrics are useful tools for the study of highly complex samples.

5.1 Introduction

Growing concerns over the impact of industry on the global environment has drawn considerable attention to a more sustainable use of the natural resources. Indisputably, major improvements in environmental performances have already been made on industrial companies, but we are still striving to develop more sustainable processes. In Brazilian biofuel industry, palm oil is one of the feedstocks used in biodiesel production. Palm oil is mainly composed of triglycerides, a lower amount of free fatty acids and 1% of minor components, such as carotenoids (500-700 ppm), coenzyme Q10 (10-80 ppm), vitamin E (600-1000 ppm), sterols (250-620 ppm), squalene (200-600 ppm) and phospholipids (20-100 ppm) [14], [18]. During biodiesel production, pigments and other minor components are removed to produce light-colored oils which represent a loss of a potential source of these valuable compounds. Recovery of carotenoids and coenzyme Q10 from palm oil before the refining process might be economically viable due to the high value of these bioactive compounds and their wide range of applications in industry. Carotenoids form an important class of natural pigments that are found in microorganisms, plants and animals. There are more than 600 carotenoids in nature, but the most studied are beta-carotene, alfa-carotene, lycopene, lutein, astaxanthin, fucoxanthin and canthaxanthin. Approximately 50 carotenoids are consumed in human diet and only 12 account for most of the dietary intake [83]. Carotenoids are fat-soluble compounds that play an important role in physiological and biological processes. In addition to the pro-vitamin A activity of some carotenoids, these compounds have been associated with a number of health benefits [84]. Several studies have shown that their antioxidant capacity help prevent cancer, diabetes and cardiovascular diseases [20], [79]. Besides their medicinal use, the importance of carotenoids has also increased due to their use in the food, cosmetic and feed industries [46], [84].

Coenzyme Q10 (ubiquinone-10) is a fat-soluble, vitamin-like nutrient that has a very low solubility in water ($< 1\mu$g/L) [85]. Its structure consists of an isoprenoid side chain attached to a benzoquinone ring [86]. Coenzyme Q10 is the only lipid soluble antioxidant synthesized in the human body and plays an important role in the mitochondrial respiratory chain [3], [87], [88], [89]. It is found in high levels in cells with high energy requirements such as heart, brain and liver cells [87]. Like

carotenoids, coenzyme Q10 is also a powerful antioxidant. Its antioxidant capacity is ten times greater than vitamin E. Many therapeutic values of coenzyme Q10 have been reported, such as prevention of lipid peroxidation and oxidative damage of hemoglobin [17], [28], [84], [90]. Coenzyme Q10 has also been implicated as a potential therapy for neurodegenerative disorders and cardiovascular diseases [87], [91], [92]. Furthermore, it has been used to treat some skin conditions-e.g., facial vitiligo or as anti-aging ingredient in cosmetic products [85], [87], [93].

Ultra-High Performance Supercritical Fluid Chromatography (UHPSFC) is a separation technique that combines the unique properties of supercritical CO_2 with the use of sub-2μm particle columns to improve the separation efficiency, speed and selectivity [94]. UHPSFC has been employed to determine minor constituents of palm oil. Choo *et al.* (2005) determined total carotenoid content in palm oil by UHPSFC [9]. Another study reported the recovery and quantification of coenzyme Q10 [10]. As of our knowledge no attempts have been made to separate and quantify lycopene, beta-carotene, coenzyme Q10 and lutein from palm oil by UHPSFC. A study using UHPSFC coupled with photodiode array (PDA) detection for the separation of bioactive compounds from palm oil is presented here.

5.2 Materials and Methods

5.2.1 Chemicals and Reagents

Propane (99.5%) was supplied by White Martins. HPLC-grade hexane, ethanol (EtOH) and methyl tert-butyl ether (MTBE) were acquired from Panreac. Tetrahydrofuran (THF) was bought from J.T.Baker. The water used in the clean-up procedures was purified on a Milli-Q system (Millipore). Solid-phase extraction (SPE) cartridges packed with C18 and ENVI-8 (500 mg/3 mL) phases were purchased from Supelco. Dispersive solid-phase extraction (d-SPE) sorbent, Bondesil primary secondary amine (PSA) 40μm was acquired from Agilent. Graphitized carbon black (GCB) for d-SPE was purchased from Varian. Amberlite XAD7HP resin was obtained from Supelco. Ultrapure CO_2 (99.99%) was provided by White Martins. Analytical standards of lycopene, beta-carotene, coenzyme Q10 and lutein were

acquired from Sigma-Aldrich. Palm oil was extracted at Universidade Tiradentes (Sergipe, Brazil).

5.2.2 Instrumentation

All experiments were performed on a Waters Acquity UPC^2 system equipped with a binary solvent delivery pump used to supply the organic modifier and the CO_2, an autosampler that included partial loop volume injection system, two-position column oven compatible with 150 mm length columns, a single column heater compatible with 300 mm length columns, a photo-diode array detector (PDA) including a high pressure UV cell (400 bar) with a volume of 8 μL and a dual-stage backpressure regulator (BPR) consisting of a static and a dynamic part [35], [40], [43], [95], [96]. Empower 2 software (Waters) was used for instrument control and data analysis.

5.2.3 Methodology

Palm Oil Extraction

Oil palm fresh fruit bunches (*Dura* variety) was provided by Empresa Baiana de Desenvolvimento Agrícola (EBDA). A method previously developed employing supercritical fluid was used [97]. Fruits were separated from bunches, washed and peeled manually. Palm fiber was dried in a circulating air oven (Nova Ética, 400/4N) at 60 ℃ for 18 hours. After drying, palm fiber was ground in a knife mill, classified on a series of Tyler sieves and particle size between 8 to 24 mesh were selected. Samples were kept under refrigeration at 10 ℃ prior to extraction.

Extraction was carried out in a semi-batch laboratory scale equipment. The equipment was comprised of a syringe pump (ISCO model 500D) for compressed fluid displacement, a cylindrical vessel (25 x 2.0 (i.d.) cm, 157.3 cm^3), a flow control valve, two thermostatic baths for fluid and extraction temperature control and a pressure transducer (Huba Control, pressure transmitter type 691) to manage system pressure [97]. An amount of 25 g of palm fiber was loaded into the extraction vessel. Propane was pumped into the system. Temperature and pressure were set at 40 ℃

and 150 bar. System was kept at experimental condition for 40 min and extraction was performed at flow rate of 1 mL/min.

Clean-up Procedures

Clean-up procedures employing Supelclean C18 and ENVI-8 SPE cartridges, d-SPE with PSA and GCB, liquid-liquid extraction (LLE) with hexane, Amberlite XAD7HP resin and saponification were tested in order to physically reduce interference of matrix components. Palm oil sample was also prepared without the clean-up step. An amount of 1750 mg was weighted and dissolved in 5 mL MTBE.

Chromatographic conditions employed in the experiments were: Acquity UPC^2 HSS C_{18} SB 3.0 x 150 mm column with particle size of 1.8 μm. CO_2 and ethanol (84.5:15.5, v/v) were used as mobile phase. Pressure was set at 1500 psi, column temperature 40 ℃, sample manager temperature 5 ℃, flow rate 1.5 mL/min and injection volume 2 μL [84]. All injections were carried out in duplicate and the average was calculated. After scanning in the 210-600 nm range, analytes were detected at 275 nm (coenzyme Q10) and 450 nm (carotenoids).

Solid-Phase Extraction

Two types of SPE cartridges were used in the clean-up procedure, C18 and ENVI-8. A cartridge was placed in a vacuum-elution apparatus, and conditioned by consecutive passing 5 mL ethanol and 5 mL MTBE. The vacuum was released to prevent drying of the cartridge. A sample of palm oil (1750 mg) was weighted and dissolved in 5 mL MTBE. The palm oil sample was applied to the cartridge and the fraction was recollected in a 10 mL flask. Then, another 3 mL MTBE was added to elute the analytes and was recollected in the preceding volumetric flask. The volume was adjusted to 10 mL. An aliquot (1 mL) of the final solution was filtered and injected into the UHPSFC system. The cartridge was washed with 5 mL ethanol to elute polar compounds and the volume was recollected in another volumetric flask. An aliquot (1 mL) of this solution was filtered and injected into the UHPSFC system [98], [99], [100], [101].

Dispersive Solid-Phase Extraction

A combination of PSA and GCB sorbents were investigated in the d-SPE procedure. A sample of palm oil (1750 mg) was weighted and dissolved in 5 mL MTBE. An amount of 10 mg of PSA sorbent was added to palm oil sample, centrifuged for 3 minutes and filtered to remove PSA sorbent. Then, an amount of 10 mg of GCB sorbent was added to the sample, centrifuged again for 3 minutes and filtered to remove GCB sorbent. An aliquot (1 mL) of the extract solution was injected into the UHPSFC system [98].

Liquid-Liquid Extraction with Hexane

A sample of palm oil (1750 mg) was weighted and dissolved in 15 mL hexane. The palm oil sample was kept under mechanical stirring for 1 hour. After precipitation of the lipid components, the upper layer was collected, filtered and injected into the UHPSFC system [99], [100].

Amberlite XAD7HP Resin

Amberlite XAD7HP is a polymeric adsorbent, which is comprised of non ionic aliphatic acrylic polymer. It has high surface area (500 m^2/g) and relatively large pores (450 Å). Due to its properties, Amberlite XAD7HP resin is suitable for the adsorption of large molecules from plant extracts [102], [103].

The clean-up procedure was carried out according to the method of Bijttebier *et al.* (2014). Briefly, a sample of palm oil (1750 mg) was weighted and dissolved in 5 mL MTBE. Approximately 0.5 g of Amberlite XAD7HP resin was added to palm oil sample and the mixture was kept under magnetic stirring for 30 minutes. The extract solution was collected, filtered and injected into the UHPSFC system. The resin was washed 3 times with 5 mL MTBE. The combined MTBE extracts were also analyzed by UHPSFC [104].

Saponification

A sample of palm oil (1750 mg) was weighted and dissolved in 5 mL MTBE. Next, the sample was mixed with 5 mL of 50% potassium hydroxide in ethanol and kept under magnetic stirring for 1 hour at room temperature (25 ℃). Then,

the saponified sample was extracted 3 times with 50 mL of 10% deionized water in hexane. The extracts were combined and washed with 10% ethanol in deionized water to remove alkali. The extract was evaporated to dryness under a stream of nitrogen and redissolved in 3 mL MTBE. An aliquot (1 mL) of the extract solution was filtered and injected into the UHPSFC system [9], [105].

Two-step Procedure

A combination of two clean-up procedures were also investigated. In the first two-step procedure, LLE with hexane and SPE with C18 cartridge were employed. In the other one, Amberlite XAD7HP resin and SPE with C18 cartridge were evaluated. All steps were carried out as previously described, except for the following changes: C18 cartridges were conditioned by consecutive passing 5 mL ethanol and 5 mL deionized water, and analytes were eluted with 3 mL chloroform. In the step with Amberlite XAD7HP resin, palm oil sample was dissolved in 5 mL acetone.

5.2.4 Experimental Design

Experimental design was developed based on a previous study with the standard compounds [84]. The experimental domain was defined taking into account some constrains, such as maximum pressure of the system, maximum temperature limit of the column, and carotenoids and coenzyme Q10 sensitivity to heat. Considering that, the maximum allowed temperature for Viridis HSS C_{18} SB column is 60 ℃, a temperature range of 25-50 ℃ was selected. Ethanol percentage range (16–24, v/v) was chosen based on preliminary experiments. Pressure range of 1500-2200 psi was evaluated to allow the use of ethanol range selected previously.

A Central Composite Design (CCD) was used to design a series of experiments to provide data to determine the relationship between the three operating parameters, pressure, temperature and ethanol percentage and the responses, retention factors (k) and separation factors ($\alpha = k_n/k_{n-1}$). The CCD consisted of 19 experiments, run in a randomized order to estimate the model coefficients and their corresponding errors. More specifically, 8 factorial runs (2^x, x is the number of studied variables), 6 axial runs (2x, on axes at a distance of $\pm\ \alpha$ from the center) and 5 replicates of

the central point were carried out [84], [106]. The range and levels of experimental variables investigated are presented in Table 5.1.

Table 5.1: Coded and actual levels of the independent variables for UHPSFC experiments.

Symbol	**Variables**	**Coded Levels**		
		-1	**0**	**+1**
A	Pressure (psi)	1500	1850	2200
B	Temperature (℃)	25	37.5	50
C	Ethanol percentage (%)	16	20	24

Statistical analyzes were carried out by Design Expert software version 9.0 (Stat-Ease Inc.). All retention factors were transformed logarithmically to ln k. The second order model was obtained as follows:

$$y = \beta_0 + \sum_{j=1}^{k} \beta_j X_j + \sum \sum_{i<j} \beta_{ij} X_i X_j + \sum_{j=1}^{k} \beta_{jj} X_j^2 \tag{5.1}$$

where β_0, β_j, β_{ij} and β_{jj} are regression coefficients for intercept, linear, interaction and quadratic coefficients respectively and X_i and X_j are coded independent variables [49]. The regression models for each response was assessed by analysis of variance (ANOVA). This analysis includes the model F-value and the Prob>F value to evaluate the model overall significance and its associated probability, the coefficient of determination (R^2) which measures the goodness of fit of the regression model and the prediction error sum of squares (PRESS) [107], [108].

Chromatographic conditions employed in the experiment were: Viridis HSS C_{18} SB 3.0 x 150 mm column with particle size of 3.5 μm, sample manager temperature 17 ℃, equilibration time between injections 4 minutes, flow rate 1.5 mL/min and injection volume 2 μL. All injections were carried out in triplicate and the average was calculated. After scanning in the 210-600 nm range, analytes were detected at 275 nm (coenzyme Q10) and 430 nm (carotenoids). Palm oil sample (1250 mg) was weighted and dissolved in 5 mL MTBE. Coenzyme Q10 (4.2 mg) was dissolved in 5 mL MTBE.

5.2.5 Quantification of Carotenoids and Coenzyme Q10 in Palm Oil Extract

Quantification of carotenoid and coenzyme Q10 was carried out with palm oil samples spiked with each standard. The concentration range was: 50 to 500 μg/mL for beta-carotene, 8 to 100 μg/mL for coenzyme Q10 and 8 to 60 μg/mL for lutein. Lycopene was not evaluated due to the low purity of its secondary standard (7.2%). Palm oil sample (1250 mg) was weighted and dissolved in 5 mL MTBE. Beta-carotene and coenzyme Q10 were dissolved in MTBE and lutein in THF.

Chromatographic conditions employed in the experiment were: Viridis HSS C_{18} SB 3.0 x 150 mm column with particle size of 3.5 μm, CO_2:EtOH (82:18, v/v), pressure 1600 psi, column temperature 40 ℃, sample manager temperature 17 ℃, equilibration time between injections 4 minutes, flow rate 1.5 mL/min and injection volume 2 μL. All injections were carried out in triplicate and the average was calculated. After scanning in the 210-600 nm range, analytes were detected at 275 nm (coenzyme Q10), 430 nm (lutein) and 440 nm (beta-carotene). Data analysis was carried out by MCR-ALS using the toolbox MVC2 (multivariate calibration 2) written for MATLAB [109].

5.3 Results and Discussion

5.3.1 Clean-up Procedures

In a previous study, an analytical method for the separation of carotenoids and coenzyme Q10 was developed employing a model mixture [84]. The optimized operating conditions were then evaluated with palm oil extract. In the preliminary results, it was observed co-elution of some matrix components and the analytes. Furthermore, lower S/N ratios and retention time shifts of the analytes in palm oil extract in relation to their standards were also observed which made it difficult to identify and quantify the target compounds. Due to these challenges, the addition of a clean-up procedure to physically reduce interference of matrix constituents followed by UHPSFC analysis was investigated.

Clean-up procedures showed similar qualitative chromatographic profiles, but with quantitative differences. In addition, the operating conditions optimized with standard compounds did not allow a proper identification and quantification of the analytes. The chromatogram of saponification procedure showed peaks with intensity similar to the ones observed on the chromatograms of Amberlite XAD7HP resin and LLE with hexane (chromatograms are shown in Figure 5.1). The results suggest that loss of carotenoid content was not significant after saponification. Although saponification can lead to carotenoid degradation, it is an effective means to hydrolyze carotenol esters and remove lipids and chlorophylls which may interfere in their chromatographic detection [27]. Some authors suggest that its use should be evaluated according to carotenoid content of the sample [105], [110]. The chromatogram of the washing solvent used in the Amberlite XAD7HP resin procedure showed that part of the analytes remained adsorbed on the resin (data not shown).

The chromatograms of SPE and d-SPE procedures showed less intense peaks than those observed on the chromatograms of saponification, Amberlite XAD7HP resin and LLE with hexane (chromatograms are shown in Figure 5.2). In the d-SPE procedure, PSA and GCB sorbents were chosen because PSA has higher ion-exchange capacity for removal of fatty acids while GCB adsorb pigments [103]. Chromatograms of the washing solvents used in the SPE procedures had no peak indicating that the SPE cartridges were not selective in separating the analytes and matrix components.

Chromatograms of the two-step procedures showed low intensity peaks which can be attributed to degradation and/or loss of analytes (chromatograms are shown in Figure 5.3). The chromatogram of palm oil sample without a clean-up procedure (chromatogram is shown in Figure 5.3) and the chromatogram of d-SPE procedure had similar profile suggesting that the clean-up procedure was not effective on removing interferences. Considering these results, a separation method was developed with palm oil extract, and a chemometric method, Multivariate Curve Resolution with Alternating Least Squares (MCR-ALS), was used to analyze data and mathematically remove interferences.

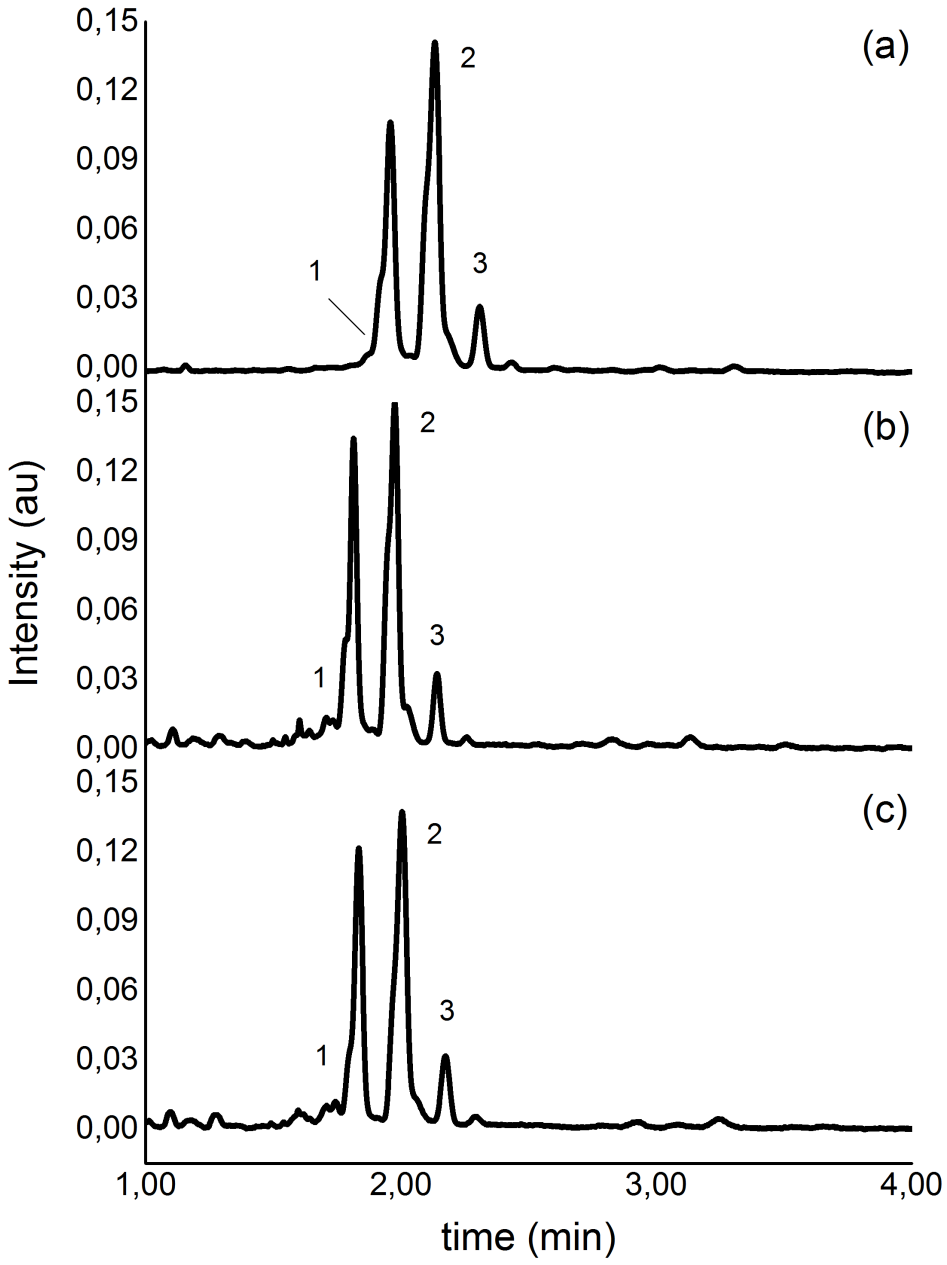

Figure 5.1: Chromatograms at 450 nm: 1. Lycopene, 2. Beta-carotene, 3. Coenzyme Q10. Clean-up procedures: (a) saponification; (b) Amberlite XAD7HP resin and (c) LLE with hexane. Chromatographic conditions: Acquity UPC^2 HSS C_{18} SB 3.0 x 150 mm, 1.8 μm column, mobile phase CO_2:EtOH (84.5:15.5, v/v), pressure 1500 psi, column temperature 40 ℃, sample temperature 5 ℃, flow rate 1.5 mL/min and injection volume 2 μL.

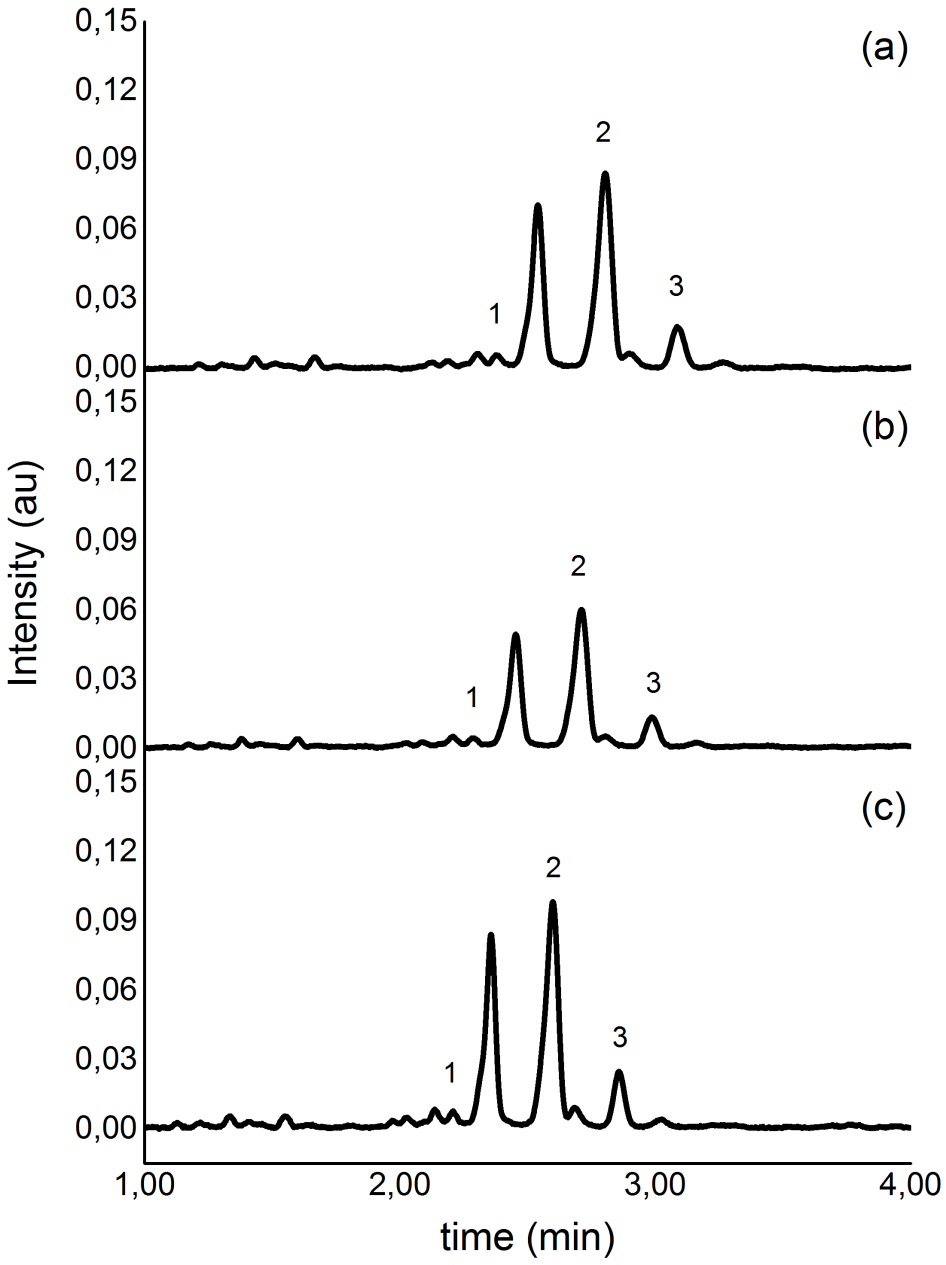

Figure 5.2: Chromatograms at 450 nm: 1. Lycopene, 2. Beta-carotene, 3. Coenzyme Q10. Clean-up procedures: (a) C18 SPE cartridge; (b) ENVI-8 SPE cartridge and (c) d-SPE with PSA and GCB sorbents. Chromatographic conditions: Acquity UPC^2 HSS C_{18} SB 3.0 x 150 mm, 1.8 μm column, mobile phase CO_2:EtOH (84.5:15.5, v/v), pressure 1500 psi, column temperature 40 ℃, sample temperature 5 ℃, flow rate 1.5 mL/min and injection volume 2 μL.

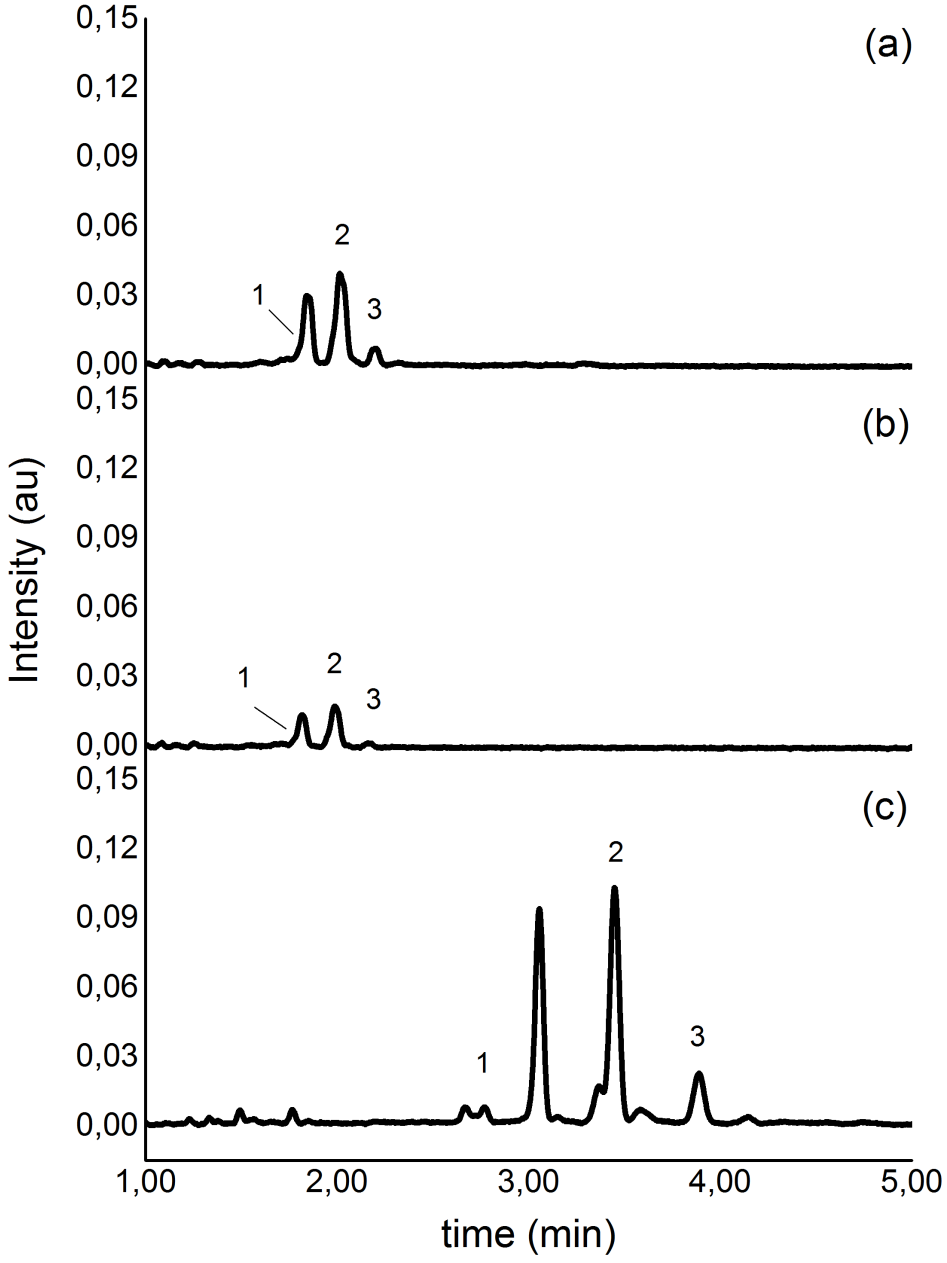

Figure 5.3: Chromatograms at 450 nm: 1. Lycopene, 2. Beta-carotene, 3. Coenzyme Q10. Clean-up procedures: (a) LLE with hexane and C18 SPE cartridge; (b) Amberlite XAD7HP resin with C18 SPE cartridge and (c) without clean-up procedure. Chromatographic conditions: Acquity UPC^2 HSS C_{18} SB 3.0 x 150 mm, 1.8 μm column, mobile phase CO_2:EtOH (84.5:15.5, v/v), pressure 1500 psi, column temperature 40 ℃, sample temperature 5 ℃, flow rate 1.5 mL/min and injection volume 2 μL.

5.3.2 Experimental Design

The influence of pressure (A), temperature (B) and ethanol percentage (C, C_E) on retention and separation factors of carotenoids and coenzyme Q10 in palm oil extract was investigated by design of experiments. Regression models were built for lycopene, beta-carotene and coenzyme Q10. Lutein is present in a low concentration and its peak is observed only with addition of the standard compound. Experiments with palm oil samples spiked with the standard mixture were also performed, but it was observed retention time shifts and changes in peak intensities due to sample precipitation which can be attributed to diluent volatility and also to differences in analyte solubility (data not shown). Carotenoid solubility depends on the presence of different functional groups. Carotenes, compounds containing only carbon and hydrogen in their backbone, are soluble in non-polar solvents, such as hexane, ethyl acetate and MTBE, while xantophylls, derivatives containing also oxygen, are soluble in polar solvents like ethanol and acetone [27]. Because of their differences in solubility, the stability of carotenoid mixture at high concentrations should be evaluated [27].

The chromatograms of some operating conditions employed in the design of experiments are shown in Figure 5.4. The results showed that at low pressure, retention times were more affected by an increase in ethanol percentage (Figures 5.4a and 5.4c) than at high pressure (Figures 5.4b and 5.4d). The results also showed that at the same temperature and ethanol percentage, retention times were slightly lower at high pressures than at low pressures (Figures 5.4a and 5.4b) while no significant changes were observed at high ethanol percentage (Figures 5.4c and 5.4d). The results clearly showed that lycopene peak shape was more affected by changes in the operating conditions than beta-carotene and coenzyme Q10 peaks.

Retention Factor

ANOVA showed that the quadratic model was suitable to describe the retention of lycopene, beta-carotene and coenzyme Q10 where Prob<0.05 indicates that the model coefficients are significant in a 95% confidence level (Table 5.2). The F-values of regression significance were 329.29, 679.02 and 30.13 for lycopene, beta-carotene and coenzyme Q10 models, respectively, indicating that the retention strongly de-

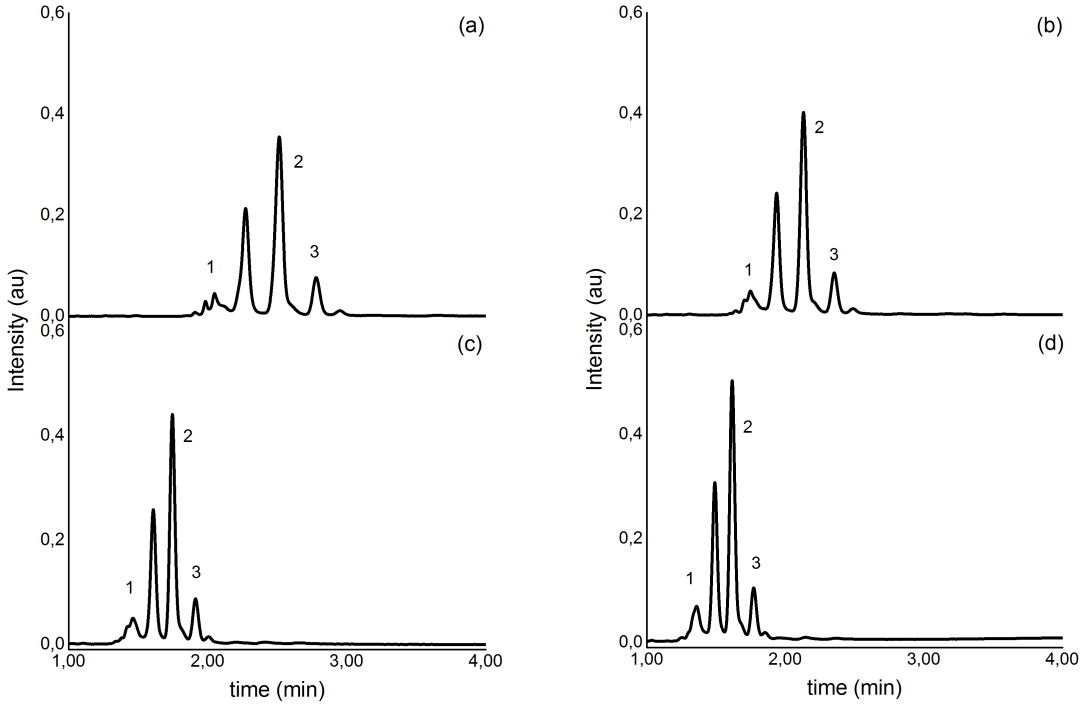

Figure 5.4: Chromatograms of the experimental design at 430 nm: 1. Lycopene, 2. Beta-carotene, 3. Coenzyme Q10. Experimental conditions: (a) 16% of ethanol, temperature 25 ℃ and pressure 1500 psi; (b) 16% of ethanol, temperature 25 ℃ and pressure 2200 psi; (c) 24% of ethanol, temperature 25 ℃ and pressure 1500 psi; (d) 24% of ethanol, temperature 25 ℃ and pressure 2200 psi.

pends on the operational conditions within the studied range of the factors. The results indicated that linear and interaction coefficients were significant for the three models. Additionally, the second-order effect C^2 (ethanol percentage, C_E) was also significant for all models. The second-order effect B^2 (temperature) was significant only for lycopene and beta-carotene models while the second-order effect A^2 (pressure) was not significant.

As shown in Table 5.3, the F-values of lack of fit were 11.72, 5.73 and 1.53 for lycopene, beta-carotene and coenzyme Q10, respectively, indicating that only for the lycopene model a lack of fit was observed (the tabulated value of F 5.4, 95% is 6.26). The coefficients of determination (R^2) were > 0.96 while the adjusted coefficients of determination (adjusted R^2) were > 0.95 for all models. The prediction R^2 were 0.9434, 0.9794 and 0.8267 for lycopene, beta-carotene and coenzyme Q10 models, respectively. The adjusted R^2 and the prediction R^2 values were in reasonable agreement, as the difference between these two values was less than 0.2. The

Table 5.2: ANOVA for the quadratic model for the retention factors of lycopene, beta-carotene and coenzyme Q10.

Source	Sums of squares	DF	Mean square	F value	Prob> F
Lycopene					
Model	0.46	9	0.052	329.29	< 0.0001
A-P	0.10	1	0.10	641.24	< 0.0001
B-T	0.012	1	0.012	75.20	< 0.0001
C-C$_E$	0.32	1	0.32	2034.60	< 0.0001
AB	0.011	1	0.011	72.08	< 0.0001
AC	6.9×10^{-3}	1	6.9×10^{-3}	43.94	< 0.0001
BC	2.9×10^{-3}	1	2.9×10^{-3}	18.34	0.0020
A²	1.5×10^{-4}	1	1.5×10^{-4}	0.99	0.3467
B²	2.3×10^{-3}	1	2.3×10^{-3}	14.99	0.0038
C²	1.3×10^{-3}	1	1.3×10^{-3}	8.41	0.0176
Beta-carotene					
Model	0.53	9	0.058	679.02	< 0.0001
A-P	0.10	1	0.10	1195.46	< 0.0001
B-T	0.014	1	0.014	162.04	< 0.0001
C-C$_E$	0.37	1	0.37	4363.82	< 0.0001
AB	0.010	1	0.010	120.39	< 0.0001
AC	4.9×10^{-3}	1	4.9×10^{-3}	56.96	< 0.0001
BC	4.0×10^{-3}	1	4.0×10^{-3}	46.47	< 0.0001
A²	1.7×10^{-4}	1	1.7×10^{-4}	2.02	0.1894
B²	2.7×10^{-3}	1	2.7×10^{-3}	31.47	0.0003
C²	1.6×10^{-3}	1	1.6×10^{-3}	18.31	0.0021
Coenzyme Q10					
Model	0.13	9	0.015	30.13	< 0.0001
A-P	0.017	1	0.017	35.20	0.0002
B-T	4.0×10^{-3}	1	4.0×10^{-3}	8.07	0.0194
C-C$_E$	0.091	1	0.091	184.26	< 0.0001
AB	5.4×10^{-3}	1	5.4×10^{-3}	11.03	0.0089
AC	4.5×10^{-3}	1	4.5×10^{-3}	9.21	0.0141
BC	5.0×10^{-3}	1	5.0×10^{-3}	10.14	0.0111
A²	3.8×10^{-4}	1	3.8×10^{-4}	0.78	0.4002
B²	1.8×10^{-5}	1	1.8×10^{-5}	0.038	0.8506
C²	5.3×10^{-3}	1	5.3×10^{-3}	10.73	0.0096

low PRESS values, 0.011-0.026, suggest that the regression models are suitable for predictive applications. The values of coefficient of variation (CV) were 0.50, 0.35 and 1.42 for lycopene, beta-carotene and coenzyme Q10, respectively. Adequate precision values were 73.848, 105.070 and 23.346 for lycopene, beta-carotene and coenzyme Q10. These values measure the signal to noise ratio and a ratio greater than 4 is desirable [82], [107].

Table 5.3: Statistical parameters for the quadratic model of lycopene, beta-carotene and coenzyme Q10.

Statistical parameters	**Lycopene**	**Beta-carotene**	**Coenzyme Q10**
Lack of fit	11.72	5.73	1.53
R^2	0.9970	0.9985	0.9679
Adjusted R^2	0.9939	0.9971	0.9538
Prediction R^2	0.9434	0.9794	0.8267
PRESS	0.026	0.011	0.024
C.V. %	0.50	0.35	1.42
Adequate precision	73.848	105.070	23.346

The graphical representation of the coefficients for the regression models of the retention factors is presented in Figure 5.5. The main effect of ethanol percentage (C_E, C) was the most significant parameter for the retention of all analytes, with negative effect, i.e., a decrease in ethanol percentage in the mobile phase lead to an increase on the retention factor. Pressure (A) was the second most significant factor studied and it had nearly the same influence on the retention factors of lycopene and beta-carotene while it had a lower influence on the retention factor of coenzyme Q10. Temperature (B) had a minor effect on the retention factors as illustrated in Figure 5.5. The second order models obtained for the retention factors in terms of coded factors were:

$$\begin{aligned} lnk_{lycopene} &= 2.45 - 0.10A - 0.034B - 0.18C - 0.038AB + 0.029AC \\ &\quad - 0.019BC + 7.516 \times 10^{-3}A^2 + 0.029B^2 + 0.022C^2 \end{aligned} \tag{5.2}$$

$$\begin{aligned} lnk_{beta-carotene} &= 2.65 - 0.10A - 0.037B - 0.19C - 0.036AB + 0.025AC \\ &\quad - 0.022BC + 7.961 \times 10^{-3}A^2 + 0.031B^2 + 0.024C^2 \end{aligned} \tag{5.3}$$

$$\begin{aligned} lnk_{coenzymeQ10} &= 1.55 - 0.042A - 0.020B - 0.095C - 0.026AB + 0.024AC \\ &\quad - 0.025BC - 0.012A^2 - 2.607 \times 10^{-3}B^2 + 0.044C^2 \end{aligned} \tag{5.4}$$

Figure 5.6 shows surface response plots of lycopene, beta-carotene and coenzyme Q10 retention factors illustrating the dependency of these responses on ethanol percentage and pressure at 25 ℃ and 50 ℃. The correlation between the retention factors and the independent variables can be readily seen in the response surface plots. It is interesting to point out that an increase in pressure at high ethanol

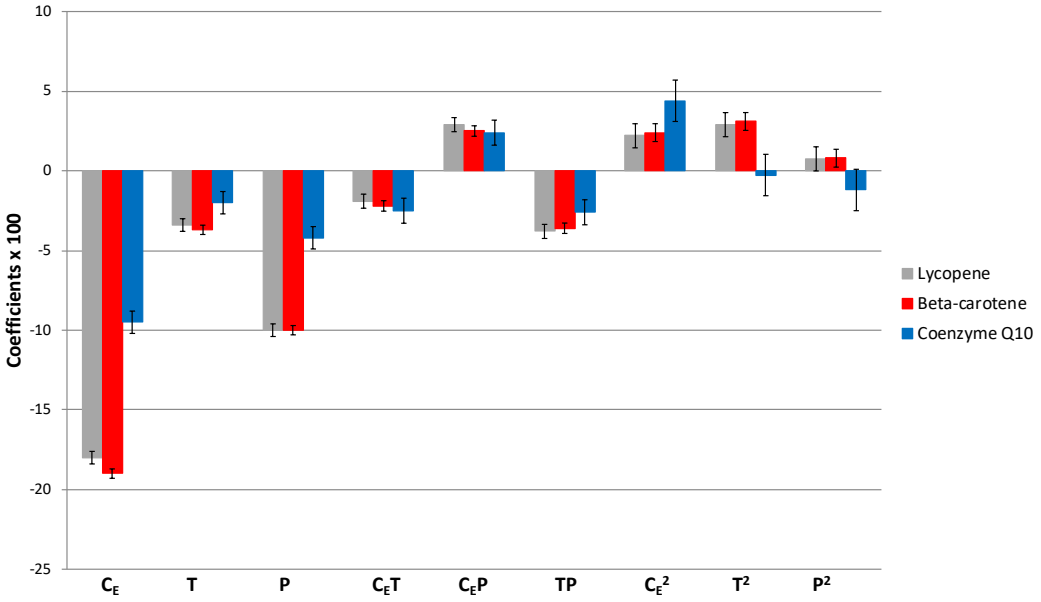

Figure 5.5: Coefficients of the model for the retention factor of lycopene, beta-carotene and coenzyme Q10. The error bars represent the 95% confidence interval of the coefficients. A is the pressure, B is the temperature and C is the ethanol percentage (C_E); AB, AC and BC are the interaction terms; A^2, B^2 and C^2 are the second-order terms.

percentage did not affect significantly the retention factors while significant changes were observed at low ethanol percentage.

Selectivity

The polynomial regression models were not in good agreement with experimental results. Carotenoids and coenzyme Q10 eluted in close proximity and minor changes in the operating conditions resulted in beta-carotene and coenzyme Q10 co-elution. This pair of peaks was considered critical in the method development. Then, two additional operating conditions were selected by evaluating the chromatograms. The additional experiments were carried out in order to obtain adequate overall separation between beta-carotene and coenzyme Q10. Experiments were performed with palm oil samples spiked with coenzyme Q10 to evaluate the separation. One experiment was carried out at pressure of 1850 psi, column temperature 25 ℃ and 18% ethanol and the other one was conducted at pressure of 1600 psi, column temperature 40 ℃ and 18% ethanol. Chromatograms obtained under these operating conditions are shown in Figure 5.7. It was observed co-elution between beta-carotene and coen-

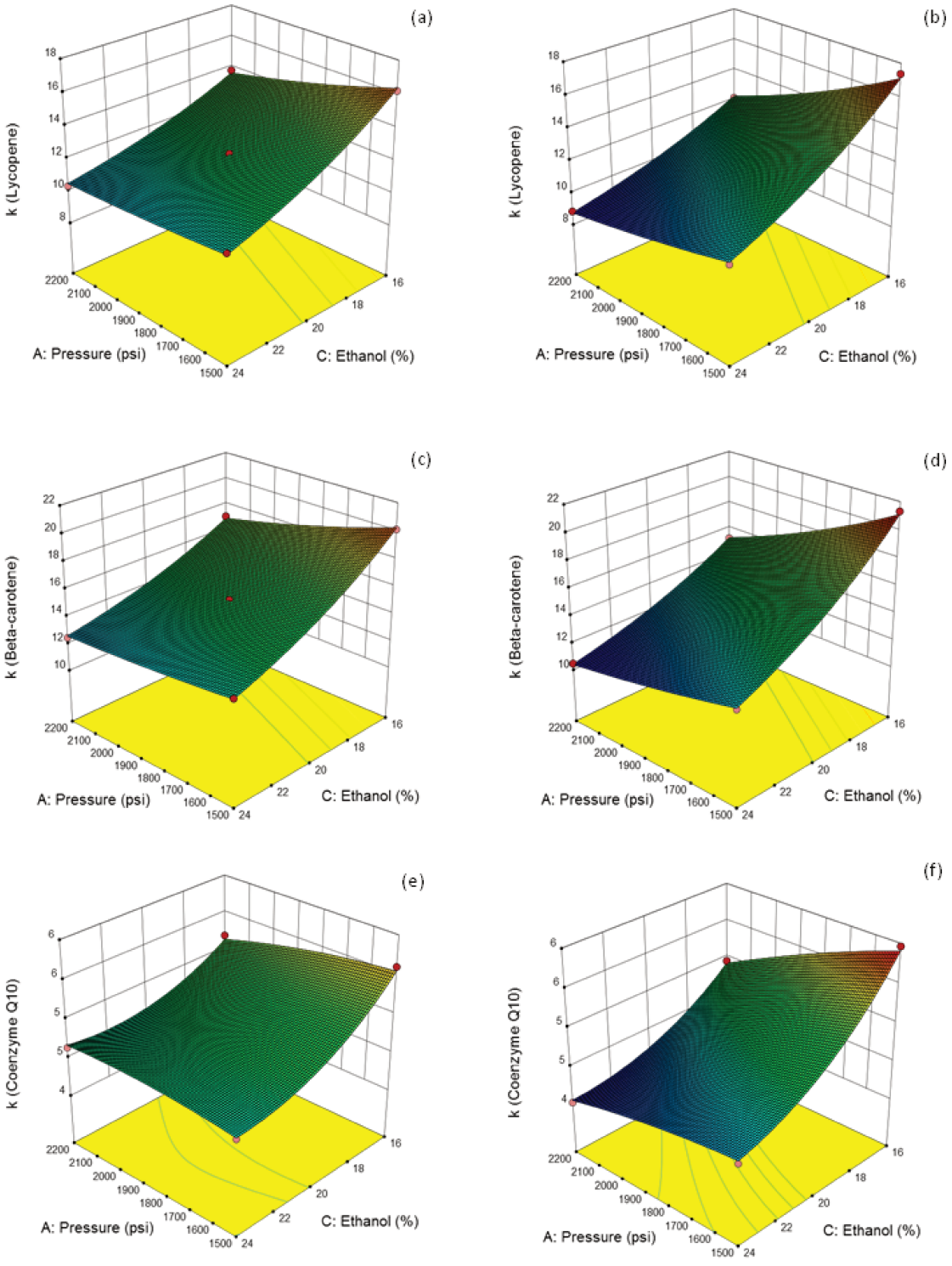

Figure 5.6: Response surface plots of the retention factors as a function of ethanol percentage and pressure at 25 ℃ on the left and 50 ℃ on the right.

zyme Q10 peaks in the first condition (Figure 5.7a), while baseline resolution was achieved in the second one. Based on these results, the operating conditions se-

lected for quantification of carotenoids and coenzyme Q10 in palm oil extract were: pressure 1600 psi, column temperature 40 ℃ and 18% of ethanol.

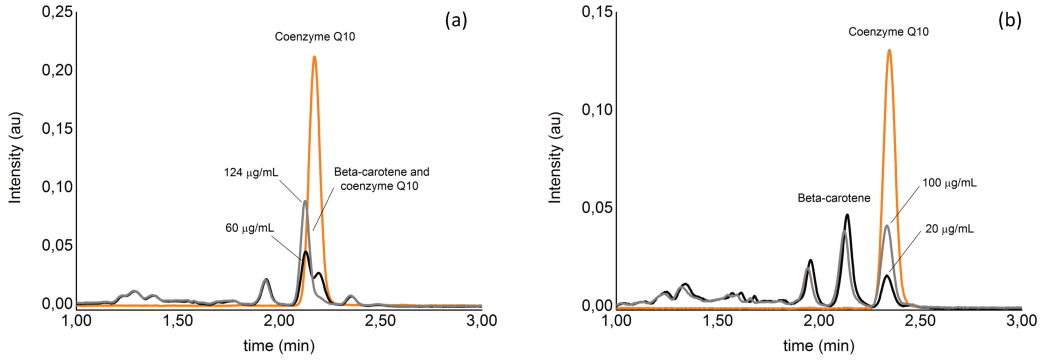

Figure 5.7: Chromatograms of palm oil samples spiked with coenzyme Q10 at 275 nm. Chromatographic conditions: (a) pressure 1850 psi, column temperature 25 ℃ and 18% of ethanol, and (b) 1600 psi, column temperature 40 ℃ and 18% of ethanol.

5.3.3 Quantification of Carotenoids and Coenzyme Q10 in Palm Oil Extract

Quantification of carotenoid and coenzyme Q10 was carried out by UHPSFC. Palm oil samples were spiked with each standard compound in the concentration range: 50 to 500 μg/mL for beta-carotene, 8 to 100 μg/mL for coenzyme Q10 and 8 to 60 μg/mL for lutein. Calibration curves were built separately due to differences in analyte solubilities. Chromatograms of palm oil samples spiked with beta-carotene, coenzyme Q10 and lutein are shown in Figure 5.8.

Palm oil is a highly complex matrix. The broad variety of constituents and the difficulty in separating carotenoid geometrical isomers represented an additional degree of complexity on the separation and quantification of beta-carotene, coenzyme Q10 and lutein. The chemometric method MCR-ALS was used to resolve some interference co-eluting with the target compounds. MCR-ALS method has been widely used to solve co-elution, retention time shifts, among other chemical problems found in chromatographic data [111], [112], [113], [114], [115]. The assumption of MCR-ALS method is that the experimental data fulfills a bilinear model. The method decomposes the data into two matrices C and S^T as described in equation

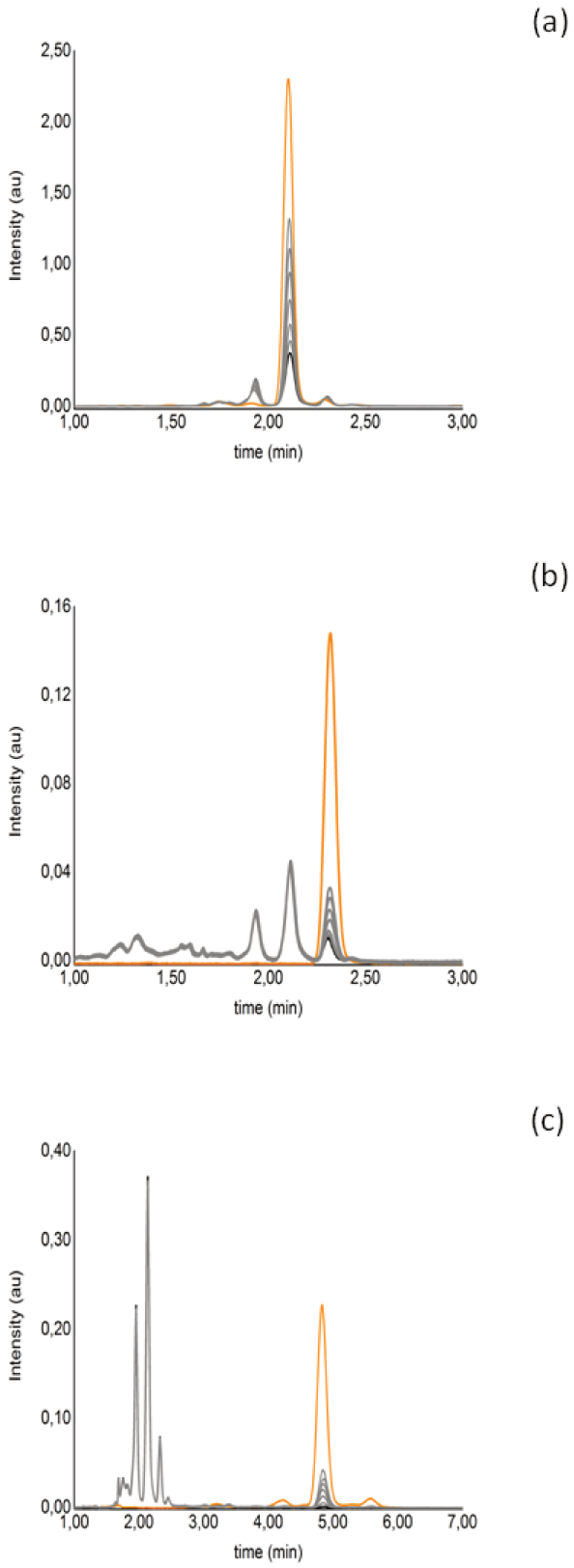

Figure 5.8: Chromatograms of palm oil samples spiked with (a) beta-carotene, (b) coenzyme Q10 and (c) lutein. Chromatogram colors refer to palm oil samples (black), fortified palm oil samples (grey) and standard compounds (orange).

5.5:

$$D = CS^T + E \tag{5.5}$$

where D is the cube data set of spectral profile at each wavelength for samples with different concentration of the analytes, and C and S are matrices with the concentration and spectra profiles of the components in the mixture. E is the matrix of the data variance not explained by the components in C and S [114], [115].

Palm oil chromatographic data was evaluated by MCR-ALS to properly identify and quantify beta-carotene, coenzyme Q10 and lutein. Elution and spectral profiles of the target compounds were retrieved by solving equation 5.5 iteratively by alternating least squares optimization under the constrains, non-negativity and unimodality. Elution and spectral profiles retrieved by MCR-ALS are illustrated in Figure 5.9. As can be seen in Figure 5.9a, beta-carotene co-eluted with an unknown compound. It is interesting to note that the unknown compound has an UV/Vis spectrum characteristic of a carotenoid with respect to the fine structure (Figure 5.9b). Coenzyme Q10 also co-eluted with an unknown compound (Figures 5.9c and 5.9d). The results suggest that this unknown compound might be a lutein isomer. Lutein peak was only observed in fortified palm oil samples (Figures 5.9e and 5.9f). However, a comparison among the spectra of unknown compounds 1 and 2 with lutein standard showed great similarity in their fine structure (Figure 5.10). The difference between the spectrum of the unknown compound 2 and the others is the position of the *cis* peak around 330 nm. Lutein geometrical isomers, 13-Z and 13'-Z, 9-Z and 9'-Z, have been reported in literature [116]. Additionally, the intensity of the *cis* peak gives insight into the position of the *cis* double bond, its intensity increases as the position of the double bond approaches the center of the molecule [117].

Carotenoids are present in 500-700 ppm in palm oil. Beta-carotene is the major carotenoid and accounts for 50-56.02% of total carotenoid content in palm oil. Lycopene is 1.0-1.3% while xanthophylls, which include lutein, accounts for 2.2%. Coenzyme Q10 is present in 10-80 ppm. Table 5.4 shows the concentration of beta-carotene, coenzyme Q10 and lutein in palm oil extract determined by MCR-ALS. Pseudo-univariate calibration curves for the MCR-ALS models for beta-carotene,

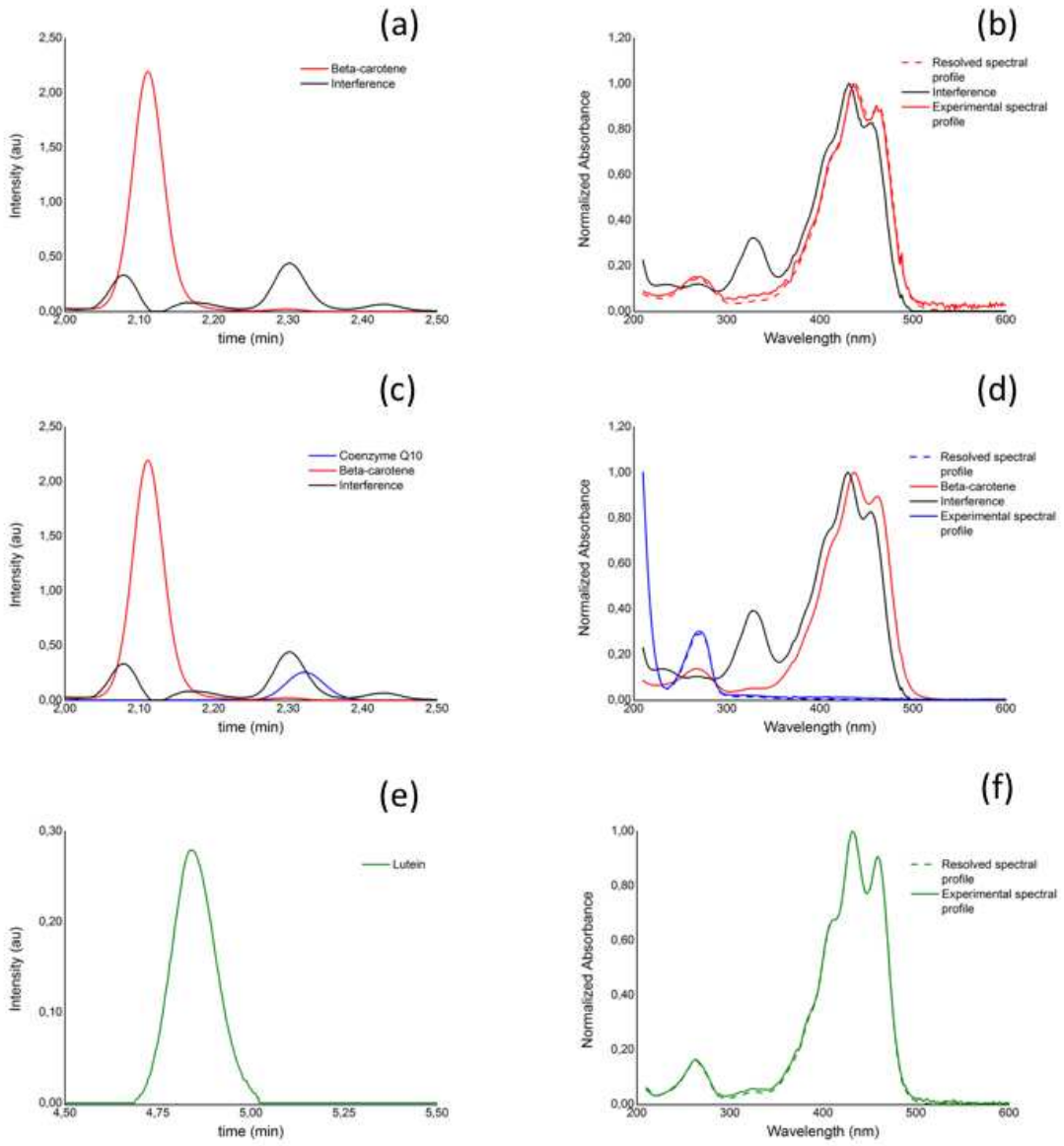

Figure 5.9: MCR-ALS recovery of elution profiles of (a) beta-carotene, (c) coenzyme Q10 and (e) lutein. Recovered and experimental spectral profiles of (b) beta-carotene, (d) coenzyme Q10 and (f) lutein.

coenzyme Q10 and lutein are shown in Figures 5.11, 5.12 and 5.13 in Supplementary Material.

Beta-carotene concentration was found to be 176 μg/mL in palm oil extract. A study developed by Choo *et al.* (2005) employed SFC in a quantitative analysis of carotenoids and other minor components from palm oil. Ethanol (4%) was used as organic modifier and carotenoids, vitamin E, sterols and squalene were isolated in less than 20 minutes. Carotenoids were quantified as total beta-carotene since it is the major carotenoid in palm oil. The amount of carotenoids in crude palm

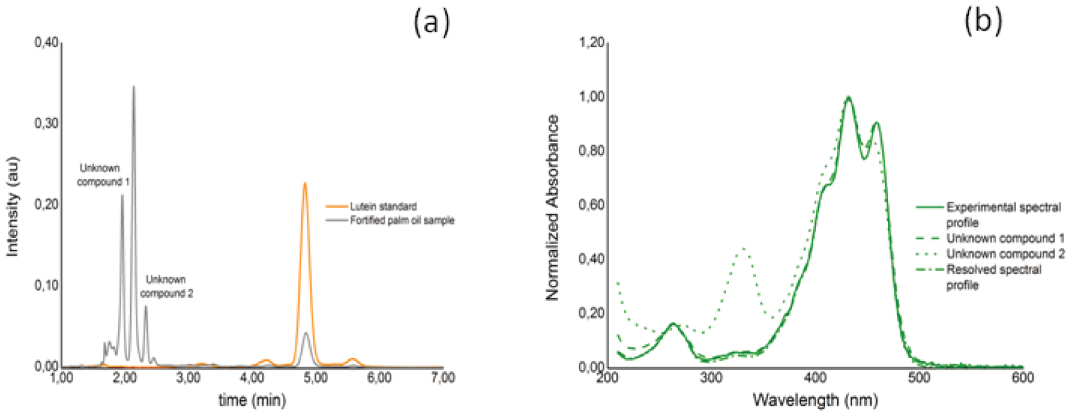

Figure 5.10: (a) Chromatograms of lutein standard compound (orange) and fortified palm oil sample with lutein (grey) and (b) Comparison of spectral profiles of unknown compounds, lutein standard compound and resolved spectral profile of lutein by MCR-ALS.

Table 5.4: Linear regression data obtained for carotenoids and coenzyme Q10.

Compound	**Concentration (μg/mL)**	**Linear range (μg/mL)**	
Beta-carotene	176	50-500	
Coenzyme Q10	8.29	8-100	
Lutein	2.90	8-60	
Compound	**Slope**	**Intercept**	**R^2**
Beta-carotene	0.4022	70.825	0.9983
Coenzyme Q10	0.0857	0.7107	0.9885
Lutein	0.3913	-1.1371	0.9829

oil was 550 ± 10 ppm [9]. Mortensen *et al.* (2005) determined beta-carotene and its isomers in palm oil by HPLC. Mobile phase was MTBE:methanol:H_2O (15:81:4, v/v) as solvent A and MTBE:methanol (10:1, v/v) as solvent B in a linear gradient going from 0% to 100% of B in 75 minutes. The authors employed peak heights for quantification of beta-carotene due to peak overlapping. Total beta-carotene content in palm oil was 179.4 g/kg [118]. In another study, Darnoko *et al.* (2000) quantified 13 carotenoids in palm oil by HPLC employing methanol:MTBE:H_2O (81:15:4, v/v) as solvent A and MTBE:metanol (91:9, v/v) as solvent B. The gradient elution was 100% A to 50% A in 45 minutes followed by 100% B in the next 10 minutes and 100% A in the next 5 minutes. Concentration of beta-carotene trans-isomer was determined as being 126.58 ppm and the total beta-carotene content was 190.31 ppm which accounted for the cis-isomers [119].

Coenzyme Q10 concentration was 8.29 μg/mL in palm oil extract. Han *et al.* (2006) evaluated the separation of coenzyme Q10 from palm oil and palm fiber oil by SFC. Methanol was employed as organic modifier. The results showed that coenzyme Q10 concentration varies from 10-80 ppm in crude palm oil and 1000-1500 ppm in palm fiber oil [10].

Lutein content in palm oil extract was determined as 2.90 μg/mL. As previously discussed, it was postulated that other isomers of lutein might be present in the sample as a comparison among the spectra of unknown compounds and lutein spectrum showed great similarity in their fine structure. The results suggest that MCR-ALS analysis accounted only for the amount of lutein standard added to palm oil extracts. Aruna *et al.* (2009) determined lutein content in selected vegetable oils by HPLC using mobile phase acetonitrile:dichloromethane:methanol (6:2:2, v/v) containing 0.1% ammonium acetate in 30 minutes. Lutein content in palm oil was 11.55 μg/100 g of oil [120]. Furthermore, Darnoko *et al.* (2000) quantified lutein among other 12 carotenoids in palm oil by HPLC employing methanol:MTBE:H_2O (81:15:4, v/v) as solvent A and MTBE:metanol (91:9, v/v) as solvent B. The gradient elution was 100% A to 50% A in 45 minutes followed by 100% B in the next 10 minutes and 100% A in the next 5 minutes. Concentration of lutein in palm oil was 11.85 ppm [119].

In contrast to HPLC studies, carotenoid and coenzyme Q10 separation was accomplished in less than 7 minutes by UHPSFC. Additionally, UHPSFC analysis was carried out with a lower consumption of organic solvent in comparison with HPLC methods. Gradient elution was not considered in this study because further studies will be performed to scale-up the analytical method to preparative scale.

5.4 Conclusions

In this study, an analytical method for the recovery and quantification of beta-carotene, coenzyme Q10 and lutein in palm oil extract was developed by UHPSFC. During method development, co-elution of some matrix components and the analytes were observed. Furthermore, lower S/N ratios and retention time shifts of the analytes in palm oil in relation to their standards were also observed which made it difficult to identify and quantify the target compounds. Clean-up procedures

employing SPE cartridges, d-SPE sorbents, LLE with hexane, Amberlite XAD7HP resin and saponification were evaluated in order to physically reduce interferences. The clean-up procedures were not suitable for interference removal from palm oil matrix, and hence a clean-up procedure was not considered in the method development.

Quantification of carotenoids and coenzyme Q10 were carried out under the optimized chromatographic conditions: Viridis HSS C_{18} SB 3.0 x 150 mm column with particle size of 3.5 μm, CO_2:EtOH (82:18, v/v), pressure 1600 psi, column temperature 40 ℃, sample manager temperature 17 ℃, equilibration time between injections 4 minutes, flow rate 1.5 mL/min and injection volume 2 μL. Data analysis was performed by MCR-ALS and the results clearly showed good correlation between the experimental results and the ones recovered by MCR-ALS. Concentration of beta-carotene, coenzyme Q10 and lutein in palm oil extract determined by MCR-ALS was 176, 8.29 and 2.90 μg/mL, respectively. These results opened new perspectives in the recovery of high-value minor components from palm oil extract by UHPSFC, and an integration of carotenoid and coenzyme Q10 recovery directly into biodiesel production will advance the overall economy of industrial plants.

5.5 Supplementary Material

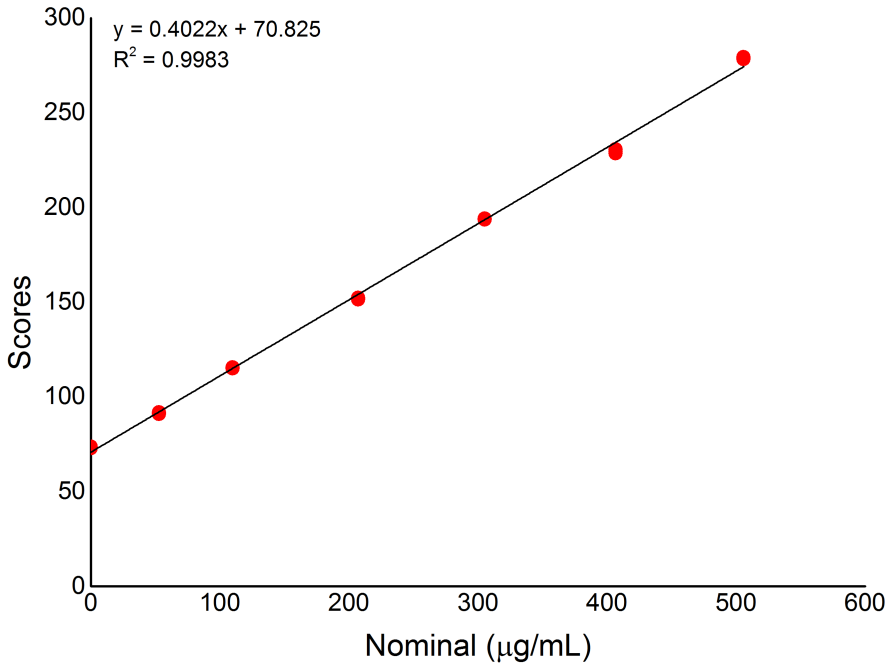

Figure 5.11: Calibration curve for the MCR-ALS model for beta-carotene.

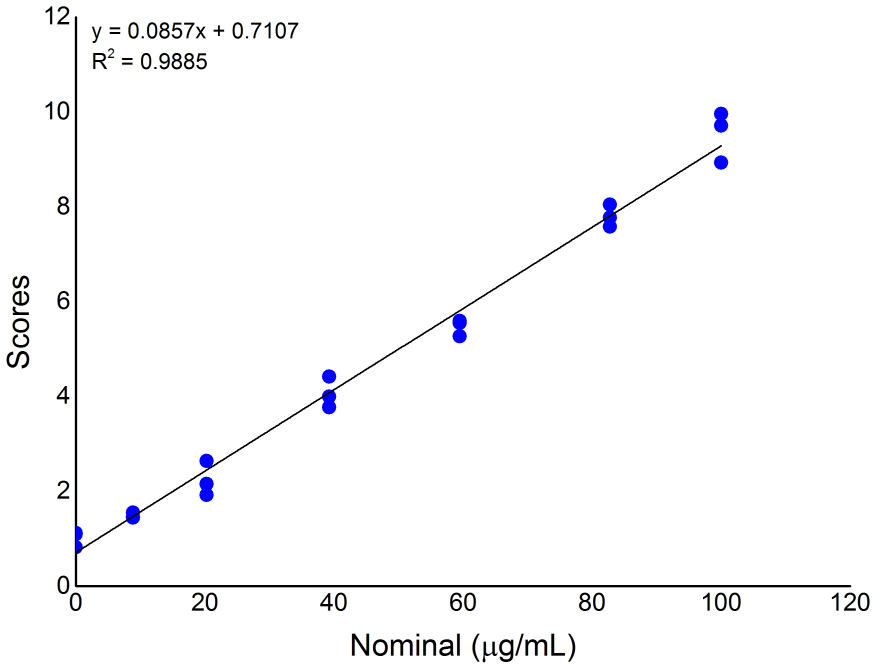

Figure 5.12: Calibration curve for the MCR-ALS model for coenzyme Q10.

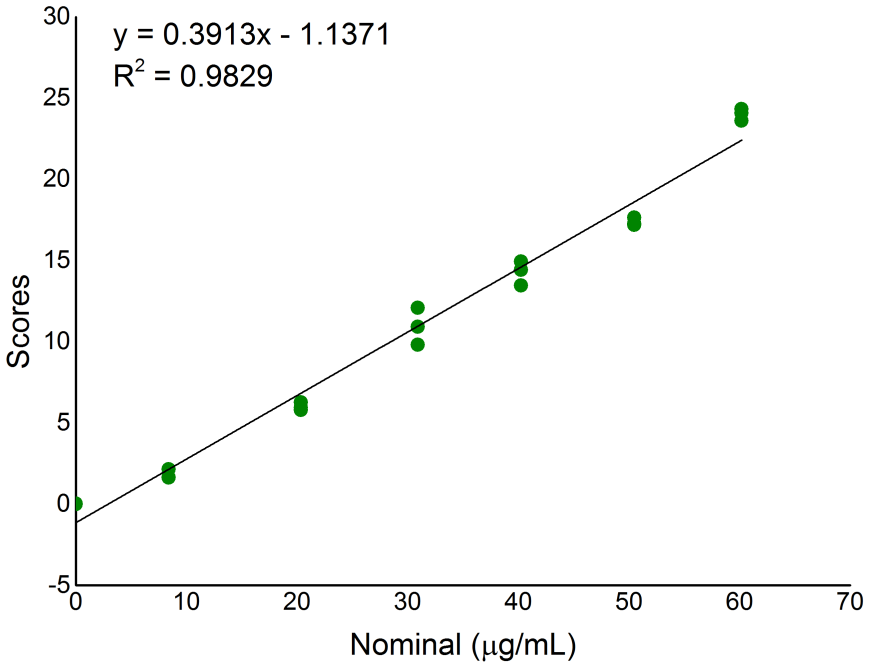

Figure 5.13: Calibration curve for the MCR-ALS model for lutein.

6 | Application of Fourier transform infrared spectroscopy (FTIR) combined with partial least squares (PLS) regression for determination of minor constituents in palm oil

Beta-carotene, coenzyme Q10 and lutein are high valuable minor constituents of palm oil (*Elaeis guineensis* Jacq.). A feasibility study for a rapid assessment of these bioactive compounds using Fourier transform infrared (FTIR) spectroscopy in conjunction with chemometrics was investigated. First, principal component analysis (PCA) was applied in the spectral data in an attempt to distinguish palm oil from beta-carotene, coenzyme Q10 and lutein standard compounds. PCA scores plot revealed four distinct clusters, and 93% of the total variance was explained by the first two components. PCA loadings plot indicated the absorption bands that most contributed to distinguish palm oil and the standard compounds arose from groups in the triglyceride constituents of the palm oil. After exploratory data analysis, calibration models were developed employing partial least squares regression (PLS). The calibration models were built with the entire spectral range (4000 to 400 cm^{-1}). Statistic performance of the models was evaluated by the coefficient of determination for calibration (R^2_{cal}), root-mean-square error of calibration (RMSEC) and standard error of calibration (SEC). The coefficients of determination (R^2_{cal}) were 0.9790, 0.8935 and 0.9591 for beta-carotene, coenzyme Q10 and lutein models, respectively. Beta-carotene, coenzyme Q10 and lutein content in palm oil determined by PLS regression were 178, 12.8 and 2.90 μg/mL, respectively. These values showed good agreement with the reference values obtained by ultra-high performance supercritical fluid chromatography (UHPSFC). The results demonstrated the feasibility of FTIR spectroscopy coupled with chemometrics for quantifying beta-carotene, coenzyme Q10 and lutein content in palm oil.

6.1 Introduction

Oil palm (*Elaeis guineensis* Jacq.) is a perennial plant that originated in West Africa [121]. From *E. guineensis* fruits two distinct types of oil are produced: crude palm oil (CPO) extracted from the mesocarp which contains 20-22% of oil and palm kernel oil (PKO) obtained from the kernel which has 38-55% of oil content [14], [121]. CPO is used to produce biodiesel, food products, industrial chemicals, cosmetics and pharmaceuticals while the main use of PKO is as component of personal care products [122], [123]. Owing to its price competitiveness, palm oil is the most globally traded vegetable oil whose production volume is expected to jump from 70.46 million metric tons in 2017 and 2018 to 73.49 million metric tons in 2018 and 2019 [122], [124]. The five leading producing countries of *E. guineensis* are Indonesia, Malaysia, Thailand, Colombia and Nigeria. Indonesia and Malaysia account for more than 86% of the world production [125]. Although Brazil is not in the top 5 producers, its production is expected to increase from 3.04 million metric tons in 2015 up to 7.44 million metric tons in 2020 [126].

Given historical links between deforestation and palm oil development worldwide, several initiatives have been taken to promote more sustainable palm oil production [127]. In 2004, the Roundtable on Sustainable Palm Oil was established as a response for the global call for a green economy. Stemming from the Roundtable on Sustainable Palm Oil initiative, ensued environmental and social criteria, which companies must comply for them to obtain certification for sustainable palm oil production. Members of Roundtable on Sustainable Palm Oil include oil palm growers, processors and traders, consumer goods manufactures, environmental NGOs, banks, investors and retailers [128], [129]. Most of the Roundtable on Sustainable Palm Oil compliant palm oil is sourced from Indonesia and Malaysia, but Papua New Guinea and Brazil are also important suppliers of certified palm oil [129]. In 2012, given the commitment of the Brazilian largest palm oil producer, Brazil had 46% of its domestic production Roundtable on Sustainable Palm Oil certified [129]. In 2010, the Brazilian government launched the Sustainable Palm Oil Production Program to support palm oil cultivation as means to reduce environmental impact, to promote socioeconomic development and to diversify biodiesel feedstock [127].

Palm oil is mainly composed of triglycerides, a lower amount of free fatty acids and 1% of minor components, such as carotenoids (500-700 ppm), coenzyme Q10 (10-80 ppm), vitamin E (600-1000 ppm), sterols (250-620 ppm), squalene (200-600 ppm) and phospholipids (20-100 ppm) [14], [18]. Carotenoids and coenzyme Q10 are high value minor constituents of palm oil, displaying antioxidant capacity. These bioactive compounds have been associated with a number of health benefits.

Several studies have shown that their antioxidant capacity help prevent cancer, diabetes and cardiovascular diseases [20], [79]. In addition to their medicinal use, the importance of carotenoids and coenzyme Q10 has increased due to their use in the feed, food, pharmaceutical and personal care products. In order to maximize palm oil resources, extraction of minor components would add value to the whole processing operation.

Chromatographic methods, such as high-performance liquid chromatography coupled with photodiode array detector (HPLC-DAD) and high-performance liquid chromatography associated with mass spectrometry (HPLC-MS) are the most common methods used to quantify minor constituents of palm oil. However, these methods usually require sample preparation and are time-consuming. Spectroscopic techniques as Fourier transform infrared (FTIR) spectroscopy are an attractive alternative to chromatographic methods due to their low solvent requirement, little or no sample preparation, short analysis, and ease of operation [130].

Previously, spectroscopic techniques associated with chemometrics analysis have been widely used to investigate geographical origin of palm oil and to quantify major and minor constituents [68], [74], [75], [76]. Jolayemi *et al.* [131] evaluated principal component analysis (PCA) and orthogonal projection to latent structure discriminant analysis (OPLS-DA) for geographical determination of palm oils. UV-Vis data and carotenoid content among other variables were used to build statistical models. Ripeness, oil content and free fatty acid level of palm oil fresh fruit bunches were determined by a rapid portable non-contact and non-destructive approach. In this study, visible and near infrared (NIR) data and chemical analysis were used to assess fresh fruit bunches. Two statistical analyses were performed to model the quality of fresh fruit bunches, the forward-stepwise multiple linear regression (FS-MLR), and a combination of PCA with multilayer perceptron neural network

(PCA-MLP). Overall, the models built with FS-MLR methods performed better than the PCA-MLP models [132].

Szydlowska-Czerniak *et al.* (2011) applied PCA to determine whether palm oil samples could be distinguished from different refining processes. The results indicated that antioxidant capacity as well as total phenolics and carotenoids content could be employed as indicators to differentiate palm oil samples from two different refining processes [133]. In another study, Moh *et al.* (1999) evaluated FTIR and NIR spectroscopy combined with partial least squares (PLS) to assess beta-carotene content in palm oil [11]. Similarly, Ammawath *et al.* (2010) developed a method for determination of beta-carotene in refined, bleached and deodorized (RBD) palm olein using FTIR. The results showed that the accuracy of the FTIR method was comparable to the one developed by HPLC [12]. Unfortunately, no FTIR-based methdos have been developed for the simultaneous determination of beta-carotene, coenzyme Q10 and lutein in palm oil by FTIR spectroscopy combined with chemometrics. This work reports on the development of FTIR-based calibration model to be used for the determination of beta-carotene, coenzyme Q10 and lutein content in palm oil.

6.2 Materials and Methods

6.2.1 Chemicals and Reagents

HPLC-grade methyl tert-butyl ether (MTBE) and standard compounds of beta-carotene, coenzyme Q10 and lutein were purchased from Sigma-Aldrich. Palm oil extract was kept at 10 ℃ and the standard compounds at -4 ℃ until used. Palm oil was extracted at Universidade Tiradentes (Sergipe, Brazil).

6.2.2 Methodology

Sample Preparation

Calibration models were developed with palm oil samples (400 mg) spiked with beta-carotene, coenzyme Q10 and lutein. A set of 9 samples were prepared for each standard in the following concentration range: 150 to 450 μg/mL for beta-carotene,

9 to 100 μg/mL for coenzyme Q10 and 9 to 17 μg/mL for lutein. Carotenoids and coenzyme Q10 were dissolved in MTBE. Samples were heated up to 40 ℃ for 5 minutes to dissolve the standard compound in palm oil and also to remove the solvent.

Fourier Transform Infrared Spectrometer

Spectrum Two FTIR spectrometer (Perkin-Elmer, Waltham, MA) equipped with an universal attenuated total reflectance (UATR) accessory was employed in the study. Spectra were collected against air as a background over the wavenumber region of 4000 to 400 cm^{-1}. Samples were scanned 6 times, and for each spectrum 8 scans were averaged to obtain acceptable signal-to-noise ratio. Spectral resolution was set to 4 cm^{-1}. Crystal was carefully cleaned between analysis with isopropyl alcohol to remove sample resides. Spectrum 10 software was used for instrument control and data acquisition.

Data Analysis

Data analysis was performed with The Unscrambler version 9.0 (CAMO Software Inc., Woodbridge, NJ). FTIR spectra were baseline corrected, mean-normalized and the spectral resolution averaged by 4 cm^{-1}. First, a study was conducted with pure palm oil extract and the standard compounds to evaluate the capability of PCA to distinguish the samples using their full spectral profile as variables.

After exploratory data analysis, calibration models were built using PLS regression. This method was applied to model a linear relation between the FTIR spectral data and the concentrations of beta-carotene, coenzyme Q10 and lutein in palm oil. PLS models were evaluated by cross-validation (leave-one-out), and their statistic performance by means of coefficient of determination for calibration (R^2_{cal}), cross-validation (R^2_{cv}), root-mean-square error of calibration (RMSEC), standard error of calibration (SEC), root-mean-square error of cross validation (RMSECV) and standard error of cross-validation (SECV) [72].

6.3 Results and Discussion

6.3.1 Fourier Transform Infrared Spectra

FTIR spectroscopy was evaluated as a fast and non-destructive analytical technique for the determination of beta-carotene, coenzyme Q10 and lutein content in palm oil extract. It was observed during analysis that solvent removal was a critical step in sample preparation; formation on the crystal of a thin film yielded reproducible spectra. FTIR absorption spectra of pure palm oil extract and of the standard compounds, retrieved in the 4000 to 400 cm^{-1} region, are shown in Figure 6.1. The absorption bands were assigned based on literature. In the palm oil spectrum, the absorption band at 3006 cm^{-1} was assigned to C-H stretching of *cis* double bonds. The terminal CH_3 groups of the triglyceride chains showed a strong band at approximately 2921 cm^{-1} due to the C-H stretching. The CH_2 groups in the saturated fatty acid backbone showed a band at 2852 cm^{-1} corresponding to C-H stretching. The strong peak near to 1743 cm^{-1} was assigned to C=O stretching. The absorption bands from 1500-650 cm^{-1} was attributed to bending and stretching vibrations of C-H and C-O groups. Specific bands in this region were assigned to scissoring of C-H bonds in CH_3 and CH_2 groups (1465 cm^{-1}), symmetric bending of C-H bonds in CH_3 groups (1378 cm^{-1}), bending and stretching vibrations of CH_2 and C-O ester groups (1165 cm^{-1}), and rocking of CH_2 groups and HC=CH *cis* bounds (720 cm^{-1}) [63], [134], [135], [136], [137].

Beta-carotene spectrum showed absorption bands from 3100 to 2700 cm^{-1} which were attributed to asymmetric and symmetric stretching vibrations of the C-H groups. The absorption band observed near 3028 cm^{-1} was due to the trans HC=CH bonds. The band at 1446 cm^{-1} corresponded to the asymmetric vibration and the one at 1364 cm^{-1} to the symmetric vibration of the C-H groups. The sharp band at 962 cm^{-1} was assigned to the trans conjugated alkene HC=CH out-of-the plane vibration mode while the band at 826 cm^{-1} was attributed to the CH_2 groups in rocking mode [11], [12], [138].

In the FTIR spectrum of coenzyme Q10, absorption bands from 3000 to 2800 cm^{-1} were attributed to stretching vibrations of the C-H groups. The absorption at 1642 cm^{-1} was due to C=O stretching vibration while the band at 1606 cm^{-1} was

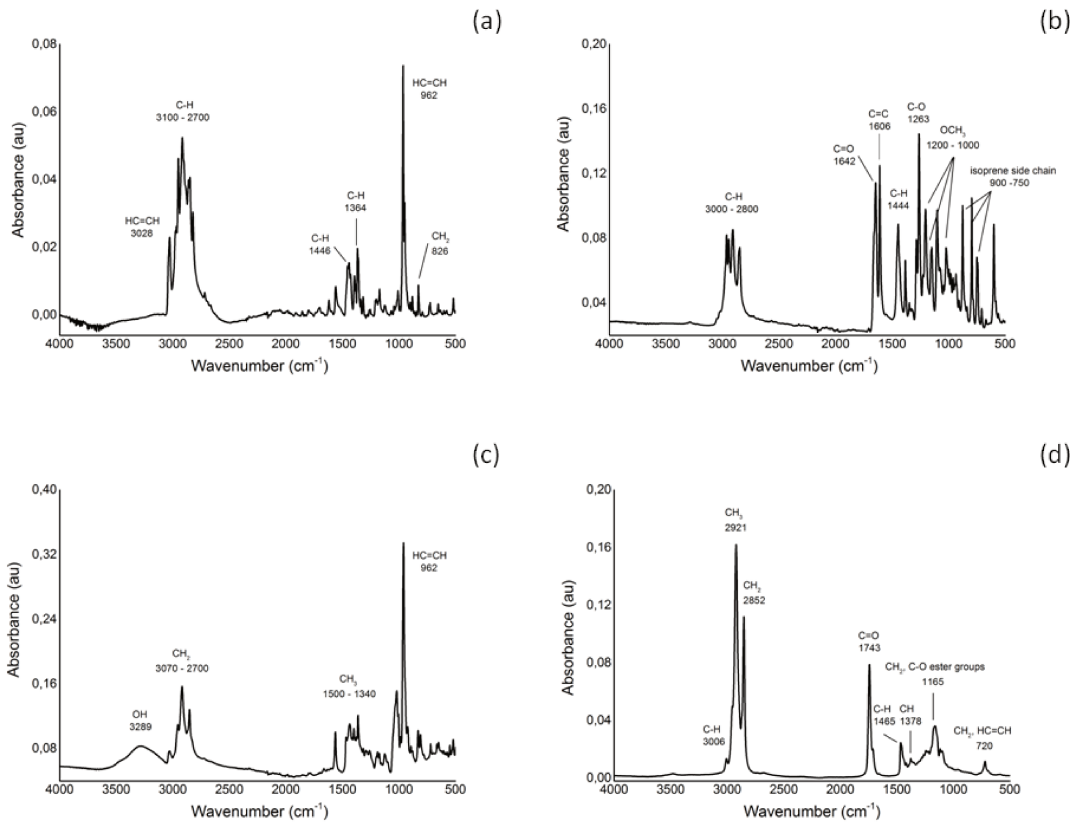

Figure 6.1: FTIR absorption spectra of (a) beta-carotene, (b) coenzyme Q10, (c) lutein and (d) palm oil extract in the 4000-400 cm^{-1} region.

assigned to C=C bonds in the quinone ring. The peak around 1444 cm^{-1} was from C-H bending while the sharp peak at 1263 cm^{-1} arose from C-O stretching. The absorption bands from 1200 to 1000 cm^{-1} were due to OCH_3 groups whereas the absorption bands from 900 to 750 cm^{-1} were attributed to all-trans isoprene side chain [139], [140], [141].

Lutein FTIR spectrum showed a broad absorption band around 3289 cm^{-1} assigned to OH stretching vibrations. The absorption bands from 3070 to 2700 cm^{-1} were from stretching vibrations of the CH_2 groups while bands corresponding to bending vibrations of the CH_3 groups were observed between 1500 and 1340 cm^{-1}. The sharp band at 962 cm^{-1} was attributed to the trans conjugated alkene HC=CH out-of-the plane vibration [142].

Beta-carotene, coenzyme Q10 and lutein are minor constituents of palm oil and are found in total concentration ranging from 500 to 700 ppm [14], [18]. Due to their lower concentration, they may have minor effects on palm oil spectrum. Because of this, a chemometric approach was used to probe these subtle changes.

6.3.2 Principal Component Analysis

As a first step, exploratory data analysis was conducted by PCA to distinguish palm oil extract and the standard compounds. This chemometric method was employed because it does not require any prior knowledge of the sample properties [61]. This chemometric method can be used to find the subspace in the space of the variables where data mostly vary [143], [144]. PCA reduces the dimensionality of a large data set into a lower number of new orthogonal variables, the principal components (PCs), so the maximum amount of variance contained in the original data set is concentrated in a small number of PCs [132], [145].

PCA scores plot showed four distinct clusters, and 93% of the total variance was explained by the first 2 components (Figure 6.2a). Palm oil samples were located on the positive portion of the PC1 axis whereas the standard compounds were grouped on the negative portion. The loadings plot for PC1 showed that the absorption bands that most contributed to distinguish palm oil extract and the standard compounds were the vibrational frequencies arising from groups in the triglycerides, as indicated in (Figure 6.2b). As expected, these absorption bands affected the PCA model since triglycerides accounted for more than 90% of palm oil content. On the other hand, the absorption bands influencing the separation of the standard compounds could be ascribed to the broad band around 3289 cm^{-1} associated to stretching vibrations of the OH groups in lutein, the peaks at 1642 cm^{-1} attributed to C=O stretching vibrations and at 1606 cm^{-1} due to the C=C bonds in coenzyme Q10, the sharp peak near 1263 cm^{-1} assigned to C-O stretching vibrations also in coenzyme Q10 and the band at 962 cm^{-1} due to C=C out-of-the plane vibrations in beta-carotene and lutein, as can be seen in the loadings plot of PC2. Beta-carotene and lutein are grouped more closely to each other than to coenzyme Q10. This can be explained by the influence of the negative peak at 962 cm^{-1} on the separation of beta-carotene and lutein from coenzyme Q10. The latter was separated from the other standard compounds by the positive peaks at 1642, 1606 and 1263 cm^{-1} as revealed in the loadings plot of PC2.

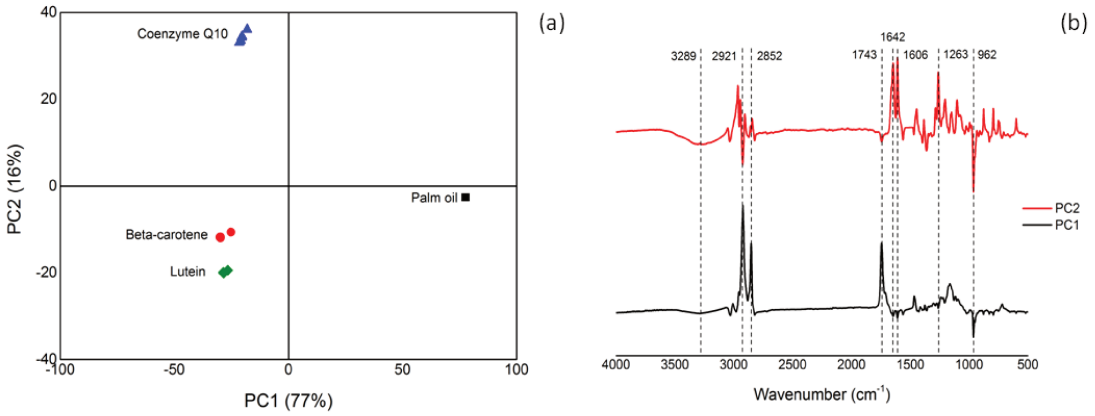

Figure 6.2: Principal component analysis of FTIR spectra for palm oil extract and the standard compounds (a) the scores plot of PC1 versus PC2 and (b) the loadings plot for PC1 and PC2.

6.3.3 Partial Least Squares

Calibration models were built using PLS regression. PLS is a chemometric method that relates the variations in one or more dependent variables (Y) to the variations of several independent variables (X) with explanatory or predictive purposes [61], [64], [146]. This chemometric method was employed to obtain chemical information from FTIR data to assemble calibration models to predict beta-carotene, coenzyme Q10 and lutein content in palm oil extract. PLS calibration models were built before quantifying the target compounds by the UHPSFC method used as reference. In Figure 6.3, FTIR spectrum of palm oil extract was compared to those of the spiked samples and the standard compounds. Differences between palm oil spectrum and those of the spiked samples, specially in the 1500 to 500 cm^{-1} fingerprint region, were observed.

Figure 6.4 shows PLS models and the regression coefficients plots. The estimated content of beta-carotene, coenzyme Q10 and lutein measured by FTIR spectroscopy showed good correlation with the reference values. Leave-one-out cross-validation was used to construct the validation set. The regression coefficients plots allowed identification of the absorption bands associated with the highest variation in the data set. For beta-carotene, the loading plot depicted peaks at the absorption region from 3000 to 2900 cm^{-1} correlated to the lipid moieties of the palm oil and also to the HC=CH bonds of the beta-carotene backbone, two sharp peaks at approximately

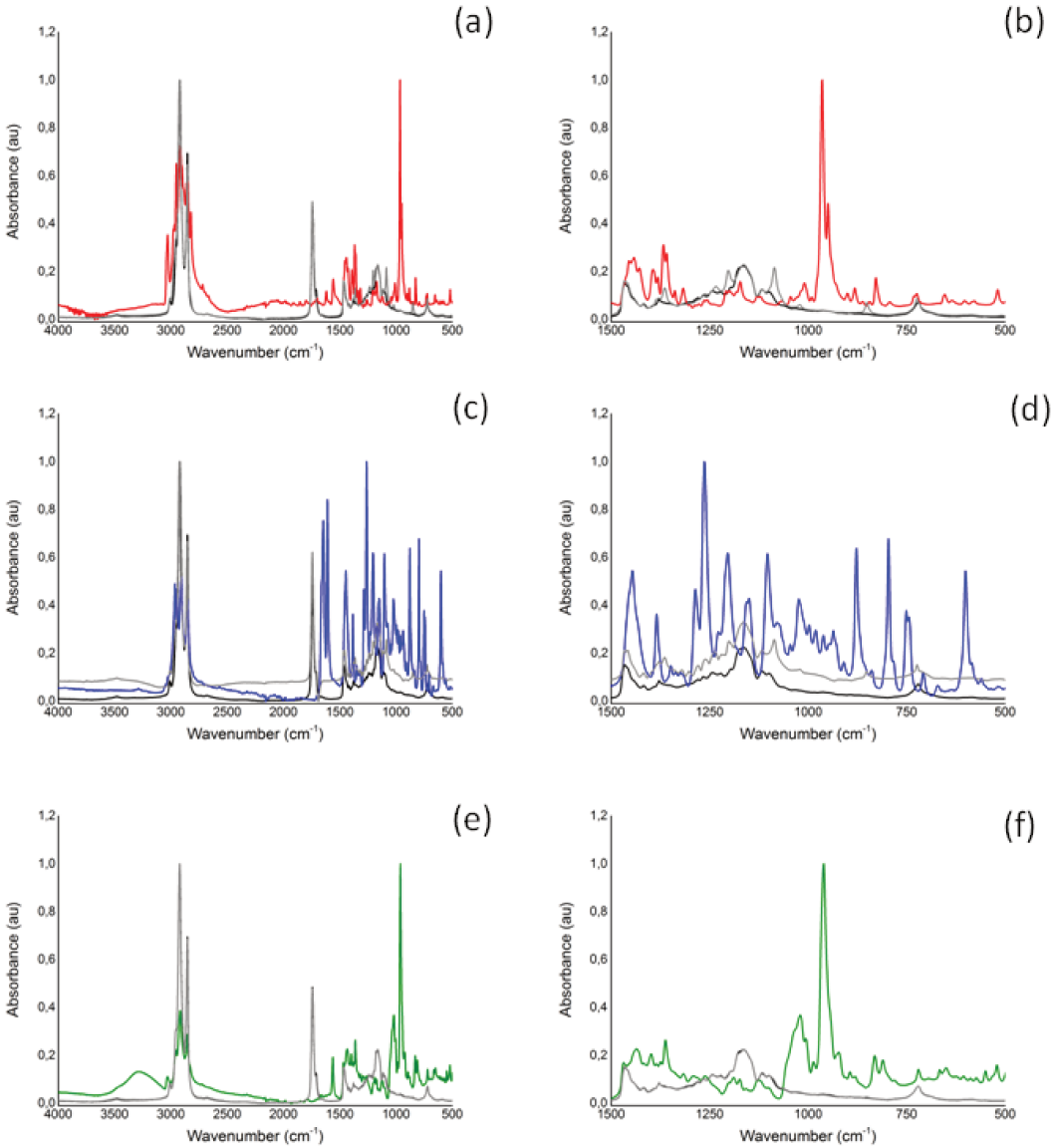

Figure 6.3: FTIR spectra and fingerprint region of fortified palm oil samples with (a and b) beta-carotene, (c and d) coenzyme Q10 and (e and f) lutein. Spectrum colors refer to beta-carotene (red), coenzyme Q10 (blue), lutein (red), palm oil samples (black) and fortified palm oil samples (grey).

1747 and 1707 cm^{-1} attributed to C=O groups of palm oil and peaks with lower intensities in the fingerprint region of beta-carotene (1500 to 500 cm^{-1}). Similar pattern was observed in the loading plot of coenzyme Q10, two sharp peaks near 2931 cm^{-1} also correlated to the triglyceride constituents of the palm oil and to the C-H groups of coenzyme Q10 isopronoid tail, two peaks near 1735 cm^{-1} correlated to C=O groups of palm oil and also to the benzoquinone ring of coenzyme Q10, and peaks in the fingerprint region. Three intense peaks were observed in the loading plot of lutein at 2919 cm^{-1} correlated to the lipid moities of the palm oil and also to

lutein backbone, a sharp peak at 1727 cm^{-1} attributed to C=O groups of palm oil and a peak at 1175 cm^{-1}.

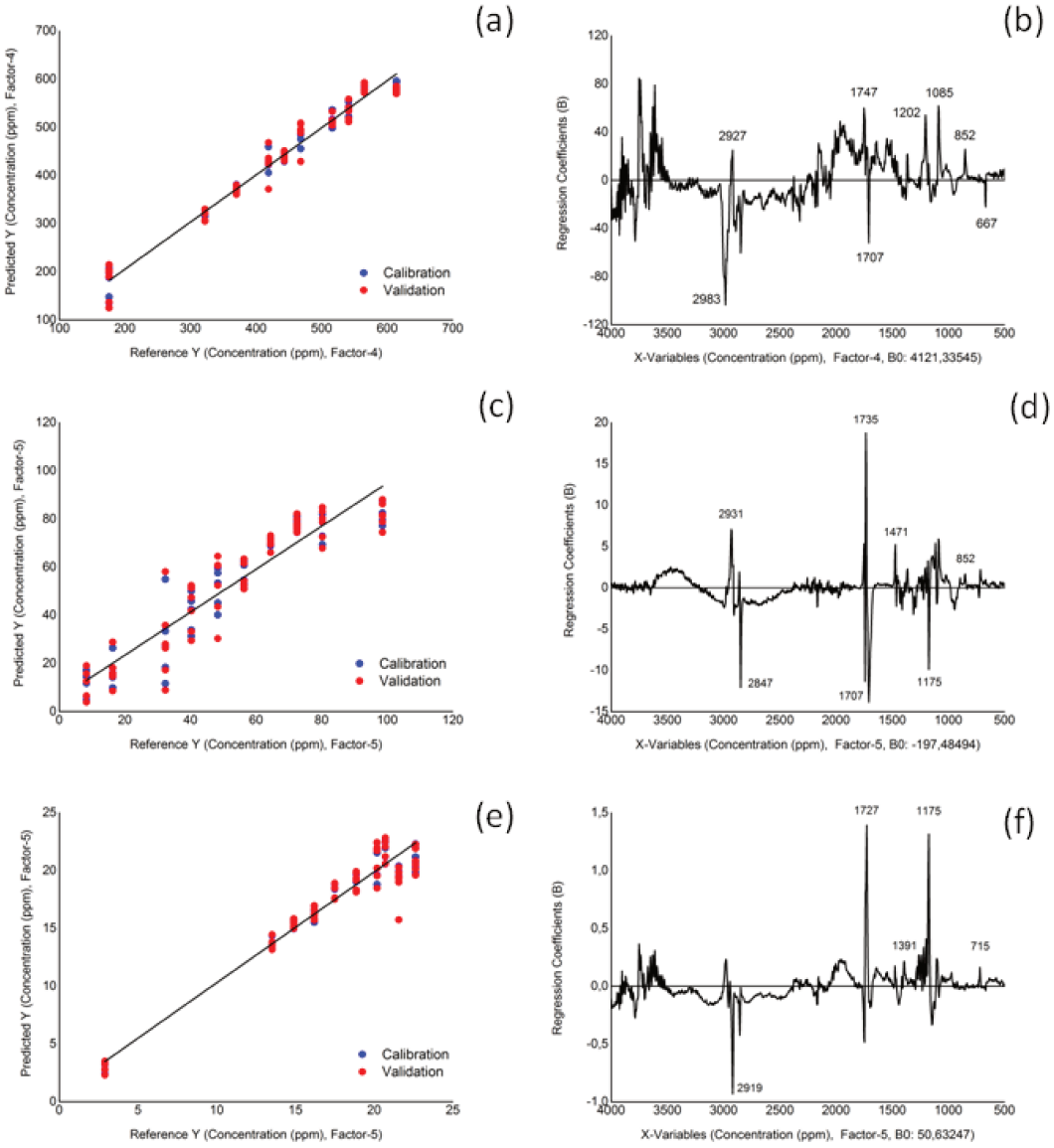

Figure 6.4: Cross-validated (leave-one-out) PLS regression plots for (a) beta-carotene, (c) coenzyme Q10 and (e) lutein content in palm oil. Regression coefficients plots for (b) beta-carotene, (d) coenzyme Q10 and (f) lutein models.

Statistic performance of the PLS models was assessed by the coefficient of determination for calibration (R^2_{cal}), root-mean-square error of calibration (RMSEC), standard error of calibration (SEC), coefficient of determination for cross-validation (R^2_{cv}), root-mean-square error of cross-validation (RMSECV) and standard error of cross-validation (SECV). Table 6.1 shows the statistic performance of the PLS models. The models gave coefficients of determination (R^2_{cal}) > 0.89 for all models,

demonstrating that FTIR data contain significant information about the content of the target compounds in palm oil. Beta-carotene and lutein models showed higher R^2_{cal} values than the coenzyme Q10 model. RMSEC values were 17.8468, 8.8072 and 1.1006 μg/mL for beta-carotene, coenzyme Q10 and lutein models, respectively. The calibration models used a reasonably low number of PLS factors, indicating that the models were not overfitted by picking up noise in the FTIR spectra. The explained predictors (X) variance and explained response (Y) variance for each model are reported in Table 6.1. In order to validate the models, cross-validation (leave-one-out) was employed. Cross-validation evaluates the data by building a model with part of the samples while the remaining samples are used for prediction. Then, a new model is constructed with a new set of samples and it is used to estimate the value for the samples that were left out. This procedure is performed until all samples have been left out once [72], [73]. The statistic performance of the cross-validation is shown in Table 6.1. The coefficients of determination (R^2_{cv}) were 0.9651, 0.8643 and 0.9353 for beta-carotene, coenzyme Q10 and lutein models, respectively. RMSECV were 23.2703 μg/mL for beta-carotene model, 10.1082 μg/mL for coenzyme Q10 model and 1.4016 μg/mL for lutein model. The SECV values were slightly higher than the RMSECV values as shown in Table 6.1.

Table 6.1: Partial least squares regression performance statistics for determination of beta-carotene, coenzyme Q10 and lutein content in palm oil extract.

Model Parameter	**Beta-carotene**	**Coenzyme Q10**	**Lutein**
	Calibration		
Number of samples	10	10	10
R^2_{cal}	0.9790	0.8935	0.9591
RMSEC	17.8468	8.8072	1.1006
SEC	17.9974	8.8815	1.1099
Number of factors	4	5	5
% X variance explained	99.7799	98.3543	99.9653
% Y variance explained	97.8979	89.3470	95.9103
	Validation		
R^2_{cv}	0.9651	0.8643	0.9353
RMSECV	23.2703	10.1082	1.4016
SECV	23.4458	10.1931	1.4107
% X variance explained	99.7368	97.7292	99.8916
% Y variance explained	96.6808	86.3513	93.7693

Beta-carotene, coenzyme Q10 and lutein content in palm oil determined by the PLS models were 178, 12.8 and 2.90 μg/mL, respectively (Table 6.2). Beta-carotene and lutein concentration showed good agreement with reference values obtained by UHPSFC. Coenzyme Q10 concentration obtained by FTIR spectroscopy was slightly higher than the one obtained by UHPSFC, but its concentration is in the range (10-80 ppm) that this constituent is expected to be found in palm oil [14].

The feasibility study showed that there is a relationship between FTIR spectra and the concentration of the target compounds in palm oil. Additionally, calibration models with reasonable precision were built for the determination of beta-carotene, coenzyme Q10 and lutein content. This approach demonstrated the utility of FTIR spectroscopy coupled with PLS regression for prediction of minor constituents in palm oil. However, these results cannot be considered exhaustive because of the small sample set used. In order to build more accurate calibration models, a group of samples covering large content variability among the target compounds should be employed.

Table 6.2: Beta-carotene, coenzyme Q10 and lutein content in palm oil extract obtained by FTIR spectroscopy and the reference method.

Palm Oil Constituent	**FTIR** μ**g/mL**	**UHPSFC** μ**g/mL**
Beta-carotene	178 ($\pm$ 31.42)	176
Coenzyme Q10	12.8 ($\pm$ 5.11)	8.29
Lutein	2.90 ($\pm$ 0.31)	2.90

6.4 Conclusions

In this study, FTIR spectroscopy coupled with chemometrics was employed for determination of beta-carotene, coenzyme Q10 and lutein content in palm oil. The chemometric method PCA was first employed with the aim to identify clustering that could influence the subsequent multivariate analyses. In PCA results, the scores plot revealed a clear differentiation between palm oil extract and the standard compounds while the PCA loadings plots showed that the absorption bands that most contributed to distinguish palm oil samples from the standard compounds arose from the lipid moieties of the palm oil. PLS regression was applied on the spectral data

to build calibration models. Beta-carotene, coenzyme Q10 and lutein content in palm oil determined by PLS regression were 178, 12.8 and 2.90 μg/mL, respectively. These results were comparable to those from the reference method, and demonstrated that the proposed method is a potential choice for a rapid determination of minor constituents of palm oil.

7 | Conclusão

Neste trabalho, método para separação e quantificação de compostos bioativos extraídos dos frutos da palmeira *Elaeis guineensis* Jacq. foi desenvolvido por UHPSFC. Além do método desenvolvido por UHPSFC, o trabalho também avaliou a viabilidade do emprego da espectroscopia FTIR associada à quimiometria para a quantificação de carotenoides e coenzima Q10 no óleo de palma.

Na primeira parte do trabalho, o método para separação e quantificação foi desenvolvido com a mistura padrão (licopeno, betacaroteno, coenzima Q10 e luteína) por UHPSFC. O estudo investigou a influência das condições de operação (pressão, temperatura e porcentagem de etanol) nos parâmetros cromatográficos (fator de retenção e fator de separação). As respostas foram usadas na construção de modelos estatísticos que descreveram o comportamento do sistema dentro da região estudada de forma a identificar as condições ótimas de separação dos analitos.

Os resultados mostraram que a porcentagem de etanol e a pressão foram os fatores que mais afetaram a retenção dos analitos. Por outro lado, a temperatura foi o fator que menos influenciou a retenção. No entanto, a faixa de variação da temperatura empregada no planejamento experimental foi pequena devido as limitações da técnica e também a baixa estabilidade térmica dos compostos estudados, o que pode ter resultado no efeito não significativo desse fator. É interessante ressaltar que o aumento da temperatura resultou na redução dos fatores de retenção do licopeno e betacaroteno, enquanto que aumento dos fatores de retenção da coenzima Q10 e luteína foram observados.

Os três fatores (pressão, temperatura e porcentagem de etanol) afetaram a separação dos analitos. Betacaroteno e coenzima Q10 foram os analitos que apresentaram as maiores limitações na separação. Gráficos de sobreposição foram empregados para identificar as condições ótimas de separação. Devido a co-eluição do betacaroteno e coenzima Q10 em alguns condições de operação e a instabilidade térmica dos

compostos, as condições de operação selecionadas foram pressão 1500 psi, temperatura 40 ℃ e porcentagem de etanol 15,5%.

Na segunda parte do estudo, as condições ótimas de operação determinadas com a mistura padrão foram avaliadas com a amostra do óleo de palma. Os resultados indicaram que essas condições não eram adequadas para a separação do licopeno, betacaroteno, coenzima Q10 e luteína presentes no óleo de palma devido à co-eluição desses compostos com componentes da matriz do óleo. Novas condições de operação foram determinadas com a amostra do óleo. Os resultados mostraram que no domínio experimental estudado, em pressões mais baixas, o aumento da porcentagem de etanol resultou em variações significativa nos fatores de retenção, enquanto que efeito menos pronunciado foi observado em pressões mais elevadas. Por outro lado, em altas porcentagens de etanol, a variação da pressão não influenciou significativamente os fatores de retenção. Apesar da temperatura ter sido o fator menos significativo, este fator foi importante para o ajuste das condições de operação e para melhorar a separação entre os picos do betacaroteno e coenzima Q10. As condições de operação selecionadas para a separação e quantificação dos compostos bioativos no óleo de palma foram pressão 1600 psi, temperatura 40 ℃ e porcentagem de etanol 18%.

O método de processamento de sinais analíticos MCR-ALS foi empregado na análise dos dados cromatográficos do óleo de palma para recuperar valores das concentrações relativas e os perfis espectrais puros dos compostos investigados. Os resultados mostraram co-eluição entre o betacaroteno e componentes da matriz e também co-eluição entre a coenzima Q10 e componentes da matriz. É importante ressaltar que o perfil espectral do composto que coeluiu com o betacaroteno e a coezima Q10 é semelhante ao perfil espectral de carotenoides. Betacaroteno e coenzima Q10 foram identificados e quantificados apesar da co-eluição, o que mostra a importância do método MCR-ALS na análise dos dados cromatográficos de amostras complexas. A concentração obtida para o betacaroteno e coenzima Q10 foi 176 e 8,29 μg/mL, respectivamente. A identificação da luteína só foi possível com a adição do padrão analítico e a concentração obtida foi 2,90 μg/mL. Os resultados obtidos pelo método MCR-ALS forneceram informações relevantes para a identificação dos compostos estudados. Além disso, a comparação do perfil espectral dos compostos

não identificados com o espectro da luteína indicou semelhança na estrutura fina desses espectros. Não foi possível a identicação desses compostos devido à pouca disponibilidade de padrões analiticos de carotenoides.

Os resultados dessa parte do estudo mostraram os desafios envolvidos na identificação e quantificação de compostos minoritários em uma matriz complexa como o óleo de palma. Além disso, a presença de isômeros demandou o uso do método quimiométrico MCR-ALS para a identificação e quantifiação dos compostos estudados.

Na terceira parte do trabalho, betacaroteno, coenzima Q10 e luteína foram quantificados por espectroscopia FTIR associada ao método quimiométrico PLS. O objetivo do estudo foi avaliar a viabilidade do uso de dados espectrais de FTIR para a quantificação de compostos minoritários do óleo de palma. Os resultados apresentaram concordância com os resultados obtidos com o método de referência (UHPSFC) e demonstraram a viabilidade do uso da técnica FTIR associada à quimiometria para a quantificação do betacaroteno, coenzima Q10 e luteína no óleo de palma. É importante ressaltar que para a construção de modelos de calibração mais robustos é necessário um conjunto representativo de amostras do óleo de palma com ampla variabilidade na concentração dos compostos de interesse.

Os resultados desse trabalho demonstraram o uso de duas técnicas sustentáveis que apresentam como vantagens menor consumo de solventes orgânicos e menor tempo de análise para a quantificação de compostos presentes em baixa concentração no óleo de palma. Os resultados do estudo poderão contribuir para uma melhor compreensão da matriz do óleo de palma, das técnicas necessárias para a quantificação dos seus constituintes, para a implementação de processos para recuperação desses constituintes e também para agregar valor ao óleo de palma comercializado para diferentes aplicações.

8 | Perspectivas

Este estudo avaliou as técnicas UHPSFC e espectroscopia FTIR para a quantificação de compostos bioativos no óleo de palma. Os resultados desse trabalho levam a novas possibilidade de pesquisa com esta matriz. Como sugestão para trabalhos futuros pode-se considerar:

- Identificação e quantificação de outros carotenoides presentes na matriz do óleo de palma por UHPSFC;
- Uso do clorofórmio como diluente devido à alta volatilidade do MTBE;
- Emprego do procedimento de saponificação da amostra com etapa de congelamento para remover a matriz oleosa;
- Isomerização do padrão dos compostos de interesse e fortificação da amostra do óleo de palma com essa mistura para auxiliar na identificação dos isômeros;
- Experimentos com a coluna Torus 1-AA(1-aminoantraceno) como alternativa a coluna C18;
- Experimentos com o equipamento UHPSFC acoplado à espectrometria de massas para auxilar na identificação dos compostos;
- Emprego de um conjunto representativo de amostras para construção de modelos robustos com dados espectrais de FTIR;
- Emprego de outros métodos de pré-tratamento dos dados espectrais;
- Avaliação da construção dos modelos de calibração com regiões do espectro infravermelho.

Bibliografia

(1) Akanda, M. J. H.; Sarker, M. Z. I.; Ferdosh, S.; Manap, M. Y. A.; Ab Rahman, N. N. N.; Ab Kadir, M. O. *Molecules* **2012**, *17*, 1764–1794.

(2) Chinembiri, T. N.; Du Plessis, L. H.; Gerber, M.; Hamman, J. H.; Du Plessis, J. *Molecules* **2014**, *19*, 11679–11721.

(3) Parmar, S. S.; Jaiwal, A.; Dhankher, O. P.; Jaiwal, P. K. *Critical Reviews in Biotechnology* **2015**, *35*, 152–164.

(4) De Dieu Ndikubwimana, J.; Lee, B. H. *Biotechnology Letters* **2014**, *36*, 1917–1926.

(5) Ye, V. M.; Bhatia, S. K. *Biotechnology Letters* **2012**, *34*, 1405–1414.

(6) Rivera, S.; Canela-Garayoa, R. *Journal of Chromatography A* **2012**, *1224*, 1–10.

(7) Lunetta, S.; Roman, M. *Journal of AOAC International* **2008**, *91*, 702–708.

(8) Laboureur, L.; Ollero, M.; Touboul, D. *International Journal of Molecular Sciences* **2015**, *16*, 13868–13884.

(9) Choo, Y. M.; Ng, M. H.; Ma, A. N.; Chuah, C. H.; Hashim, M. A. *Lipids* **2005**, *40*, 429–432.

(10) Han, N. M.; May, C. Y.; Ngan, M. A.; Hock, C. C.; Hashim, M. A. *American Journal of Applied Sciences* **2006**, *3*, 1929–1932.

(11) Moh, M. H.; Man, Y. B. C.; Badlishah, B. S.; Jinap, S.; Saad, M. S.; Abdullah, W. J. W. *Journal of the American Oil Chemists' Society* **1999**, *76*, 249–254.

(12) Ammawath, W.; bin Che Man, Y. *Asian Journal of Food and Agro-Industry* **2010**, *3*, 443–452.

(13) Teixeira, C. B.; Macedo, G. A.; Macedo, J. A.; da Silva, L. H. M.; da C. Rodrigues, A. M. *Bioresource Technology* **2013**, *129*, 575–581.

(14) Mba, O. I.; Dumont, M.-J.; Ngadi, M. *Food Bioscience* **2015**, *10*, 26–41.

(15) Damayant, S.; Andry, S.; Khairurrijal; Kartasasmita, R. E. *Journal of Applied Sciences* **2014**, *14*, 2615–2621.

(16) Guedes, L. S.; Beppu, M. M.; Melo, L. V.; Jardim, I. C. S. F.; Breitkreitz, M. C.; Santana, C. C. em *The XXI Brazilian Congress of Chemical Engineering (COBEQ)*, Fortaleza, 2016.

(17) Ng, M.; Choo, Y. *American Journal of Analytical Chemistry* **2015**, *6*, 645–650.

(18) Kamboh, M. A.; Chang, A. S.; Wan Ibrahim, W. A.; Sanagi, M. M.; Mahesar, S. A.; Sirajuddin; Hussain Sherazi, S. T. *RSC Adv.* **2015**, *5*, 50591–50596.

(19) Lesellier, E.; Krstulovic, A. M.; Tchapla, A. *Chromatographia* **1993**, *36*, 275–282.

(20) Amorim-Carrilho, K.; Cepeda, A.; Fente, C.; Regal, P. *TrAC Trends in Analytical Chemistry* **2014**, *56*, 49–73.

(21) Sy, C.; Gleize, B.; Dangles, O.; Landrier, J.-F.; Veyrat, C. C.; Borel, P. *Molecular Nutrition & Food Research* **2012**, *56*, 1385–1397.

(22) Fuller, B. B. em *Cosmetic Dermatology: Products and procedures*, Draelos, Z. D., ed.; John Wiley & Sons, Ltd: West Sussex, 2010; cap. 35, pp. 281–291.

(23) Abrahamsson, V.; Rodriguez-Meizoso, I.; Turner, C. *Journal of Chromatography A* **2012**, *1250*, 63–68.

(24) Marz, U. *The global market for carotenoids*; rel. téc. FOD025E, Acesso em: 01/06/2019; Wellesley, MA: BCC Research, 2019.

(25) Mercadante, A. Z.; Rodrigues, D. B.; Petry, F. C.; Mariutti, L. R. B. *Food Research International* **2017**, *99*, 830–850.

(26) Tee, E.-S.; Lim, C.-L. *Food Chemistry* **1991**, *41*, 147–193.

(27) Rivera, S.; Canela, R. *Molecules* **2012**, *17*, 11255–11268.

(28) Xia, S.; Xu, S.; Zhang, X. *Journal of Agricultural and Food Chemistry* **2006**, *54*, 6358–6366.

(29) Zhao, Y.; Sun, Y.-H.; Li, Z.-Y.; Xie, C.; Bao, Y.; Chen, Z.-J.; Gong, J.-B.; Yin, Q.-X.; Chen, W.; Zhang, C. *Journal of Solution Chemistry* **2013**, *42*, 764–771.

(30) Bunaciu, A. A.; Aboul-Enein, H. Y.; Fleschin, S. *Applied Spectroscopy Reviews* **2010**, *45*, 206–219.

(31) Shafaa, M. W.; Elshazly, A. H.; Dakrory, A. Z.; Elsyed, M. R. *Advanced Pharmaceutical Bulletin* **2018**, *8*, 1–9.

(32) Ahmed, N.; Ahmed, M.; Gehad, E. A.; Yasmin, E.; Yasmein, H.; Yasmin, H.; Samar, E. g.; Samar, F.; Yomna, R. *CNS & Neurological Disorders - Drug Targets* **2016**, *15*, 45–53.

(33) Fan, L.; Feng, Y.; Chen, G.-C.; Qin, L.-Q.; Fu, C.-l.; Chen, L.-H. *Pharmacological Research* **2017**, *119*, 128–136.

(34) Alvaro, S.; Javier, D.-C.; Mario, P.-M.; Naroa, K.; Rafael, G.; Julio J., O. *Current Drug Metabolism* **2016**, *17*, 345–358.

(35) Nováková, L.; Perrenoud, A. G.-G.; Francois, I.; West, C.; Lesellier, E.; Guillarme, D. *Analytica Chimica Acta* **2014**, *824*, 18–35.

(36) Santana, C. C.; Jr., I. J. S.; Azevedo, D. C. S.; Jr., A. G. B. em *Downstream industrial biotechnology: Recovery and purification*, Flickinger, M. C., ed.; John Wiley & Sons: New Jersey, 2013, pp. 147–178.

(37) Lesellier, E.; West, C. *Journal of Chromatography* A **2015**, *1382*, 2–46.

(38) Saito, M. *Journal of Bioscience and Bioengineering* **2013**, *115*, 590–599.

(39) Tarafder, A.; Guiochon, G. *Journal of Chromatography* A **2011**, *1218*, 4569–4575.

(40) Bernal, J. L.; Martín, M. T.; Toribio, L. *Journal of Chromatography A* **2013**, *1313*, 24–36.

(41) Taylor, L. T. *The Journal of Supercritical Fluids* **2009**, *47*, 566–573.

(42) Waters UPC^2 strategy for scaling from analytical to preparative SFC separations., Application Note APNT134770356, 2013.

(43) Desfontaine, V.; Tarafder, A.; Hill, J.; Fairchild, J.; Perrenoud, A. G.-G.; Veuthey, J.-L.; Guillarme, D. *Journal of Chromatography A* **2017**, *1511*, 122–131.

(44) Knofel, T. Ultra-performance convergence chromatography: Expanding selectivity for clinical laboratory., 2013.

(45) McLaren, L.; Myers, M. N.; Giddings, J. C. *Science* **1968**, *159*, 197–199.

(46) Ahmad, A.; Chan, C.; Shukor, S. A.; Mashitah, M. *Separation and Purification Technology* **2010**, *73*, 279–285.

(47) Barros Neto, B.; Scarminio, I. S.; Bruns, R. E. em *Como fazer experimentos: Pesquisa e desenvolvimento na ciência e na indústria*, Barros Neto, B., Scarminio, I. S., Bruns, R. E., eds.; Editora da Unicamp: Campinas, 2001; cap. 6, pp. 251–299.

(48) Montgomery, D. C. em *Introduction to statistical quality control*, Montgomery, D. C., ed.; John Wiley & Sons, Inc.: Hoboken, 2009; cap. 14, pp. 602–628.

(49) Bas, D.; Boyacı, I. H. *Journal of Food Engineering* **2007**, *78*, 836–845.

(50) Teófilo, R. F.; Ferreira, M. M. C. *Química Nova* **2006**, *29*, 338–350.

(51) Bezerra, M. A.; Santelli, R. E.; Oliveira, E. P.; Villar, L. S.; Escaleira, L. A. *Talanta* **2008**, *76*, 965–977.

(52) Ferreira, S. L. C.; Bruns, R. E.; da Silva, E. G. P.; dos Santos, W. N. L.; Quintella, C. M.; David, J. M.; de Andrade, J. B.; Breitkreitz, M. C.; Jardim, I. C. S. F.; Neto, B. B. *Journal of Chromatography A* **2007**, *1158*, 2–14.

(53) Asberg, D.; Enmark, M.; Samuelsson, J.; Fornstedt, T. *Journal of Chromatography* A **2014**, *1374*, 254–260.

(54) De Tarso Vieira e Rosa, P. em *Biomateriais aplicados ao desenvolvimento de sistemas terapêuticos avançados*, de Sousa, H. C., Braga, M. E. M., Sosnik, A., eds.; Imprensa da Universidade de Coimbra: Coimbra, 2015; cap. 15, pp. 599–633.

(55) Waters Qualitative and quantitative analysis of β-carotene using UPC^2., Application Note APNT134719455, 2013.

(56) Lesellier, E.; West, C.; Tchapla, A. *Journal of Chromatography A* **2003**, *1018*, 225–232.

(57) Poole, C. F. *Journal of Chromatography A* **2012**, *1250*, 157–171.

(58) Collins, C. H. em *Fundamentos de Cromatografia*, Collins, C. H., Braga, G. L., Bonato, P. S., eds.; Editora da Unicamp: Campinas, 2006; cap. 1, pp. 17–42.

(59) Snyder, L. R.; Kirkland, J. J.; Glajch, J. L. em *Practical HPLC method development*, Snyder, L. R., Kirkland, J. J., Glajch, J. L., eds.; John Wiley & Sons, Ltd: Danvers, 2012; cap. 2, pp. 21–58.

(60) Kawano, Y. em *Técnicas de caracterização de polímeros*, Canevaloro Jr., S. V., ed.; Artliber Editora: São Paulo, 2017; cap. 1, pp. 17–40.

(61) Capuano, E.; van Ruth, S. em *Encyclopedia of food and health*, Caballero, B., Finglas, P., Toldra, F., eds.; Academic Press: Oxford, 2016, pp. 424–431.

(62) Lu, X.; Rasco, B. A. *Critical Reviews in Food Science and Nutrition* **2012**, *52*, 853–875.

(63) Dobson, G. *European Journal of Lipid Science and Technology* **2001**, *103*, 815–815.

(64) De Nardo, T.; Shiroma-Kian, C.; Halim, Y.; Francis, D.; Rodriguez-Saona, L. E. *Journal of Agricultural and Food Chemistry* **2009**, *57*, 1105–1112.

(65) Stuart, B. H. em *Infrared spectroscopy: Fundamentals and applications*, Stuart, B. H., ed.; John Wiley & Sons, Ltd: Chichester, 2005; cap. 2, pp. 15–44.

(66) Coillet, E. Structural characterization of thin non-crystalline layers for low thermal noise optic., PhD thesis, Université de Lyon, 2017.

(67) FT-IR Spectroscopy Attenuated Total Reflectance ATR., 007024B_01; PerkinElmer Life e Analytical Sciences, 2005.

(68) Karim, M.; Karim, S.; Rana, A.; Masum, S.; Mondol, A.; Israt, S. *Bangladesh Journal of Scientific and Industrial Research* **2015**, *50*, 233–240.

(69) Ferreira, M. M. C., *Quimiometria: Conceitos, métodos e aplicações*; Editora da Unicamp: Campinas, 2015.

(70) Rinnan, A.; Norgaard, L.; van den Berg, F.; Thygesen, J.; Bro, R.; Engelsen, S. B. em *Infrared spectroscopy for food quality analysis and control*, Sun, D.-W., ed.; Academic Press: San Diego, 2009; cap. 2, pp. 29–50.

(71) Rohman, A.; Setyaningrum, D. L.; Riyanto, S. *International Journal of Spectroscopy* **2014**, *2014*, 1–5.

(72) ASTM Standard practices for infrared multivariate quantitative analysis (E1655-05).; ASTM International, West Conshohocken, 2012.

(73) Rohman, A.; Man, Y. C. *Food Research International* **2010**, *43*, 886–892.

(74) Nokkaew, R.; Punsuvon, V.; Inagaki, T.; Tsuchikawa, S. *International Journal of* GEOMATE **2019**, *16*, 92–98.

(75) Che Man, Y.; Aye, W.; Tan, C.; Abdulkarim, S. *Journal of Food Lipids* **2009**, *16*, 475–483.

(76) Man, Y. C.; Ammawath, W.; Mirghani, M. *Food Chemistry* **2005**, *90*, 323–327.

(77) Rasaruddin, N. F.; Hasan, M. N.; Ruah, M. E. N. M.; Fong, S. S.; Jaafar, M. Z. em *IEEE 10th International Colloquium on Signal Processing and its Applications*, IEEE: Kuala Lumpur, 2014, pp. 95–99.

(78) Siddique, B. M.; Muhamad, I. I.; Ahmad, A.; Ayob, A.; Ibrahim, M. H.; Ak, M. O. *Journal of Food Science and Technology* **2015**, *52*, 1444–1452.

(79) Rivera, S. M.; Christou, P.; Canela-Garayoa, R. *Mass Spectrometry Reviews* **2014**, *33*, 353–372.

(80) Kaczmarski, K.; Poe, D. P.; Tarafder, A.; Guiochon, G. *Journal of Chromatography* A **2012**, *1250*, 115–123.

(81) Ahmadi, M.; Vahabzadeh, F.; Bonakdarpour, B.; Mofarrah, E.; Mehranian, M. *Journal of Hazardous Materials* **2005**, *123*, 187–195.

(82) Myers, R. H.; Montgomery, D. C.; Anderson-Cook, C. M., *Response surface methodology: Process and product optimization using designed experiments*, 3ª ed.; Wiley Series in Probability and Statistics; John Wiley & Sons, Inc.: Hoboken, 2009.

(83) Karppi, J.; Nurmi, T.; Olmedilla-Alonso, B.; Granado-Lorencio, F.; Nyyssönen, K. *Journal of Chromatography B* **2008**, *867*, 226–232.

(84) Guedes, L. S.; Jardim, I. C. S. F.; de Melo, L. V.; Beppu, M. M.; Breitkreitz, M. C.; Santana, C. C. *The Canadian Journal of Chemical Engineering* **2017**, *95*, 2306–2314.

(85) Couto, R.; Seifried, B.; Moquin, P.; Temelli, F. *Journal of* CO_2 *Utilization* **2018**, *24*, 315–320.

(86) Shukla, S.; Dubey, K. K. *3 Biotech* **2018**, *8*, 249–259.

(87) Bank, G.; Kagan, D.; Madhavi, D. *Journal of Evidence-Based Complementary & Alternative Medicine* **2011**, *16*, 129–137.

(88) El-Leithy, E. S.; Makky, A. M.; Khattab, A. M.; Hussein, D. G. *Drug Development and Industrial Pharmacy* **2018**, *44*, 316–328.

(89) Zhang, Y. *IOP Conference Series: Earth and Environmental Science* **2019**, *242*, 042003.

(90) Huang, E.; Quek, S. Y.; Fu, N.; Wu, W. D.; Chen, X. D. *Journal of Food Engineering* **2019**, *247*, 45–55.

(91) López-Lluch, G.; del Pozo-Cruz, J.; Sánchez-Cuesta, A.; Cortés-Rodríguez, A. B.; Navas, P. *Nutrition* **2019**, *57*, 133–140.

(92) Ortiz-Estrada, C.; Díaz-Díaz, C. Y.; Cruz-Olivares, J.; Pérez-Alonso, C. *Revista Mexicana de Ingeniería Química* **2015**, *14*, 49–59.

(93) Kaci, M.; Belhaffef, A.; Meziane, S.; Dostert, G.; Menu, P.; Velot, É.; Desobry, S.; Arab-Tehrany, E. *Colloids and Surfaces B: Biointerfaces* **2018**, *167*, 165–175.

(94) Ashraf-Khorassani, M.; Yang, J.; Rainville, P.; Jones, M.; Fountain, K.; Isaac, G.; Taylor, L. *Journal of Chromatography B* **2015**, *983-984*, 94–100.

(95) Lemasson, E.; Bertin, S.; Hennig, P.; Lesellier, E.; West, C. *Journal of Chromatography A* **2016**, *1472*, 117–128.

(96) *Acquity UPC*^{2} *system instrument specifications.*, 720004226EN; Waters Corporation, 2013.

(97) Jesus, A. A.; Almeida, L. C.; Silva, E. A.; Filho, L. C.; Egues, S. M.; Franceschi, E.; Fortuny, M.; Santos, A. F.; Araujo, J.; Sousa, E. M.; Dariva, C. *The Journal of Supercritical Fluids* **2013**, *81*, 245–253.

(98) Muhamad, H.; Zainudin, B. H.; Bakar, N. K. A. *Food Chemistry* **2012**, *134*, 2489–2496.

(99) Nováková, L.; Vlčková, H. *Analytica Chimica Acta* **2009**, *656*, 8–35.

(100) Mateos, R.; García-Mesa, J. A. *Analytical and Bioanalytical Chemistry* **2006**, *385*, 1247–1254.

(101) Moreno, P.; Salvadó, V. *Journal of Chromatography A* **2000**, *870*, 207–215.

(102) Amberlite® *XAD7HP.*, PDS 0529 A; Rohm e Haas Company, 2003.

(103) Sandhu, A. K.; Gu, L. *Journal of Agricultural and Food Chemistry* **2013**, *61*, 1441–1448.

(104) Bijttebier, S.; D'Hondt, E.; Noten, B.; Hermans, N.; Apers, S.; Voorspoels, S. *Food Chemistry* **2014**, *163*, 147–153.

(105) Aman, R.; Biehl, J.; Carle, R.; Conrad, J.; Beifuss, U.; Schieber, A. *Food Chemistry* **2005**, *92*, 753–763.

(106) Dejaegher, B.; Heyden, Y. V. *Journal of Pharmaceutical and Biomedical Analysis* **2011**, *56*, 141–158.

(107) Gharibzahedi, S. M. T.; Mousavi, S. M.; Hamedi, M.; Khodaiyan, F. *Food and Bioprocess Technology* **2013**, *6*, 456–469.

(108) Huang, W.; Li, Z.; Niu, H.; Li, D.; Zhang, J. *Journal of Food Engineering* **2008**, *89*, 298–302.

(109) Olivieri, A. C.; Wu, H.-L.; Yu, R.-Q. *Chemometrics and Intelligent Laboratory Systems* **2009**, *96*, 246–251.

(110) Rodriguez-Amaya, D. B.; Kimura, M., *HarvestPlus handbook for carotenoid analysis. Harvest Plus technical monograph 2*; Washington DC. International Food Policy Research Institute (IFPRI) e International Center for Tropical Agriculture (CIAT): 2004.

(111) Jaumot, J.; de Juan, A.; Tauler, R. *Chemometrics and Intelligent Laboratory Systems* **2015**, *140*, 1–12.

(112) Ruckebusch, C.; Blanchet, L. *Analytica Chimica Acta* **2013**, *765*, 28–36.

(113) Jaumot, J.; Gargallo, R.; de Juan, A.; Tauler, R. *Chemometrics and Intelligent Laboratory Systems* **2005**, *76*, 101–110.

(114) Tauler, R. *Chemometrics and Intelligent Laboratory Systems* **1995**, *30*, 133–146.

(115) Zagatto, E. A.; Oliveira, C. C.; Townshend, A.; Worsfold, P. J. em *Flow analysis with spectrophotometric and luminometric detection*, Zagatto, E. A., Oliveira, C. C., Townshend, A., Worsfold, P. J., eds.; Elsevier: Amsterdam, 2012; cap. 8, pp. 295–448.

(116) Dachtler, M.; Glaser, T.; Kohler, K.; Albert, K. *Analytical Chemistry* **2001**, *73*, 667–674.

(117) Rodriguez-Amaya, D. B., *A guide to carotenoid analysis in food*; Washington, D.C. OMNI Research: 2001.

(118) Mortensen, A. *Food Research International* **2005**, *38*, 847–853.

(119) Darnoko, D.; Cheryan, M.; Moros, E.; Jerrel, J.; Perkins, E. G. *Journal of Liquid Chromatography & Related Technologies* **2000**, *23*, 1873–1885.

(120) Aruna, G.; Mamatha, B.; Baskaran, V. *Journal of Food Composition and Analysis* **2009**, *22*, 632–636.

(121) Bergmann, J.; Tupinambá, D.; Costa, O.; Almeida, J.; Barreto, C.; Quirino, B. *Renewable and Sustainable Energy Reviews* **2013**, *21*, 411–420.

(122) Brandão, F.; Schoneveld, G. *The state of oil palm development in the Brazilian Amazon*; Working Paper 198; Indonesia: Center for International Forestry Research, 2015.

(123) Talbot, G. em *Reducing saturated fats in foods*, Talbot, G., ed.; Woodhead Publishing Series in Food Science, Technology and Nutrition; Woodhead Publishing: 2011, pp. 3–28.

(124) Statista Palm oil: Global production volume 2012/13 – 2018/19., 2019-03-23, `https://www.statista.com/statistics/613471/palm-oil-production-volume-worldwide/`.

(125) Bezerra, F. W. F.; da Costa, W. A.; de Oliveira, M. S.; Andrade, E. H. A.; de Carvalho, R. N. *The Journal of Supercritical Fluids* **2018**, *136*, 136–143.

(126) Brasil *Plano Nacional de Energia 2030 / Ministério de Minas e Energia; colaboração Empresa de Pesquisa Energética*; rel. téc. 12; Brasília: Ministério de Minas e Energia, 2007.

(127) Benami, E.; Curran, L. M.; Cochrane, M.; Venturieri, A.; Franco, R.; Kneipp, J.; Swartos, A. *Environmental Research Letters* **2018**, *13*, 1–13.

(128) RSPO*: T*ransforming markets to make sustainable palm oil the norm*; Malaysia: Roundtable on Sustainable Palm Oil, 2019.

(129) Potts, J.; Lynch, M.; Wilkings, A.; Huppe, G.; Cunningham, M.; Voora, V. *The state of sustainability initiatives review 2014:* S*tandards and the green economy*; Technical Report; Winnipeg: International Institute for Sustainable Development & International Institute for Environment e Development, 2014.

(130) Cozzolino, D. *Antioxidants* **2015**, *4*, 482–497.

(131) Jolayemi, O. S.; Ajatta, M. A.; Adegeye, A. A. *Food Science & Nutrition* **2018**, *6*, 773–782.

(132) Makky, M.; Soni, P. *Journal of Food Engineering* **2014**, *120*, 248–259.

(133) Szydłowska-Czerniak, A.; Trokowski, K.; Karlovits, G.; Szłyk, E. *Food Chemistry* **2011**, *129*, 1187–1192.

(134) Wong, Y. H.; Goh, K. M.; Abas, F.; Maulidiani, M.; Nyam, K. L.; Nehdi, I. A.; Sbihi, H. M.; Gewik, M. M.; Tan, C. P. *LWT* **2019**, *100*, 404–408.

(135) Maarof, S.; Ali, A. A.; Hashim, A. M. *Materials Today: Proceedings* **2019**, *7*, 770–775.

(136) De la Mata, P.; Dominguez-Vidal, A.; Bosque-Sendra, J. M.; Ruiz-Medina, A.; Cuadros-Rodríguez, L.; Ayora-Cañada, M. J. *Food Control* **2012**, *23*, 449–455.

(137) Nor Hayati, I.; Che Man, Y. B.; Tan, C. P.; Nor Aini, I. *International Journal of Food Science & Technology* **2009**, *44*, 152–161.

(138) Da Silva, H. R. G.; Quintella, C. M.; Meira, M. *Journal of the Brazilian Chemical Society* **2017**, *28*, 2348–2356.

(139) Coates, J. em *Encyclopedia of analytical chemistry*, Meyers, R. A., ed.; John Wiley & Sons Ltd: Chichester, 2000, pp. 10815–10837.

(140) Castresana, J.; Alonso, A.; Arrondo, J.-L. R.; Goñi, F. M.; Casal, H. *European Journal of Biochemistry* **1992**, *204*, 1125–1130.

(141) Sommer, P.; Kofler, M. *Vitamins and Hormones* **1966**, *24*, 349–399.

(142) Boonnoun, P.; Nerome, H.; Machmudah, S.; Goto, M.; Shotipruk, A. *The Journal of Supercritical Fluids* **2013**, *77*, 103–109.

(143) Obisesan, K. A.; Jiménez-Carvelo, A. M.; Cuadros-Rodriguez, L.; Ruisánchez, I.; Callao, M. P. *Talanta* **2017**, *170*, 413–418.

(144) Camacho, J.; Picó, J.; Ferrer, A. *Chemometrics and Intelligent Laboratory Systems* **2010**, *100*, 48–56.

(145) Cichelli, A.; Pertesana, G. P. *Journal of Chromatography A* **2004**, *1046*, 141–146.

(146) Héberger, K. em *Medical applications of mass spectrometry*, Vékey, K., Telekes, A., Vertes, A., eds.; Elsevier: Amsterdam, 2008; cap. 7, pp. 141–169.